TAMPERE UNIVERSITY OF TECHNOLOGY

JANNE KOIVISTO

DIFFERENTIATION OF HUMAN INDUCED PLURIPOTENT STEM CELLS INTO PERIPHERAL NEURAL CELLS

Master of Science Thesis

Examiner: Professor Minna Kellomäki

Examiner and topic approved in the Automation, Mechanical and Materials Engineering Department Council meeting on 4th April 2012

TIIVISTELMÄ

TAMPEREEN TEKNILLINEN YLIOPISTO
Materiaalitekniikan koulutusohjelma
KOIVISTO, JANNE: Ääreishermoston solujen erilaistaminen ihmisen uudelleenohjelmoiduista pluripotenteista kantasoluista
Diplomityö, 96 sivua, 2 liitesivua
Tammikuu 2013
Pääaine: Biomateriaalitekniikka
Tarkastaja: professori Minna Kellomäki
Avainsanat: Kantasolu, iPS, tuntohermosolu, kalsium-kuvantaminen, soluväliaineproteiinipinnoite, atomivoimamikroskopia

Ihmisen ääreishermoston kehitys ei ole solutasolla yhtä tunnettu kuin keskushermoston, mutta parin viime vuoden aikana on julkaistu ensimmäiset soluviljelyprotokollat, joilla voidaan tuottaa ääreishermoston soluja laboratoriossa kantasoluista. Erittäin monikykyisten kantasolujen muuttumista jonkin solutyypin soluiksi kutsutaan erilaistumiseksi. Erilaistamalla soluja laboratoriossa saadaan niitä tuotettua sovelluksiin, kuten lääkeaineja myrkyllisyyskokeisiin, mallinnettua niillä tauteja solutasolla tai käytettäviksi lääketieteessä kliinisissä hoidoissa. Ääreishermoston tuntoaistiin liittyvät solut, kuten myeliinitupettomat kipua aistivat C-neuronit, ovat yksi mielenkiintoinen kohde niin lääkeainekehitykselle kuin tautimalleillekin.

Erilaistusprotokollien on osoitettu toimivan alkion kantasoluilla, mutta tätä työtä aloitettaessa ei vielä ollut saatavilla dataa aikuisen uudelleen ohjelmoitujen kantasolujen, eli iPS-solujen, erilaistamisesta ääreishermoston soluiksi. Tärkeimpänä tavoitteena työssä oli siis todistaa, että ääreishermoston kipuhermoja voidaan tuottaa julkaistuilla menetelmillä myös iPS-soluista. Erilaistettujen solujen luonnetta tutkittiin niin morfologian kuin fenotyyppiin liittyvän proteiinien ekspression kautta immunosytokemialla ja RT-PCR:llä, kuin myös toiminnallisuutta kalsium-kuvantamismenetelmällä.

Solujen erilaistuksen lisäksi tutkittiin myös niiden kasvualustana toimivia, soluväliaineproteiineilla pinnoitettuja pintoja. Tavoitteena oli löytää neljästä parhaiten ääreishermoston soluille sopivasta kasvualustavaihtoehdosta sopivin, sekä tutkia pinnoitteiden fysikaalisia eroja. Tutkitut pinnoitteet olivat laminiini, fibronektiini, Matrigel™ ja gelatiini. Pinnoitteiden tutkimiseen käytettiin atomivoimamikroskopiaa, kontaktikulma mittauksia neste-kiinteä -rajapinnalla sekä vasta-aineisiin perustuvaa fluoresenssileimausta.

Työhön valitulla protokollalla onnistuttiin erilaistamaan kalsium-signalointia ilmentäviä hermosoluja, mutta erilaistumistehokkuus oli vaihteleva. Morfologialtaan ja toiminnallisuudeltaan yleisesti hermosoluja vastaavia soluja saatiin kuitenkin tuotettua paljon, mutta spesifisemmin C-neuronien kaltaisia kipuhermoja vain vähän ja niidenkin luonne oli kyseenalainen. Tutkituista proteiinipinnoitteista laminiini vaikutti paremmalta kuin muut, mutta ero erityisesti soluviljelyissä ei kahta poikkeusta lukuun ottamatta ollut suuri. Jatkossa näiden solujen erilaistamisessa kannattaisi siirtyä uuteen, tämän työn aloituksen jälkeen julkaistuun protokollaan ja käyttää tulosten arviointiin tässä työssä opittuja analyysimenetelmiä.

ABSTRACT

TAMPERE UNIVERSITY OF TECHNOLOGY
Master's Degree Programme in Materials Science and Engineering
KOIVISTO, JANNE: Differentiation of human induced pluripotent stem cells into peripheral neural cells
Master of Science Thesis, 96 pages, 2 Appendix pages
January 2013
Major: Biomaterials
Examiner: Professor Minna Kellomäki
Keywords: Stem cell, iPS, peripheral sensory neuron, calcium-imaging, extracellular matrix protein coating, atomic force microscopy

The development of human peripheral nervous system is not as well known on the cellular level as the central nervous system, but during the last few years there have been published cell culture protocols that can produce peripheral sensory neural cells. Changing pluripotent stem cells into some specific cell type is called differentiation. Differentiating cells in laboratory can produce them for applications such as drug and toxicology screening, modeling diseases on cellular level or for use in clinical applications in medicine. The peripheral sensory neurons, such as unmyelinated C nerve fibers that are responsible for sense of pain are good targets for drug development and disease models.

The differentiation protocols work for human embryonic stem cells, but when this thesis was started, no data about the use of induced pluripotent stem cells, or iPS cells, for peripheral neural differentiation were published yet. The most important aim of this thesis was to prove that peripheral sensory neurons can be produced from iPS cells with this protocol. The nature of differentiated cells was studied according to morphology and phenotype by protein expression studies in immunocytochemistry and RT-PCR and functionality was studies by calcium-imaging.

In addition to cell differentiation, the extracellular matrix protein coatings used as cell culture surface, were studied as well. The aim was to find the best out of four coatings suitable for peripheral neurons and study the physical differences of these coatings. The studied coatings were laminin, fibronectin, Matrigel™ and gelatin. Coatings were studied by atom force microscopy, contact angle measurement from liquid-solid interface and antibody based fluorescence labeling.

It was possible to differentiate neural cells that have calcium signaling, with the protocol selected for the thesis, but the differentiation efficiency varied a lot. Cells with general neural morphology and functioning calcium signaling were produced, but more specifically C-fiber-like peripheral sensory neurons were only detected in very small amounts and their nature was uncertain. Out of the studied protein coatings, laminin seemed better than the others, but the difference especially in cell culturing was not big, except for two occasions. In the future the differentiation of these kinds of cells should be done with a new protocol published after starting this thesis, and use the analysis methods learned from this thesis to evaluate the differentiation results of the newer protocol.

PREFACE

This work was done in Heart group in Institute of Biomedical Technology (IBT), a part of BioMediTech, joint life science institute of Tampere University and Tampere University of Technology. The work was funded partly by Pirkanmaa Hospital District researcher fund and partly by the Hydrogel project of the biomaterials research group.

First of all, I would like to express my gratitude to my supervisor Mari Pekkanen-Mattila and our group leader Katriina Aalto-Setälä, for letting me get to know the exciting fields of tissue engineering and cell biology in great detail and giving me this interesting subject to study in my master's thesis. Especially Mari's advice has been invaluable during the course of this work. I would also like to thank my supervisor and examiner Minna Kellomäki for valuable feedback on my work and also for igniting my interest in biomaterials and tissue engineering in the first place as a lecturer.

In addition, I would like to thank Henna Venäläinen and Markus Haponen for teaching me how *in vitro* cell culturing works, Niina Ahola and Maiju Hiltunen for help with AFM imaging, Kim Larsson and Kirsi Kujala for teaching me the basics of calcium imaging and Joose Kreutzer for teaching the contact angle measurements. I would also like to thank the whole Heart group and all the people of ex-Regea for valuable conversations and great work atmosphere. A warm thank goes also for my friends both from MIK and from outside the Tampere University of Technology, you have made sure I have a life outside of studies and work.

Finally I want to thank my parents and my dear brother Mikko for supporting me, giving very valuable feedback on whatever the topic and understanding me and my goals. Thank you for believing in me throughout my studies.

Tampere, 21.01.2013

_____

Janne Koivisto

TABLE OF CONTENTS

ABBREVIATIONS AND TERMS

AFM	Atomic force microscopy
bFGF	Basic fibroblast growth factor
Brn3a	Marker protein for developing peripheral neurons
C-fiber	Unmyelinated axon of peripheral neural cells responsible for sense of pain and heat
Ca-imaging	Computer and microscope assisted research method that allows the study of cellular calcium influx and efflux
Capsaicin	Active component of chili that causes the burning sensation
Collagen	A type of ECM protein
CNS	Central neural system
Contact angle	An angle between the surface of a droplet of liquid and a solid surface and the gas phase
DAPI	Fluorescent stain used to mark cell nuclei, 4',6-diamidino-2-phenylindole
DRG	Dorsal root ganglion
ECM	Extracellular matrix, consists of a cocktail of proteins
EHS	Engelberth-Holm-Swarm, mouse tumor with abundant basement membrane, from where Matrigel™ and laminin-1 can be extracted
Fibroblast	Common cell type of connective tissues
Fibronectin	A type of ECM protein
Fura-2	Ratiometric dye for calcium imaging
Gelatin	Collagen derivative used as coating for cell culture
Glutaraldehyde	A fixative
hESC	Human embryonic stem cell
in vitro	Latin for “in glass”, referring to research done in laboratory without living animals or patients
in vivo	Latin for “in body”, referring to research done with animals or in clinical use
iPS cell	Induced pluripotent stem cell
Laminin	A type of ECM protein
Matrigel™	Commercial ECM protein cocktail used as biomaterial gel and coating for cell culture
Myelin sheat	A protective layer over some peripheral neural axons, that affects the signal conduction rate
NCSC	Neural crest stem cell
NGF	Neural growth factor
Nociceptor	Peripheral neuron responsible for sensation of pain
Noxious	Harmful or dangerous
p75	Neural crest marker protein

PA6	A specific commercial mouse stromal cell line
PFA	Paraformaldehyde, a fixative
PBS	Phosphate buffered saline solution
Peripherin	Intermediate filament protein of peripheral neural cells
PS	Polystyrene, polymer used to make cell culture plates
PSN	Peripheral sensory neuron
QCM-D	Dissipative quartz crystal microbalance
RGD	Sequence of three amino acids arginine-glycine-aspartaic acid. Well known as cell binding site in ECM.
RT-PCR	Reverse transcription polymerase chain reaction
SDIA	Stromal-derived inducing activity, basis of PSN differentiation protocol used in this study
SEM	Scanning electron microscope
SNA1	Neural crest marker protein
SOX9	Neural crest marker protein
TGF-β	Transforming growth factor β, important growth factor for many different cell types
TrkA	Receptor for NGF, expressed in nociceptors
TRPA1	Transient receptor potential ankyrin 1, ion channel in neural cells responsible for sensation of pain
TRPV1	Transient receptor potential vanilloid 1, ion channel in neural cells responsible for sensing noxious heat and also activated by capsaicin
Tyrodes solution	Perfusion solution for Ca-imaging representing the composition of cerebrospinal fluid

1 INTRODUCTION

The primary goal of this thesis was to produce peripheral neural cells from human induced pluripotent stem cells (iPS cells) with a differentiation protocol established for human embryonic stem cells and prove that it works for iPS cells as well. The differentiation of stem cells into peripheral neural cells as well as their calcium signaling was studied. Another goal was to test and characterize selected extracellular matrix (ECM) proteins as coating material for cell culturing purposes and especially their effect on peripheral neural cell differentiation. These coatings are used in everyday cell culturing, but the exact principles of how they work are not always well known, so they were studied to get more detailed information on their characteristics.

Human embryonic stem cells have been under extensive research for over a decade now and they are capable to differentiate into all human cell lines found in adults. However, human iPS cells lack the ethical and antigenic problems inherent to embryonic cells. The iPS cells have been made by reprogramming adult human skin fibroblast cells into being pluripotent again. These kinds of cells have the advantages of having the same genotype as the patient donating them so they are called patient and disease specific and they do not have the same ethical problems in their production that are present in embryonic stem cell production. [1]

The stem cell differentiation protocol used in this work was obtained from data published by Pomp et al. 2008 [2] and Goldstein et al. 2010 [3] and used with little modification. Cell differentiation was studied by immunocytochemical staining and fluorescence microscopy, by observing morphological changes in cells with phase contrast microscope and studying mRNA obtained from living cells. Calcium signaling of cells was tested with calcium imaging by studying cell responses to changes in potassium concentration and capsaicin. Refining the cell culture protocol and research methods to suit our purposes was done during this work, so this was an iterative process.

The ECM protein coatings were studied with atomic force microscopy (AFM) contact angle measurement, fluorescent labeling and tested in use in cell cultures. They were chosen both by literature reviewing proteins suitable to neural cells and by having already been preliminarily tested in other studies in our research group and the ones used were readily available. The main characteristics of ECM protein coatings studied were thickness, coverage and hydrophilicity. One more objective was to find best ways to study biological and wet coatings with AFM.

2 THEORETICAL BACKGROUND

Studying human cells gives us understanding of diseases and healing mechanisms of human body and tissues. Making cells grow in laboratory on plastic plates and in incubators is called *in vitro* cell culturing. The cells of all kinds of living organisms can be cultured *in vitro*. Using human cells in cell culture is the best way to understand them, even though their upkeep is more expensive than using other mammalian or lower organism cells. When grown *in vitro*, cells usually need special surfaces to attach to and grow on. A bioactive surface or coating reacts biologically with cells and can also help cell differentiation. [4]

2.1 Stem cells and iPS cells

A living human has cells of over 300 different cell types, but the most important categorization is between stem cells and differentiated, mature cells. Stem cells can be further divided according to their differentiation potential. Totipotent cells of fertilized embryo are capable to grow into a full human being, differentiating into all the cell types found in adult humans. Pluripotent stem cells are almost as potent in differentiation as totipotent cell, but they lack the ability to grow into the supporting structures that embryo needs inside the womb to grow into a full human being. The pluripotent cells also have the ability to grow indefinitely while maintaining their potency. Multipotent cells can differentiate into a few cell types and have more limited self-renewal capability. Examples of multipotent cells are mesenchymal stem cells and the neural crest stem cells studied here. Unipotent stem cells have lost their self-renewal capability and only differentiate further in their own pathway. [4]

Because of their ability to grow into fully mature adult tissue, stem cells can be used for therapeutic transplantations in regenerative medicine, for screening drugs and toxicological agents or for creating developmental and disease models. Because of their great potential, much effort has been invested in optimization of stem cell culturing *in vitro*. Human embryonic stem cells (hESC) are usually cultured over a feeder cell layer, for example mouse or human fibroblasts, or more recently on biomaterials mimicking the ECM or consisting of ECM proteins. [5]

Even though hESCs have been used in research for many years, there are problems in their use. They are derived from aborted embryos, which raises controversies and ethical questions about the rights to use them for research and clinical applications. Their production and use is even prohibited in many countries. They can also have problems if used therapeutically, as their antigenicity can induce tumor growth and inflammatory reactions if transplanted into living tissue. Another problem is that embry-

onic stem cells are not disease or patient specific, so research done with them does not necessarily correlate with actual patients and health problems. [1]

In year 2007 Takahashi et al. [1] were the first to publish a defined method to produce human pluripotent stem cells from already differentiated adult skin fibroblasts. These reprogrammed cells are called induced pluripotent stem cells. The method of reprogramming is based on delivery, or transduction, of four transcription factors into the fibroblast using retroviruses. The transcription factors used in iPS cell production are Oct3/4, Sox2, Klf4 and c-Myc. These factors are genes that are active in the stem cells but not in mature differentiated cells. The cells produced this way are very similar to embryonic stem cells in characteristics used to confirm cell's pluripotency, such as morphology, proliferation, gene and protein expression and teratoma formation and many others. [1] However, there has been a call for more consistent standard of pluripotency as some iPS cell lines have passed these tests even though they have had abnormalities on their functioning. But before new standards for pluripotency are agreed on, the research will continue on the old basis. So even if many of the ethical problems are solved with iPS cells there are still other pros and cons to consider. [6]

Differentiation of cells is a process where stem cells come to be of some specific cell type, i.e. differentiate. In mature differentiated cells only the genes needed by that specific cells purpose are active and produce messenger-RNA, mRNA, which then guides the production of morphogens and proteins and the cell functionality. Other genes are inactive as proteins they code are not needed. Not all the mechanisms affecting cell differentiation are known yet. [4; 7]

The current iPS cell production is not yet suitable for clinical use, as tumor formation ability of these cells is not understood well enough and there can be detected differences between hESC and iPS in DNA microarray analysis. Also the retroviruses used to reprogram these cells might still be active in them and pose a health risk and the cells are currently considered as genetically modified organisms. So for now the iPS cells are used for creating models of cell differentiation and diseases, in screening drugs and toxicological agents, but not for therapeutics in clinical use directly. [1] And there have even been questions about reliability of toxicological assays done with iPS cells and stem cells in general compared to assays with live animals or primary cells extracted from live animals. However, iPS cells should have an upper hand over hESCs, as the genetic composition and expression is better known as the cells are from live individual, not from an aborted embryo. There has also been raised a question on do iPS cell lines from one individual have more similarities with each other in their sensitivity to chemicals than iPS lines from multiple individuals. It needs to be studied more on how iPS cells differ from each other and what actually is an iPS cell or stem cell. [6; 7]

2.2 The peripheral nervous system

The nervous system is divided into central and peripheral parts. The central nervous system (CNS) consists of brains and the spine while the peripheral nervous system consists of all the other neurons divided throughout the body, divided into afferent and efferent neurons of which the first means neurons that bring information to the brain and the latter a vice versa. Examples of efferent are somatic neurons, which are the ones a person can control voluntarily, while autonomic neurons work independently of persons will controlling inner organs, glands and smooth muscles. [4; 8]

Peripheral sensory neurons (PSN) are afferent neurons and they have important functions in transmitting information about the world around us, for example heat, pain, cold and touch are sensed by the PSN. These sensations are then transferred as neural impulses to central nervous system to be interpreted and reacted upon. Other senses such as sight, taste and smell are composed of afferent neurons as well. The dorsal root ganglion (DRG) is part of the spine, where the peripheral sensory neurons originate and come in contact with the CNS. [2; 4]

The neural axons can be myelinized or unmyelinized, meaning that the supporting Schwann cells produce a protective myelin sheath around some subtypes of PSN cell axons. The myelinization affects the signal transmission rate along the axons. Fast sense of pain is transmitted along myelinized Aδ-group neuronal fiber and slower version of pain, like inflammatory or injury sourced pain and also the sense of heat, is transmitted along the group C-fibers. [4]

Cells of human CNS have been differentiated from hESCs for some years now and their differentiation is better known than that of the peripheral cells. But the peripheral neural cells have equal importance, even though their differentiation is much less studied. Common diseases like diabetes damage the PSNs, so generating sensory neurons for preclinical studies, and perhaps later for clinical use as well, is an important matter. There are also viruses and diseases called neurocristopathies that can damage the sensory neurons or their processes, synapses and axons. [2]

2.2.1 The differentiation of peripheral neural cells and the neural crest

The peripheral sensory neurons, that are objective of this study, develop in the embryos during differentiational phase called the neural crest, which forms in the dorsal root ganglion and migrates from there in two waves. In humans this phase of development is not very well known on the cellular and molecular level, as it is present only in very young embryos, except for some special medical cases. The knowledge of neural crest development is mostly based on studies with model organisms as the human 3-5 week old embryos, where the neural crest is present, are not usually obtained from abortions as the pregnancy might not even be known at that stage. These cells differentiate into a multitude of different cell types, including myofibroblasts, melanocytes and almost all cells of peripheral nervous system, including the sympathetic and parasympathetic gan-

glia, somatic and sensory neurons and the supporting glia and Schwann cells. As the progeny of the neural crest is so diverse, there are also many clinical syndromes proposed to arise from malfunctions in the neural crest derived cells and their development. To study this phase of peripheral nervous system's differentiation and growth, a method to differentiate stem cells into multipotent neural crest stem cells, or NCSCs, is needed. And once the NCSCs can be produced *in vitro*, it will be possible to study the peripheral neural cells differentiated via this phase. [2; 4; 9]

During embryonic development, the cells divide into endo-, meso- and ectodermal germ layers and the neural crest hails from the ectodermal layer [9]. The differentiation and isolation of neural crest stem cells from hESCs *in vitro* is based on changing growth conditions and the signals directing the differentiation. It has been shown that neural crest spontaneously emerges from hESC cultures and that it can be regulated and directed with extrinsic signals. Example of which signaling molecules produce which cells is shown in Figure 2.1 [9; 10]. It was at some point under consideration, whether or not *in vitro* cultures are representative for the *in vivo* development as the culture conditions could regulate the cell in non-physiological way [11]. However, now it is widely accepted that there are reliable ways to produce NCSCs and further produce their progeny, such as the PSN. [3; 9; 10]

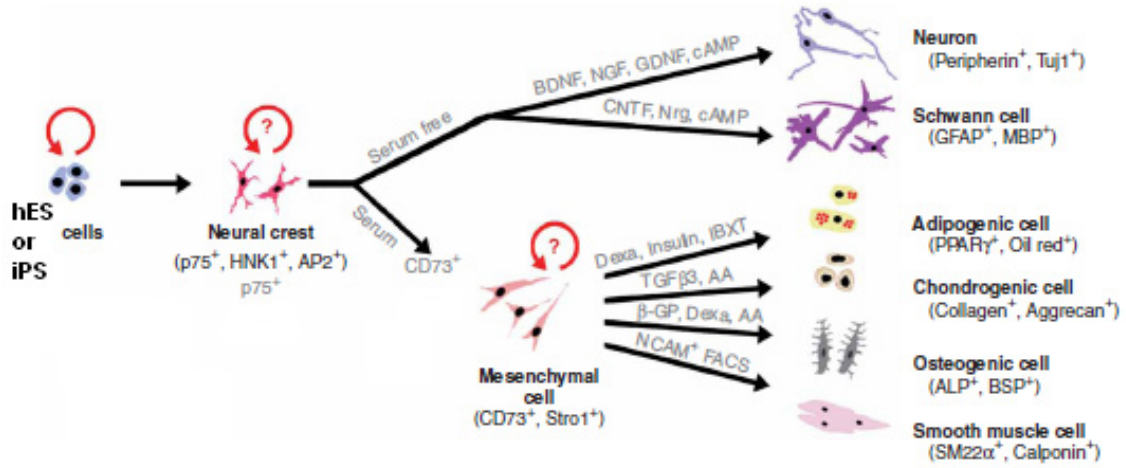

Figure 2.1: *Differentiation pathways of neural crest stem cells. Cell types and their marker proteins and growth factors affecting the differentiation listed. Modified from reference* [10].

The term sensory neurogenesis is used for the process of PSN differentiation and it is a tightly scheduled process in embryonic development [12]. Stem cells do not grow well alone, but prefer culture over a feeder cell layer and a feeder layer is also used in PSN differentiation. The so-called stromal-derived inducing activity (SDIA) was shown to induce neurons from mice and primate ESCs when co-cultured with mouse stromal cell line PA6. It had also been used to enrich neural precursors in hESC colonies, so Pomp et al. 2005 [13] were the first to use it to create human peripheral neural cells and that procedure was later developed further to create the protocols used by Pomp et al.

2008 [2] and Goldstein et al. 2010 [3] and also used this thesis. The protocol is based on mimicking the growth factors and other signals that cells receive during embryonic development. The SDIA method for peripheral neural differentiation was also the first to produce putative neural crest cells with neural crest markers such as SNAI1 (zinc finger protein), SOX9 (transcription factor SOX9) and p75 (low-affinity nerve growth factor receptor). [13] The differentiation pathway shown in Figure 2.1 is based on protocol by Lee et al. 2007 [10] and it differs from this SDIA-protocol, mainly as it requires fluorescence-activated cell sorting by flow cytometry and use of more growth factors and as the reported efficiency is not as good for the PSN cells as the SDIA-protocol, so it was not used here. [2; 10; 14]

In the SDIA-protocol the first phase of PSN differentiation is induction of hESCs to PA6 feeder cell layer where they grow into colonies positive for early universal neural markers. The colonies can be roughly divided into two categories: homogenous and heterogenous, as seen in Figure 2.2. Moving the homogenous colonies after 12 days into suspension culture makes them to grow into aggregates similar in shape as the neurospheres of CNS differentiation. The heterogenous colonies would grow into more cystic aggregates and they resemble the early embryoid bodies and in later part of culturing express endodermal markers, such as FOX2 (RNA binding protein FOX2) and GATA6 (transcription factor GATA6), which means they are wrong cells for PSN differentiation. [2; 13]

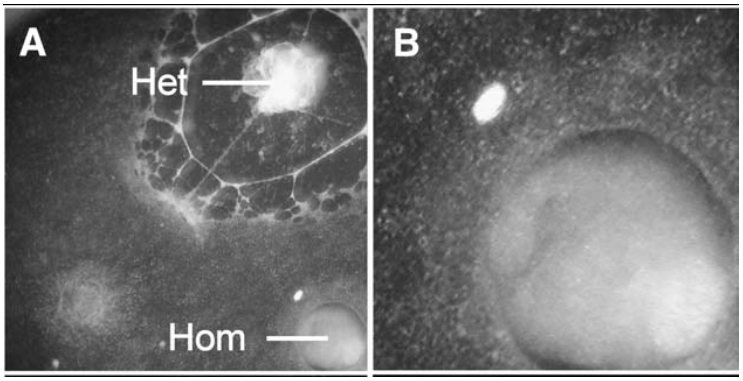

Figure 2.2: *Typical example of colonies in the first phase of the SDIA-protocol. A) Larger heterogenous and smaller homogenous colony during PA6 induction phase of PSN differentiation. B) higher magnification of the homogenous colony in A.* [2]

The neurospheres start to express markers of ectodermal origin and neural crest within one month, such as FOXA2 (forkhead box protein A2), for ectoderm and SNAI1, SOX9, MSX1 (homeobox protein MSX1), AP2 (activating protein 2), PAX3 (paired box protein PAX3) and p75 for neural crest. There is no one specific marker for only the neural crest, so the interpretation of cells as NCSCs is always based on expressing a set of neural crest marker genes, such as the ones mentioned above and the neurospheres can also express CNS markers. The propagation of differentiation in neurospheres is shown by lack of expression of hESC pluripotency markers after one month of culture. Growing the cells as neurospheres for longer time increases the yield of PSN

in the final phase of the differentiation, as they have more time to first grow into neural crest cells and only afterwards into full peripheral neurons and the schedule also follows the actual differentiation times during embryonic development. [2; 15]

The growth factors that affect neural crest development are fibroblast growth factor (FGF) and bone morphogenic proteins (BMP). Use of these growth factors significantly increases neural crest marker genes expression. [10] But it has also been tested to use BMP antagonist noggin in PSN differentiation, and this also produced putative peripheral neurons, however, the yield of PSN cells is far better without noggin. [2; 16]

The final phase of PSN differentiation is again culture over PA6 stromal layer, as the neuron inducing activity is even higher for neural crest cells compared to pluripotent cells. After replating neurospheres back to PA6 feeder layer the young neurons need neural growth factor (NGF) to grow and extend their neuronal processes with apparently 1 ng/ml concentration of NGF giving the maximal results.[2; 17] The use of different growth factors than NGF would result in differentiation to another cell type and use of NGF alone seems to cause apoptosis of CNS type cells of neurospheres, making the culture more pure in peripheral neurons. [2; 16] It was written by Pomp et al. 2008 [2] that the use of neurosphere phase increases the PSN yield from 1 % by 10-fold and the final PA6 phase increases it by a further 25 %, compared to just growing stem cells over PA6 feeder layer and using growth factors, as in continuing longer in the first phase of this protocol. [2]

But one possible problem with the SDIA-protocol is the use of feeder cells of non-human origin, which can introduce new harmful factors to the differentiation process and possible contaminations, especially if the research later advances to clinical stage. The issue of these xenogenous factors can be addressed by culturing cells in feeder-free conditions with different components of only human origin. Steps towards this were taken in this study when using the ECM protein coatings instead of PA6 feeder layer in the third phase and also testing the use of PA6 conditioned medium. The use of laminin instead of PA6 feeders is also reported to suit long time culturing of mature PSN. But the protocol used here is still far from being xenofree. [2; 14]

There are also other differentiation protocols for PSN than the one reviewed above, but most of them do not have as good efficiency, so in this study the SDIA-PSN generation method was used. Exception to this is the small molecule inhibition protocol by Chambers et al. 2012 [15], which was indeed published nine moths later than this thesis started, so it was not possible to use it here exclusively, but it can be used in later studies. That protocol is based on blocking all the irrelevant signaling pathways for developing neurons, leaving them the only option to differentiate straight to peripheral neurons, which quickens the differentiation a lot. The Wnt signaling pathway, which regulates a wide variety of differentiation pathways in the development, is a key here. [12; 15]

2.2.2 The peripheral sensory neural cells

The peripheral sensory neurons are the afferent nerve cells responding to external stimuli and transmit their information to the central nervous system. Sensory neurons can further be divided into following subtypes: cells responsive to pain or itching stimulus are called nociceptors, responsive to mechanical touch are mechanoreceptors, responsive to temperature changes are thermoreceptors and responsive to muscle movement and sensing relative position are proprioceptors. During embryonic development, nociceptors form in later part of neurogenesis, while proprioceptors and low-threshold mechanoreceptors form early [12; 18].

The morphology of PSN cells is one characteristic that can be used to identify them. Immature PSN has the bipolar morphology typical for many neurons but mature PSN cells have a unique pseudounipolar morphology, which can be seen in Figure 2.3 and Figure 2.4. It serves the purpose of receiving signals from target tissue and then conducting them to central neuron synapses while the cell body resides in dorsal root ganglion. A single axon going into peripheral terminal end splits into a branch, innervating the target tissue. [13; 18]

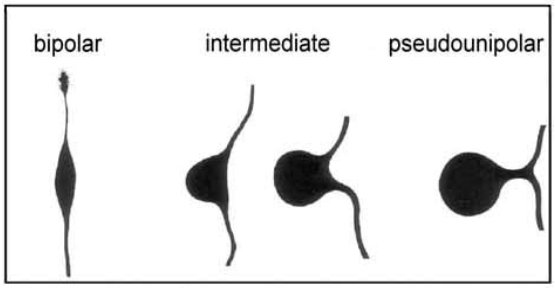

Figure 2.3: *The morphology of peripheral neurons changes during their maturation, with more immature on the left and mature on the right. Modified from reference* [13].

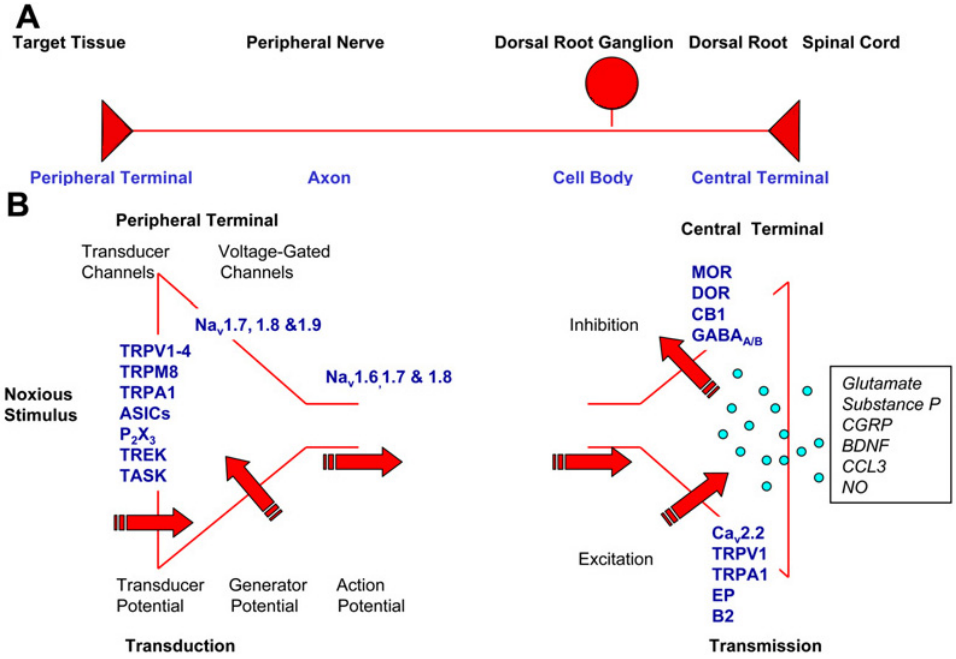

Figure 2.4: *The morphology of peripheral neuron in relation to its position in the body and functioning of PSN during nociception. Modified from reference* [18].

There is no single marker for mature peripheral sensory neuron, so their type has to be interpreted from a combination of marker proteins. The most important marker proteins for PSN are Brn3a and peripherin. If a putative cell is positive for both of these and has the PSN morphology shown above, it is considered to be a peripheral sensory neuron cell. [2; 10; 19] The cells positive for both peripherin and Brn3a usually migrate away from neurosphere clusters after plating to the third phase of differentiation. There are also universal neural markers like βIII-tubulin or Tuj1 that mark all the microtubuli of the neural cells, so PSN cells will express it as well, but it does not tell anything about subtypes of neurons. In Table 2.1 are shown protein markers of different NCSC cell progeny and in their subtypes. [13]

Table 2.1: *Marker protein or gene combinations that can be used in immunocytochemistry or PCR to identify NCSC progeny cells as being of a specific type.*

Cell type	**Marker proteins or genes**	**Reference**
Neural crest stem cell	NCAM, AP2α, p75, Sox1, Sox9, SNAI1, Ret, FOXD3	[2; 9; 10; 12; 13]
Neuroectoderm	PAX6, Sox1, Sox3	[20]
Peripheral sensory neuron (PSN)	Peripherin, Brn3a (POU4F1), Isli1, TrkC, Neurog-family	[12; 13; 15; 21--23]
Nociceptor (PSN-subtype)	TRPA1, TRPV1, TrkA, NTRK1, Neurog1, SOX10	[12; 15; 18; 24]
Proprioceptor (PSN-subtype)	Neurog2, Runx3, TrkC	[12; 15]
Mechanoreceptor (PSN-subtype)	Neurog2, TrkB, Ret	[12; 15]
Motoneuron	Islet1, Islet2, Lim3, HB9	[20]
Sympathetic neuron	TH, Peripherin	[13]
Epithelial cell	NCAM, E-cadherin	[13]
Melanocytes	MITF, Sox10	[12]
Smooth muscle cell (Myofibroblast)	SMA	[9]
Schwann cells, Glia	GFAP, MBP, Vimentin	[9; 10; 21]

The intermediate filaments form the cytoskeleton of all eukaryotic cells with microtubules and microfilaments. In the nervous system, astrocytes and neurons express intermediate filaments, but oligidendrocytes do not. The intermediate filament proteins are structurally related to lamins and keratins and the most common one of them is glial fibrillary acidic protein, or GFAP. Lamin is an intercellular and nuclear protein while laminin is an extracellular matrix protein. Peripherin is the neuronal intermediate filament protein expressed in peripheral neural cells and it is also expressed in limited brain stem and spinal cord neurons, which have projections towards peripheral structures and forming the major structure of peripheral axons. [21]

Peripherin can assemble with other neurofilament subunits or self assemble, either case it forms intermediate filament networks during embryonic growth and the expression will decrease after birth. It is also up-regulated after neural injury, likely to help axonal regeneration, but its exact function is not known as peripherin knock-out mice still grow and reproduce normally. [21; 22] The peripherin over-expression can lead to neurodegenerative diseases and neural cell death, mostly affecting motorneurons, for example, recent studies of the amyotrophic lateral sclerosis, or ALS, have shown peripherin mutations having an effect on development of the disease. [21]

Peripherin production is regulated by NGF and FGF, both growth factors used in this thesis as well, and it is a rare neuronal filament in being almost exclusive to peripheral neural systems. [25] Peripherin maybe also involved in development of diabetes mellitus as it is target autoantigen and destruction of both peripheral neurons and insulin producing islet-β cells by immune response has been shown in mice, but not yet in humans. [22] Co-expression of peripherin and Brn3a is characteristic for early sensory-like neurons, while sympathetic neurons co-express peripherin with tyroside hydroxylase, or TH, and it is considered as a more mature neurofilament marker than βIII-tubulin. The TH-peripherin co-expression also indicates sympathetic neuronal subtype and likely multipolar morphology. [2; 10; 16; 25]

The Brn3a protein belongs to the POU -gene family and as the gene coding is POU4F1 it is also sometimes called POU4F1 –protein, but in this study it is referred to as Brn3a. Its function is guiding the differentiation of neural cells and especially PSN cells and the expression is closely linked to appearance of mature sensory neurons and blocking it causes sensory neuron death. [12; 23] In addition to sensory neurons, Brn3-proteins are also expressed in retinal ganglion cells, which are specific neural cells of the eye, and where they also guide the differentiation and development. In retinal ganglion there are three Brn3 proteins expressed in close coherence, but in dorsal root ganglion the Brn3a has over 50 % higher expression than its near-identical relatives Brn3b and Brn3c, while in the brain the other two are clearly expressed and Brn3a expression is questionable and in non-neural tissues none of these are expressed. [26] In sensory neurogenesis the Brn3a is closely linked to transcription factor Islet1, their combinatory effect is needed for development as in double knock-out mice the sensory neurons fail to migrate from dorsal root and the generic neural precursors remain in undifferentiated ground state. [27]

2.3 Sensory neural cell functionality

2.3.1 Nociception and TRP -ion channels

The neurogenesis relevant to pain sensing nociceptors starts from NCSCs migrating from dorsal neural tube in quite late part of development. The earlier NCSCs form proprioceptors and low-threshold mechanoreceptors, which are the other main subtypes of sensory neurons. The high affinity NGF receptor TrkA is expressed in all newly formed embryonic nociceptors, however, all the transcription factors affecting nociceptor differentiation are not known. The Brn3a discussed in the chapter above is one of the factors required to maintain TrkA expression high, but it is not the one causing the cell fate determination in first place and it is also present in other cells. A transcription factor expressed exclusively in early nociceptors is Runx1, but its expression is also initiated some time after the TrkA expression, so it cannot be the determining factor either. [18]

Regardless of the starting factor, nociceptor development soon divides them further into peptidergic and nonpeptidergic nociceptors. These two subtypes have distinct combinations of ion channels and receptors and innervate their own target tissues. The ones that retain TrkA expression and respond to NGF become peptidergic nociceptors, while about half stops TrkA expression and start expressing glial cell-derived growth factor GDNF receptor Ret. Peptidergy means ability to use small peptides in neural signal transmission across synapses. As different sensory ion channels and receptors are expressed in partially overlapping or mutually exclusive manner and also controlled by time, the whole nociceptive neurogenesis has very complex hierarchy. [12; 18]

A distinction between sensory cell sensitivity to stimulus qualities and speed of response would be important for their full characterization. For example noxious cold and noxious heat activate different sensors, but these are both nerve fibers expressing cation ion channels from the transient receptor potential family, or TRP-family [28]. There are also other proteins related to nociception, such as the Mas-related G protein couple receptor, but the TRP-family is in focus here. [12]

An important ion channel expressed in pain sensing peripheral nerve C-fibers is called transient receptor potential ankyrin 1 (TRPA1). This is one of the channels responsible for sensing cold and there is a hypothesis that this ion channel has main role in developing symptoms called peripheral diabetic neuropathy during the disease diabetes mellitus. [24] An interesting aspect of TRP -ion channels is that in addition to heat and cold, they also react to chemicals existing in spices, such as capsaicin, mustard oil, garlic, oregano and peppermint. Of these TRPA1 reacts to cinnamon, mustard and garlic, while the primarily heat sensing vanilloid receptor 1 (TRPV1) reacts to capsaicin and to spider toxins such as inhibitor cystein knot peptides, also called vanillotoxins [18; 29]. Both TRPA and TRPV families are non-selective cat ion channels that can carry Ca^{2+}-, Na^{+}- and K^{+}-ions with varying permeability rates. An example of effect of these channels on the whole body is that tests have shown that subcutaneous injection of

capsaicin affects rat body temperature regulation causing the core body temperature to drop. While TRPV1 is essential for thermal nociception, TRPV1 null mice still react to noxious heat, even though with impaired pain behavior. The TRPA1-like channels are also identified as having some effect on mechanosensitivity on lower organisms, but there is much uncertainty in this in vertebrates. [18; 28; 30--32]

Some vanilloid nociceptors have a low response threshold, sensing even small concentrations of stimulant, like TRPV3 channel, while others only react to high and dangerous concentrations, like TRPV2 channel. Peripheral sensitization means that at a site of injury, inflammation or other continuous stimuli, many cells around PSN produce a broad range of sensitizing agents, such as enzymes and growth factors, that causes the cell's reaction threshold to lower and increases responsiveness and more molecules can now cause pain. Especially in cases where the axons are severed, spontaneous pain may arise independent of stimulus or in relation to new, innocuous stimuli, like pulsation of blood vessels. This is caused by the PSN trying to adapt to the new situation and causes permanent changes in the synapses in the dorsal root. Examples of the sensitizers are prostaglandin and bradykinin and its receptor B_1, which are present during chronic pain. The sensitizers work by binding to receptors of nociceptor membrane and activating multiple new intracellular signaling pathways and the large number of these interrelated molecules and receptors makes it difficult to selectively block and treat inflammatory pain. The successful treatment should restore the nociceptor to its normal state where only a danger to the tissue causes sense of pain and this requires understanding nociceptors in both healthy and injured states. [18]

2.3.2 Functionality studies by calcium imaging

The reason for existence of neural cells is the neural impulse that delivers the signals interpreted as sensation or other information that the neural cell has acquired from its environment. A flux of ions over the cell membrane occurs locally at the point of stimulation. This ion flux is based on a change between sodium, potassium and calcium ion concentrations inside and outside the cell through ion channels. The flux alters the membrane potential and if the stimulus is strong enough an impulse of rapidly moving change in cell membrane's electric potential, called action potential, is generated. An increased strength in stimuli is translated as higher frequency of action potentials, which in turn is perceived as stronger sensation. [4; 18; 30]

The ion flux causes the inside of cell membrane to be positively charged for a few milliseconds and outside of the membrane to be negatively charged. As the charges are reversed at rest, the flow of ions causes the surroundings of the active site to react as well when the threshold for current sensitive ion channels is reached. In normal situation the ion channels are open for only milliseconds and cannot open again immediately, so the action potential can only move in one direction, towards the brain for processing. It will also be modulated along the way by C-fibers and synapses of the dorsal root. In case of inflammatory reaction to injury or neuropathic pain the recovery phase of the channels is altered, in worst case permanently. [4; 24]

The so-called golden standard for identifying the nociceptive origin of neurons is demonstrating their functionality and appearance of neural impulses when applying noxious stimulus. The Figure 2.4 in Chapter 2.2.2 shows a schematic of the working principle of a nociceptive neuron. [18] The neural impulses and the functioning of neural cells can be studied with electrophysiology methods such as patch clamp or microelectrode array or by monitoring the calcium ion concentration changes in cells. [30]

Calcium ions are responsible for a large variety of intracellular functions and signaling, for example synaptic release of neurotransmitter molecules and second messenger signaling, gene expression, and regulating entire cell proliferation and cell death [33]. At rest a typical neuron has intracellular calcium concentration of 50-100 nM and during electrical activity this can rise inside the cell by even 100-fold very locally. [34] The TRP-channels are one of the mechanisms the neurons use for the influx of calcium, others are voltage-gated ion channels, ionotropic glutamate receptor and nicotinic acetylcholine receptor and the efflux is also affected by plasma membrane calcium ATPase and the sodium-calcium exchanger. [15; 30; 33]

The calcium imaging method is based on dyeing the cell with fluorescent calcium indicators such as quin-2, fura-2 and fluo-4, which respond to changes in calcium concentration by changing the intensity of fluorescence. Of these, fura-2 is particularly used for quantitative calcium measurements as the reactions are strong and the signal rationing can be obtained from excitation wavelengths during binding of calcium. [33; 35] The chemical reaction of fura-2 molecule chelating with Ca^{2+}-ion is shown in Figure 2.5. The fura-2 molecule is excitable by UV-light and its emission peak is between 505 nm and 520 nm and the binding of calcium causes conformational change that leads to changes in emitted fluorescence. Fura-2 is an example of a ratiometric dye, as it changes its emission in response to calcium, allowing the concentration of calcium to be determined from the ratio of fluorescence emission of 340 nm and 380 nm wavelengths and independently of the intracellular dye concentration, exposure time and many other factors. Because of the reactions with dye and Ca^{2+}-ions due to calcium buffering, the intracellular calcium dynamics do change a little after addition of the dye. So using the appropriate dye and concentration is important for reliable results. [33; 36]

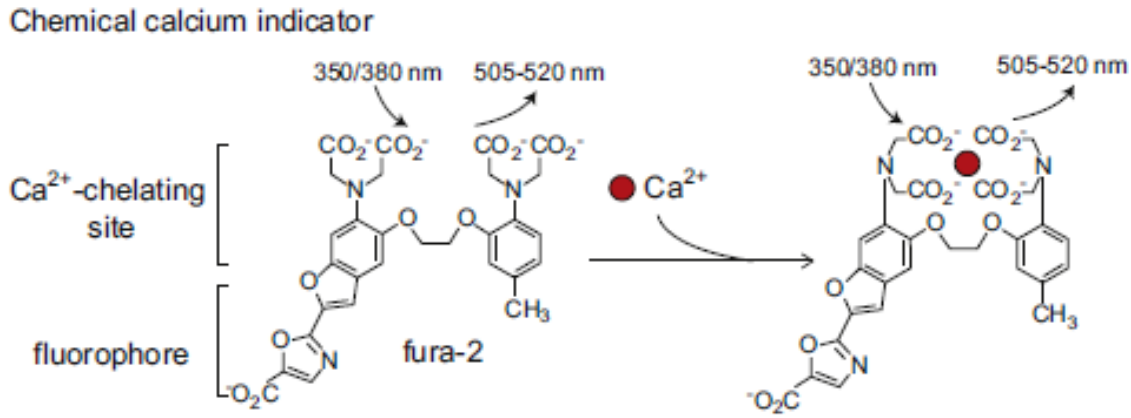

Figure 2.5: *The fluorescent chemical reaction of fura-2 reacting with Ca^{2+}-ion. Modified from reference* [33].

During the imaging, a CCD camera synchronized with UV-light source and real time DSP control unit is used to track and measure fluorescence of cells and record them on video on computer [37]. The cells are activated by changing the ion concentration of perfusion liquid or by addition of chemicals in perfusion. The cells are seen brighter as they fire action potentials as their calcium ion channels release calcium outside when reacting to changes in their environment. [36]

There are many possibilities for the liquid used in perfusion as it could be any physiological buffer or cell culture medium, except that if it has autofluorescent or colored molecules it causes problems. A good choice for perfusion for neuronal cells is Tyrodes solution, which mimics the cerebrospinal fluid found inside brain and spinal chord. When the Tyrodes solution is modified by changing NaCl and KCl concentrations while staying iso-osmolaric, the cell membranes are depolarized and ratio of fluorescence emissions changes. This reaction to potassium concentration shows that the cells are putative functioning neurons as fibroblasts and other random by-products of differentiation do not react to potassium. [18; 36]

Capsaicin, or 8-methyl-N-vanillyl-6-noneamide, is the active component of chili, which causes the burning sensation when a person eats chili. It is a lipophilic vanilloid compound and along with compounds structurally related to it, such as resinferatoxin and the antagonist capsazepine, it reacts with the vanilloid receptor TRPV1 of the peripheral terminal of PSN. [31] The chemical structures of capsaicin and its related molecules are shown in Figure 2.6.

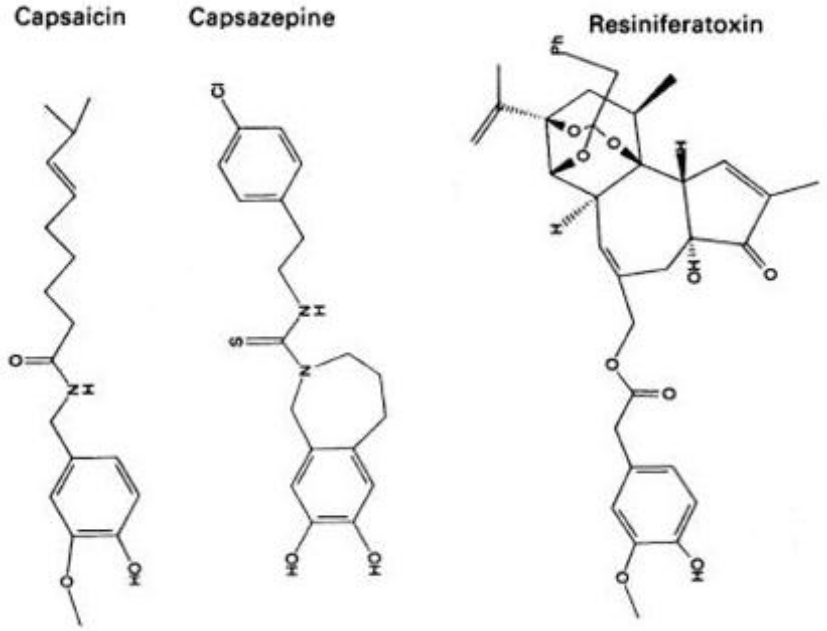

Figure 2.6: *The chemical structures of capsaicin, its antagonist capsazepine and a related biomolecule resinferatoxin. Modified from reference* [38].

When capsaicin reacts with the TRPV1 channel, it lets sodium and calcium ions pass inside the cell membrane and potassium ions to leave the cell. This causes a cascade of events that leads to firing of action potential and also to flashing fluorescence in calcium imaging. By human or other mammals this would be perceived as burning pain, as the same receptor reacts to noxious temperatures of over 47 °C and also reacts to protons of acids in pH below 5. But it seems that mammals are the only animals able to react to capsaicin and having the TRPV1 receptors. Capsaicin can also be used for desensitization of neurons, which is an important aspect when considering use of capsaicin in medicine as analgesic. [31; 32]

In calcium imaging, capsaicin is used to visualize the nociceptive functionality by addition of capsaicin to the perfusion liquid. Addition of capsaicin for a short time induces a robust response in case of pure nociceptive neurons and this is also important method of showing that differentiated cells are in fact C-fiber-like cells. Example of this is shown in Figure 2.7. The capsaicin response peak can either go up-and-down fast or have a fast rise and a prolonged decay. [39]

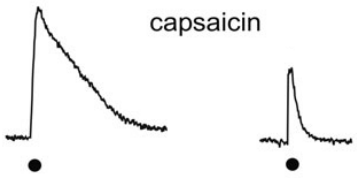

Figure 2.7: *Two example fluorescent ratio graphs of mouse nociceptive neurons reacting to capsaicin. Left is recorded from cell that only reacted to capsaicin and right is from a cell that reacted to ATP-sensitive agonist as well as to capsaicin. Modified from source* [39].

Usually in case of *in vitro* differentiated neurons the amount of capsaicin responsive cells in calcium imaging is merely a few per cents. Even with neural cultures isolated from animals, the responsiveness to capsaicin in calcium imaging is well under 50 % of whole population. [15] If the neurons have been segregated well enough from live rats, the responsiveness to capsaicin by DRG neurons has been as high as 90 % of culture [40]. Increase of capsaicin concentration also increases the amount of responsive cells, but too high concentrations cause the desensitization and cell death. The cells that do react should have a robust peak in fluorescence ratios and when a cell reacts to both potassium concentration change and capsaicin, they are C-fiber like neuronal cells. [15; 24; 28; 40]

2.4 Use of extracellular matrix proteins in cell culturing

Whether cells are cultured *in vitro* or growing as part of living human tissue *in vivo*, they are highly sensitive to their environment. Cells get continuous feedback signals from their surrounding extracellular matrix (ECM) which has part in directing their actions, such as differentiation, protein production and even apoptosis. The ECM is a complex mixture of collagen and other glycoproteins, proteoglycans, matrix metalloproteinases and other biomolecules bound to these. [41] The characteristics affecting cells are mostly in micro- and nanoscale and the nanoscale engineering of surfaces for tissue engineering is a more and more sought after goal and beginning to be a reality to some extend. [42] In addition to cell adhesion and support, ECM also has role in regulating growth factor signaling, as growth factors are bound to the ECM proteins and then possibly attached to their specific receptors in cells as well or they can be released from the ECM enzymatically. [43]

Many *in vitro* cell culture protocols require cells to attach in culture well bottom and this is acquired by coating culture wells with ECM proteins or with just the cell receptor binding parts of proteins called peptides or with biomimetic materials with similar structure to natural ECM proteins. In a more clinically relevant viewpoint, the attachment of first proteins and then cells to a surface gives information about material biocompatibility *in vivo* and the research of these topics can give information on how to make medical implants more suitable to their applications. [43] The most well known motif cellular receptors recognize is the combination of three amino acids called RGD sequence, short for arginine-glycine-aspartic acid peptide sequence. This short peptide is found in ECM proteins fibronectin, vitronectin and collagen. The incorporation of this peptide alone can make a non-adhesive surface into adhesive for cells, or it can even make a material biodegradable if integrated in the bulk material structure. As the large protein will fold randomly over a surface and the cell attachment sites might no be available for cells, the smaller RGD peptides are more likely to be in right position and to work better. Smaller molecules are also cheaper to synthesize compared to larger ones. [44] Other ECM proteins have other peptides for attaching and one cell has many receptors for different amino acid sequences. But as the ECM proteins are multifunctional, having only the binding peptide on a surface might not have same effect as the whole protein would. The signaling pathways usually have multiple components, so for cell being bound to a right combination of ECM proteins and receptors receiving right growth factor cocktail means inducing specific differentiation cascade or some other effect. [42; 44]

In addition to biological activity of the surface molecules, the ECM coating will also form nano- and micrometer scale topographical features. Grooves, ridges, nanofibers and other features and their possible symmetry all affect cell behavior, proliferation, motility, protein production and cell's own shape and orientation can change to adapt on the surface it is attached to. [42] Especially in case of coatings thicker than one molecule layer the mechanical characteristics come to play important role as well. When the

coating gets thick enough, it can be considered a gel and its elasticity starts to affect cell behavior and especially motility and growth of appendages inside the gel. This is becoming more and more important in tissue engineering with the goal to grow cells in 3D shapes. [45] Different cell types have each other their own requirements for ECM coatings both biochemically and physically, so it would be important to find the right kind of combination of all these characteristics to have optimal cell culture results. This also means that conclusions on coating's success in general cannot be drawn from just one study with one cell type. The ideal coating or scaffold would have both suitable biochemical activity and physical characteristics, including topography, and all these should be controllable in nanoscale. And to use this ideally functional material to greatest benefit, it is also needed to understand what all the different signaling pathways of cells actually react to it. [42; 45]

Cell culture *in vitro* has for now been mostly done on 2D surface. However, it is widely accepted that culture on a 3D environment in a gel or scaffold would be needed for more representative cell culturing results. The cells in living tissue usually have signals and interactions with surroundings all around in 3D. The added dimension would help to see cell proliferation, morphology and migration that could not be seen in 2D surface, where cells only get support and certain signals from one side. Most importantly, the goal of tissue engineering is at some point the ability to transfer the cell cultures and scaffolds inside human body, where the cells have to function in 3D environment. [46; 47] One answer for this problem is hydrogels, which are three-dimensional polymer networks cross-linked to form highly porous structure. Being highly hydrophilic, they have very high water uptake which also causes swelling of the gels and multiplication of the gel volume. However, they do retain the network structure intact even when dried. [45] Hydrogels made of ECM proteins are the closest thing to actual *in vivo* cell environment that can be achieved. But currently there are no methods good enough to produce hydrogel *in vitro* that would resemble the actual living tissue environment. And even if biochemically the gel would be good enough, the mechanical properties have proven to be difficult to set. The gel can have too low strength, as in case of collagen hydrogel [43], have too harsh gelation conditions for cells to survive or it can be too thick for cells to migrate and grow their processes through it. Currently the best possibility seems to be functionalizing the gels by covalently bonding ECM proteins or their peptides into the bulk or on surfaces. There are a lot of studies going on about how to produce the perfect hydrogel for cells to grow in and what are all the properties that affect cell behavior inside a gel. [42; 45]

Other possibilities for creating 3D cell culture environment are rigid scaffolds or microparticles. The architecture of scaffolds can vary a lot as they can be porous structures, interwoven fibers or some other regular or irregular shapes. And of course fibers or particles can also be combined with hydrogels to make composite structures with desired properties. All of these scaffolds can be made from polymers, but at least microparticles for bone applications are also made from ceramic materials such as hydroxyapatite and bioactive glass. [42]

2.4.1 Attachment of extracellular matrix proteins on surfaces

When material is immersed in liquid containing cells, whether it is the bottom of cell culture plate or biomaterial implant inside the body, there will always be three major stages of interaction at the surface. First the smallest molecules, which mean water, will touch the surface in nanoseconds and likely wet it. The surface tension and hydrophilicity play a great role in what kind of shell the water molecules will make over the surface. If the surface is very reactive, it can dissociate the water molecules and will be covered with OH-groups, or be hydroxylated. A surface that does not dissociate water molecules, but still binds them more strongly than hydrogen bonds of ice, is also a hydorphilic surface. On a hydrophobic surface the bond between surface and water molecule is weaker than the hydrogen bond of ice and it is said that water does not wet this kind of surface. This ability to wet the surface can be studied with contact angle measurements. On hydrophobic surfaces the proteins adsorb more irreversibly and have tendency to denature, while too hydrophilic surfaces may inhibit protein adsorption. And then there is also the electric charge of the surface and the topography, which have roles in the attachment. [47--49]

The second phase of interaction is with the larger molecules in the liquid, usually proteins but also all kinds of other molecules. Water soluble biomolecules have always also water molecules attached to them and most of the interaction is between these two water layers. The surface influences the proteins via water molecules and this will define how the protein reacts to the surface, the protein can denature, fold, attach or orientate itself in a new way. On a very hydrophilic surface, the proteins attach via their hydrophilic parts and on hydrophobic surfaces via more hydrophobic parts of their structure. In a slightly larger scale the proteins can form a uniform coverage of the surface or just remain in isolated clumps attaching mostly on other proteins or even not attach to the surface at all. [47; 48]

Finally the third phase of interaction is between cells and the surface, which actually means interaction between cells and surface attached proteins and water molecules. At this stage for example the cells receptors can finally bind to the RGD peptide and attach the cell firmly on the surface. This whole interaction cascade is illustrated in Figure 2.8 for a hydrophilic surface and it is essentially the same whether it is the coating of a cell culture well or on top of a biomaterial implant. [47; 48] Some people also include in the cell spreading as fourth phase of interaction, where the cell cytoskeleton reassembles to accommodate to being in contact with the surface. [50]

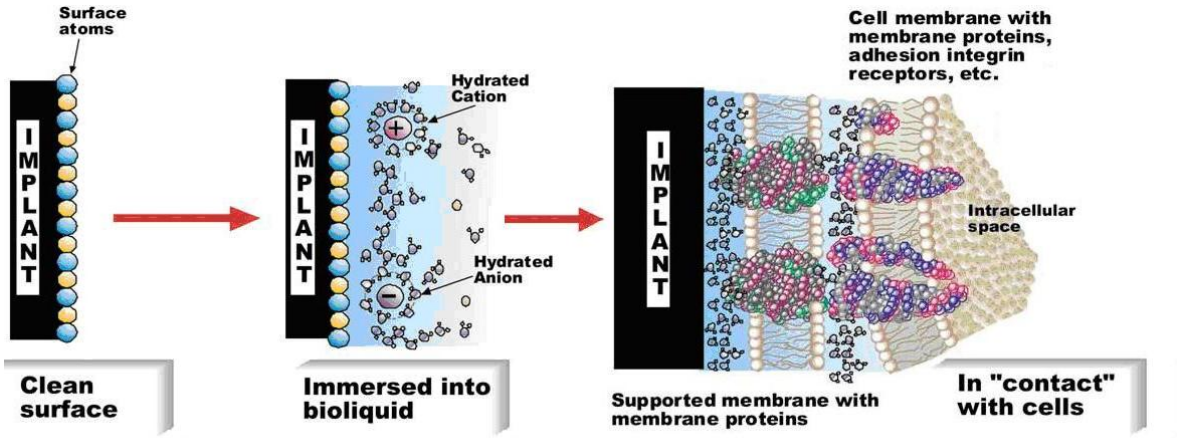

Figure 2.8: *The three stages of cell attachment on biomaterial surface. First water wets the surface, then proteins attach to it and cover it and finally cell will attach to the surface attached proteins. Modified from reference* [47].

When deliberately coating a surface, the ECM protein coating can be based on different chemical or physical reactions, depending on what is the wanted outcome. When the protein attaches itself on a surface, usually it is adsorbed irreversibly and will stay put on the surface, instead of absorbing and gradually moving inside the bulk of the material. The exact reaction during adsorption depends of surface material, or substrate, and type of protein involved, but it can be based on van der Waals interactions, polar and charged groups of the molecules, surface energy, hydrogen bonding and hydrophobic interactions. These determine the protein containing liquids ability to wet the surface, then the adsorption kinetics, the strength of the bonds and the folding of the protein. [44; 47] Depending on the case, the proteins can adsorb as isolated units, or as monolayer or as an even higher layered structures and they can unfold their own 3D-structure and denature in the process or they can stay more intact and be still active, which is usually what is wanted. If the substrate of protein attachment is rigid solid like glass, the penetration depth of the coating can be in the scale of few nanometers, while in case of some polymers capable of swelling in water and more porous microstructure, the depth can be micrometers or more. [50]

Whether creating coatings or nanoscale scaffolds, one more option is the bottom-to-top approach of self-assembly of protein layers, for which a large variety of techniques has been studied. For example layer-by-layer self-assembly can give a high degree of control over coating layer thickness compared to conventional coating but of course the protocol has many more steps and is more laborious than conventional method, where the substrate is just treated with coating liquid, incubated for a while and then removing the extra liquid. However, as this method is easy to use in laboratories and suitable also for 3D structures, it is a good choice. And when studying just the coatings and protein assembly without cell culture part, researchers often use silicon wafer as substrate, which might be inconvenient for cell applications. [42; 51--54]

The kinetics of protein adsorption is also important as the energy state in which the protein is after adsorption, is usually a metastable state, but not the permanent lowest energy state. For example in higher protein concentration of coating liquid the molecules have less time to unfold independently on the surface as there are more of them. In lower concentration there is more time for the slow structural changes without neighboring molecules preventing them physically, as shown in Figure 2.9. This can affect the biological functionality in either way, depending on how the active sites remain reachable to cells due to protein folding. The metastability of adsorption also means that at some point the adsorbed proteins can detach, or desorpt, from the surface, if conditions change to favor a lower energy state. Understanding all this leads in practice to determining the coating protocol's protein concentration and incubation times. [44; 47; 55]

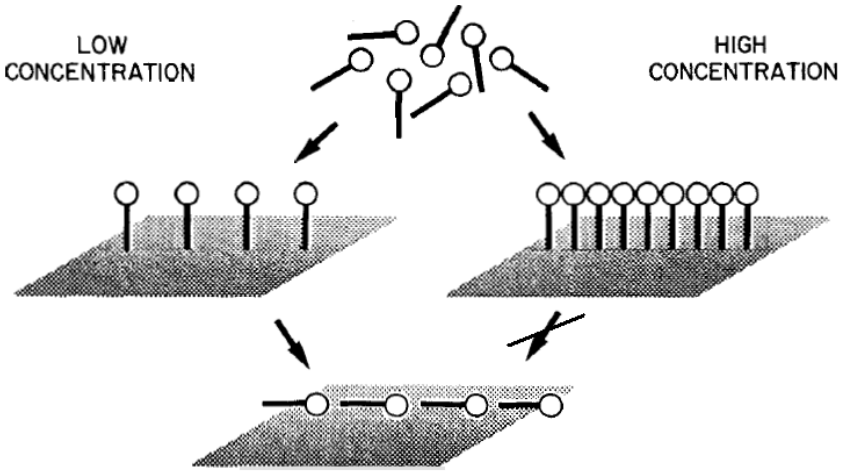

Figure 2.9: *Schematic on how the concentration affects protein adsorption on surfaces, preventing further folding after initial adsorption at high concentrations. Modified from reference* [55].

The standard coating material for cell culture in our laboratory is gelatin, which is a modified version of ECM protein collagen [52]. The gelatin is produced from mammalian bone and hide or from fish skin by thermal hydrolysis. It is a polypeptide with gelling and melting temperature below +35 °C and used a lot in food and pharmaceutical industry as well as in cell culturing and regenerative medicine research. In cell culturing it is usually used at 0.1 % concentration, when it produces a thin, rather uniform layer with some globular aggregates present throughout the coated surface. [56] Cells adhere well on this kind of gelatin coating and it does not interfere with their differentiation as many ECM proteins do [57]. In concentrations higher than 1 % gelatin will form a gel and have a fibrillar structure. The exact structure and topography of gelatin coating is difficult to examine and visualize, as the soft, wet gel will lose some of its characteristics when dried and for example will easily change its shape when imaged with atomic force microscopy. [52; 56; 58]

2.4.2 Extracellular matrix of peripheral neural cells

As the peripheral neural tissue is mostly composed of neurons and Schwann cells surrounding their axons, the extracellular matrix of peripheral neural tissue is different for example from the ECM of bone tissue or epithelium, which has a lot more ECM around the cells. [59] In addition to supporting the cells and the other usual functions, the ECM of nervous system has important role in the pathfinding of axons. [41] There is also a tight interrelation between neural cells and supporting Schwann cells, as these need contact with axons to proliferate, and axons need Schwann cells to grow and regenerate. [59] The ECM proteins mostly involved in development and regeneration of peripheral nervous system are laminin, fibronectin, collagen, thrombospondin, tenascin, agrin and many proteoglycans, like perlecan and versican. Of these, laminin and fibronectin are reviewed more closely in the next chapters, as they have most functions for peripheral nerves and they are the most studied ECM proteins after collagen. In addition to the ones listed above, there are two major glycoproteins as structural parts of the myelin sheath, named myelin-associated glycoprotein MAG and myelin protein zero P0, and these are composed of immunoglobulin-like domains. A schematic picture of the molecular structure of some important ECM proteins is presented in Figure 2.10. [41; 59]

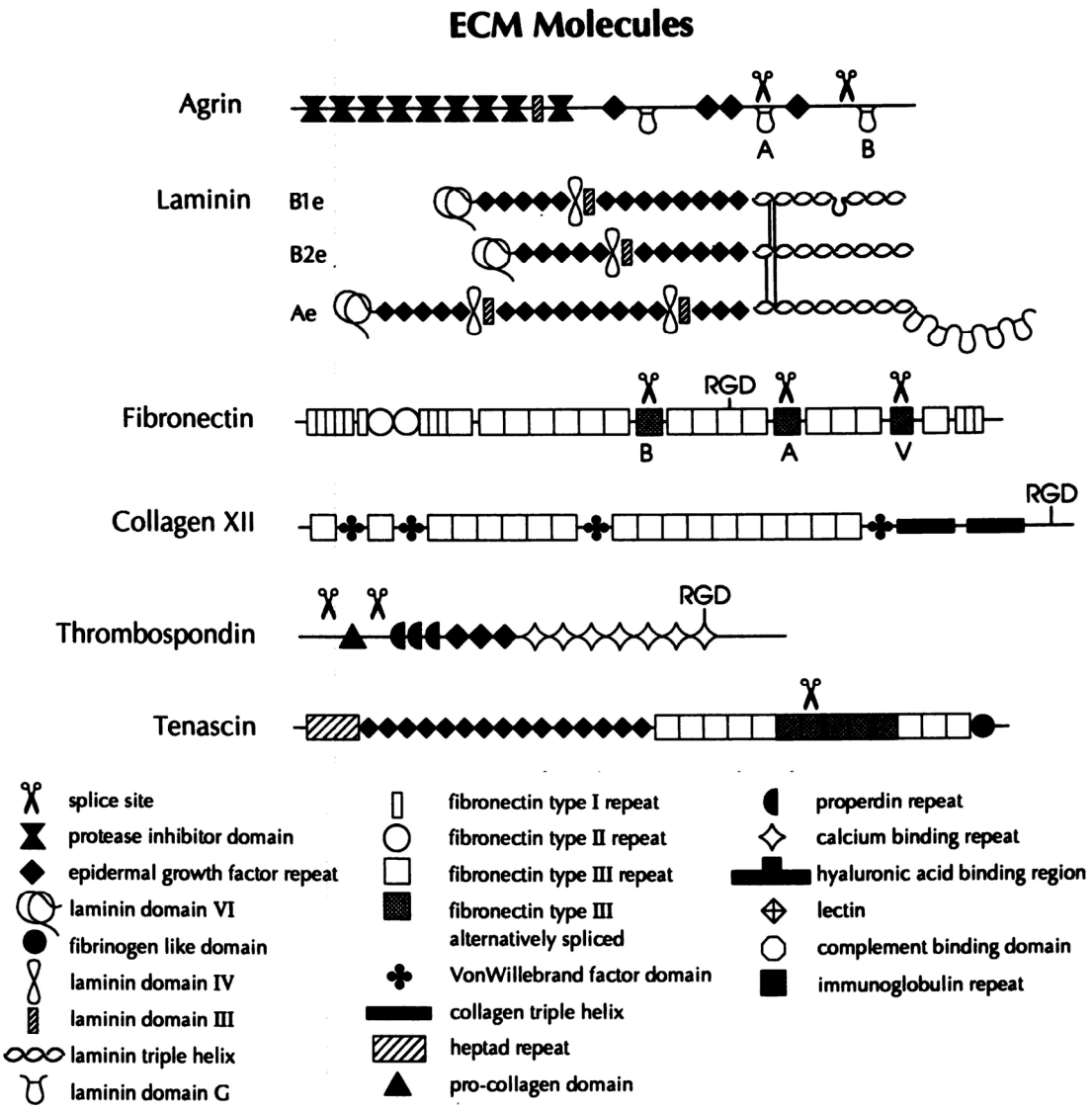

Figure 2.10: *A schematic of most important ECM proteins for neural ECM and their building blocks. Notice the repetition of several subunits and the RGD-peptide in many different molecule types. The laminin is not shown here in its characteristic cruciform shape and the tenascin consists of six out-stretched parts similar to one shown here tied to a central node. Modified from reference* [41].

Collagens are a large family of ECM proteins found in all parts of the human body and a major structural component of all ECM. Collagen IV seems to have most effect on the nervous system, as it is found in basal lamina, along developing neural crest, in the spinal cord, in the endoneurial basal lamina of peripheral nerves, at neuromuscular junctions and in the brain as well. The collagens I and IV have been shown to promote neurite outgrowth *in vitro* and the less studied collagen XII is present in the embryonic neural tube. [41] Collagen is studied a lot and many of its forms can be produced and purified from animal and human tissue. It can be made into hydrogel or a more densely packed structure and in tissue engineering it is mostly used for bone and cartilage tissue, or it can be modified further into gelatin. [43]

Thrombospondin is an ECM protein with four closely related isoforms. In general, thrombospondin is mostly found in adult tissue where cells are actively proliferating and migrating, but in nervous system it is found around embryonic central and peripheral neurons. It has a functional role in neural crest cell migration and general neurite outgrowth. It can also bind and form complexes with transforming growth factor β, or TGF-β, which is a very important growth factor for many cell types. [41]

Tenascins are a family of three ECM proteins with chemical composition slightly varying between vertebrate species. Tenascin has widespread expression in different tissues and in nervous system it is mostly expressed in migration pathways of neural crest cells, pathways of peripheral nerves and in embryonic CNS. They are very large molecules, consisting of six arms in so called hexabrachion structure. It seems to have important role in inhibiting adhesion to fibronectin-containing ECM and thus affect cell migration. It is hypothesized that tenascin prevents axons and cells from leaving the myelin sheath of a nerve. They also seem to have some role in wound healing and neovascularization, but the exact mechanisms are unknown. However, as the functions seem to be more about guidance than support, tenascin is not suitable coating material for cell culture on its own, but could be important in tissue engineering at some point for directing axonal growth in regeneration. [41; 60]

Agrin is a more limited type of protein, specifically produced by motor neurons and it is found at least in muscles, brain and kidney and their associated neurons. It seems to be essential for formation and regeneration of neuromuscular synapses. But it does have other functions in other tissue-types as well. For peripheral sensory neurons the agrin does not seem to have a specific function. [41]

2.4.3 Laminin

Laminins are a family of ECM proteins with multidomain structure built from three polypeptide chains. They were first found by Timpl et al. 1979 [61] from the epithelial basement membrane in close contact with collagen type-IV and was recognized as structurally important component of the ECM. There was a simplification to their nomenclature in article by Aumailley et al. 2005 [62]. Before the simplification, laminins were named either according to the order of discovery or rather inconsistently by the polypeptide chains as A-, B1- and B2-chains or with Greek letters in front of the number. [62; 63] Now their parts are consistently named with Greek letters as α-, β- and γ-chains accompanied with a number, telling the exact chain composition if needed to know and also guiding the naming of smaller units and domains of the molecule. For example laminin-111 and laminin-α1β1γ1 is the same thing and an even shorter version of the name is just laminin-1. [62]

The tertiary structure of a laminin molecule is very interesting as the globular and rod-like domains are extended in four arms from a middle point, forming a cruciform shape, which helps to reach distant binding sites on different cells and ECM molecules. For laminin-1 the size of this shape is around 36-48 nm for the shorter arms and 77 nm

for the longer one and it does retain its shape even in dissolutions, which has been proven by hydrodynamic measurements. Pictures of this shape can be taken with rotary shadowing technique in scanning electron microscopy and an example is shown in Figure 2.11a. The Figure 2.11b shows a schematic view of laminin structure and the most important parts repeated here as the previous Figure 2.10 does not show the cruciform shape. [63]

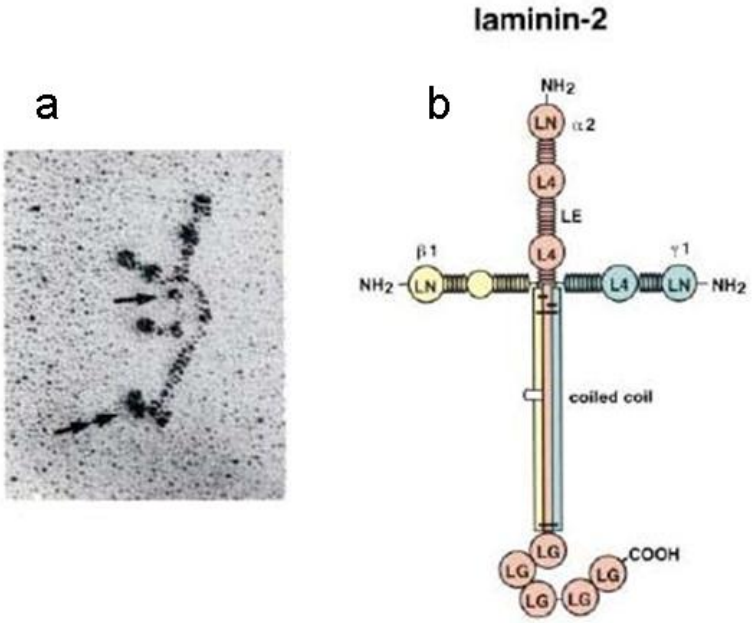

Figure 2.11: *On the left an electron micrograph produced with rotary shadowing technique of the laminin-1 molecule with bent cruciform shape. On the right a schematic of laminin-2 cruciform molecule, with different molecular domains shown in different colors. Combined and modified from references* [63; 64].

The laminins have many important functions: they bind skeletal muscle's actin cytoskeleton to other ECM, they bind agrin in neuro-muscular junctions, they have several EGF-like repeat units in the structure working like growth factors and they also polymerizes into sheets that form networks with collagen and then account for the mechanical properties of the basement membrane. [64] Laminin has even been called the most bioactive components of the basement membrane [65]. The two most important peptide sequences of laminin for cell attachment and neurite outgrowth are named IKVAV (isoleucine-lysine-valine-alanine-valine) and LQVQLSIR (leucine-glutamine-valine-glutamine-leucine-serine-isoleucine-arginine), but it has also been found that the cell binding and neurite growth functions can be separated by modifying the laminin with or without glycosylation. Different laminin isoforms are expressed more in different tissues and at different parts of development with mostly laminin-2, or laminin-211, present around muscle and nerve cells, laminin-3, or laminin-121, in neuromuscular junctions and laminin-4, or laminin-221, in Scwann cells and skeletal muscles and others in non-neural tissues. So laminin-2, also sometimes called merosin, is the main form of laminin in peripheral nervous system. [66]

In non-neural tissues, such as blood vessels and epithelium, the laminins form the highly structured basement membrane but in developing nervous system it is much less organized. In nervous system laminin is associated with neuronal and glial cells and axon tracts and in peripheral with the Scwann cell's own basement membrane. In higher vertebrates laminin is not expressed in adult CNS. [67]

For promoting the neurite outgrowth and extension, laminin-2 seems to be the most effective ECM molecule and it is up-regulated in case of nerve injury. The growing or regenerating nerve end has so-called growth cone on its tip, where most of the action occurs. Laminin, fibronectin and collagen are all present in the growth cone, but laminin is the best at promoting the growth at the very tip of the cone, while the others have greater degree of contact with cells. The growth cone cells have extensions called filopodia to search for the best growth route. The choice of ECM growth substrate the cone makes seems to depend on the order it reaches the ECM substrates. It has also been demonstrated that laminin concentration does not affect the behavior, so as long as laminin is present, it allows the growth of neurite, but it does not bind the neurite permanently or have problems with over-expression. Even though it is possible for neurites to detach from laminin, it does reduce the filopodia retractions as it reacts with the cell surface drawing cell organelles to the filopodia and thus making it less likely to turn back from the growth route. [59; 66] But while laminin-2 has major function in neurite outgrowth, laminin-3 has been proposed to work as inhibitory agent for motoneuron growth as it affects and promotes the formation of neuromuscular junctions. [67]

The laminin use in this thesis is laminin-α1β1γ1 or just laminin-1 that is produced in pure form relatively easily in Engleberth-Holm-Swarm mice tumor and is commercially available. It is the first laminin isoform found and the most studied one. No human version of this exact isoform is available in large scale and the human laminins commercially available are isolated from placenta or made with recombinant technology and are more expensive than laminin-1. It is possible and even likely that functions reported with laminin-1 are not relevant to all other isoforms. [68; 69] In humans, laminin-1 is mostly present in developing embryo and in some rare cell types [67]. But besides these differences, laminin-1 coating is also used for long time culture by Pomp et al. who also published the differentiation protocol for this thesis [2].

2.4.4 Fibronectin

Fibronectins are glycoproteins of the ECM found in most tissues and have been called the most important non-collagenous protein for mechanical properties of the ECM. The fibronectin molecules have more subtle changes between themselves than laminins and they are usually all just called fibronectin without distinguishing the slightly different molecular domains. The molecular structure is asymmetric, elongated and flexible shape of two identical subunits, or monomers, consisting of smaller and compact globular domains. [70] The globular domains have been named fibronectin modules F1, F2 and F3, with very little else than alternating sequence of these modules builds up the whole

molecule. Some of these same modules have later been found in other ECM proteins as well, as was shown in Figure 2.10 and here in Figure 2.12 are shown the numbering of fibronectin modules for later reference. [71]

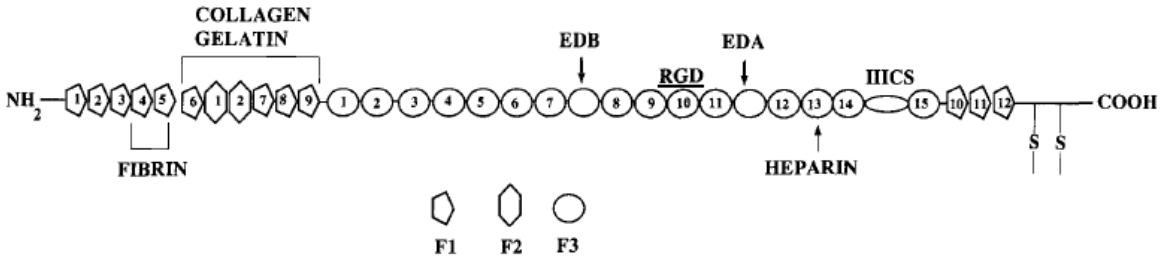

Figure 2.12: *A schematic of one monomer of fibronectin modular structure. Different repeating modules of F1, F2 and F3 have been numbered and the non-consistent modules are also marked. One very important aspect for cell binding is the RGD-peptide in 10th F3 module. Modified from reference* [71].

The fibronectin modules can function as individual fragments of varying sizes as long as they can fold in the right shape over a surface or in liquid. For example, the fragment from 7th F3 module to 10th F3 module is very important fragment for cell binding as it folds by expose the RGD-peptide as an easily reachable loop for other molecules or cells. [71; 72]

The fragment from 6th F1 module to 9th F1 module as it is the collagen and gelatin binding site, which means that cells attaching to gelatin coating probably use this fragment of fibronectin for attachment and the formation of ECM as whole is linked to this fragment. [71] And also many other molecules of the neural ECM have fibronectin F3 repeats in their structure having functional roles. [59]. The size of fibronectin protein is more difficult to measure than size of laminin, as fibronectin in elongated state forms a very easily extended fiber and it can be difficult to ascertain when a single molecule is at its full length. The approximate length of a fibronectin fiber is in the scale of tens of micrometers and the diameter is around 3 μm. The fibers can endure even 700 % strain and still return to normal elastically. [73] In globular form the dimensions of one fibronectin molecule are around 15-100 nm diameter and few nanometers in height. [74] An elongated fibronectin molecule on polystyrene surface has been measured by SEM to be 130 nm long [75]. So the size of fibronectin molecule greatly depends on the measuring conditions and protein unfolding.

In the human body, fibronectin is found in two main forms, the cold insoluble globular form found mostly in plasma and lesser amounts in other body fluids and the cellular fibronectin in fibrillar form that is found in basement membrane and soft connective tissues. Some examples of cell types synthesizing fibronectin are fibroblasts, endothelial cells, chondrocytes, macrophages, hepatocytes, and all the early embryonic tissues. [70] In neural tissues fibronectin is present in the ECM and plays a role in neuronal cell migration and regeneration. In peripheral nervous system it is expressed along neural crest migration and neurite outgrowth, as stated in Chapter 2.4.3. As fibronectin expression is up-regulated after nerve injury, it is needed in the growth cone because of high cellular

adhesivity to fibronectin, even though laminin is more important for the actual guidance of neurites. Experiments have shown that dorsal root ganglion neurons are heterogenous in their preference for laminin or fibronectin when given the possibility to grow on either one in alternating parallel coated surfaces *in vitro*. This means that laminin and fibronectin patterns guide the neurite outgrowth during development *in vivo*. [66]

The adsorption of fibronectin coating on a polystyrene surface is as much dependant on fibronectin concentration as on surface hydrophilicity, meaning that there are multiple ways for a protein to attach to a surface and fold while attaching. Comparison of two polystyrene surfaces, of which one was treated to be hydrophilic and the other being untreated and hydrophobic, showed that at low concentration more fibronectin adsorbs to the hydrophobic surface, but at higher concentrations the adsorption densities are similar. However, testing mammalian cell spreading showed far more effectivity on the hydrophilic surface even though the protein density on the surface was far lower. This is explained by the orientational changes in adsorbed fibronectin molecule and thus different amounts of reachable binding sites. The adsorption on hydrophobic surfaces is also pH independent while on hydrophilic surfaces it is pH dependent. The bond on hydrophobic surface is also stronger than on hydrophilic surface and as would be expected, desorption is faster from hydrophilic than hydrophobic surface, so the underlying chemical reactions are different. [55] As fibronectin assumes the elongated form when on polystyrene substrate, it can be assumed that the coating is actually a composition of random elongated fibers. [75]

2.4.5 Matrigel™

Matrigel™ is one of the commercial names used for basement membrane extracted protein cocktail that is usable as a surface for cell culture. Other names for Matrigel™ are Cultrex™ and EHS matrix. It forms a 3D gel in +37 °C temperature by physical cross-linking and is easily soluble below that temperature. Matrigel™ was found and is produced in Engelberth-Holm-Swarm mouse tumors as these tumors have abundance of basement membrane while normally the membrane is so thin that it is very difficult to study. The tumor consists of many different biomolecules, with highest concentrations being the ECM proteins laminin-1, collagen type-IV, perlecan and enactin and the laminin-1 used in this thesis is further extracted from here. Composition also includes proteases, growth factors such as EGF, FGF and TGF-β and other proteins. This tumor is good for the basement membrane production as it grows rapidly, is benign and simple to obtain in relatively large quantities. The large amount of different bioactive components means that the various mechanisms and responses of cells to Matrigel™ are not yet understood fully. Matrigels™ of different compositions are available, as it can be produced in a growth factor reduced form or the amount of collagen type-IV can also be increased by manipulating the diet of mice where the EHS tumors are produced. [76]

In cell culture, Matrigel™ is very bioactive growth surface, which initiates the differentiation of many different cell types. The first cells used in culture with Matrigel™

were neural crest cells from chicken embryos, which showed very good outgrowth ability on this material [77]. It has also been shown that Matrigel™ promotes myelin formation of DRG cells and differentiation of Schwann cells, so it is a favorable growth surface for neural cell applications. Other examples of the effect it has on cells are capillary formation of endothelial cells, gland-like structures produced by epithelial cells, cartilage formation of chondrocytes and can also be used with larger tissue explants. Matrigel™ has been used to replace xenogenous feeder cells in hESC cultures, so it can be also used to make the cells remain in pluripotent state. Since the first studies with neural crest cells, Matrigel™ has been used with many different stem cells and it for example affects the differentiation and maturation of cardiomyocytes. [76; 78]

The physical characteristics of Matrigel™ have been studied along the bioactive ones. For example, it has been used as model and reference for the topographical features of corneal epithelial basement membrane. The topographical features such as elevations, pores and fibers of Matrigel™ have dimensions roughly from 50 nm to 200 nm, studied by SEM and AFM. [79] The mechanical properties of Matrigel™ have also been studied by the force spectroscopy mode of AFM with elastic modulus being from 400 to 1 000 kPa, which resembles the elastic modulus of the softer tissues of body. As typical to Matrigel™ in general, this also has great lot-to-lot variations and the stiffness was also shown to vary with temperature. [80] A recent study by Koch et al. 2012 [81]claims that this is the stiffness range, which is good for peripheral neurons to grow on but also significantly larger than where CNS neurons like to grow. [81]

2.5 ECM protein coating characterization

The physical characteristics of a surface can have as big role in cellular response as bioactivity has. In practice, many conventional coating methods produce an undefined coating layer and if the coating works well, it might be produced the same way every time, but the real reason why it works is not known. Typical example of this kind of coating procedure are the ones used in this thesis as well, where the coating is just produced by applying an ECM protein containing liquid on top of a surface and incubated for certain time to allow adsorption of proteins. This way there is no control or knowledge on how much proteins there actually are attached to the surface, which is why the coatings were studied in this thesis. On the other hand, when self-assembling, nanostructured surfaces are produced, they are monitored carefully, to be able to control the self-assembly. [49; 54]

2.5.1 Methods for protein characterization

As the physical characteristics of protein coatings are being viewed as more and more important aspects, there is a need for techniques to study them. Many of the characterization tools and methods usable here belong to the field of physics called surface science. But when studying biologically altered surfaces, the ultra-high vacuum commonly used with surface science methods can also be a limiting and unwanted factor. As proteins are fragile and denature easily, the methods need either sophisticated sample preparation, such as freeze drying, or need to work at wet conditions and preferably at +37 °C temperature. Here are some examples of methods usable for studying proteins, their attachment and protein coatings, but this is not a complete review of this subject. The two methods used in this thesis are reviewed in more detail in Chapters 2.5.3 and 2.5.4. [45; 47; 54]

One much used technique for studying protein adsorption kinetics is dissipative quartz crystal microbalance, or QCM-D, which is based on measuring the frequency shifts of a piezoelectric quartz crystal sensor oscillating in an externally applied electric field. The small additions of mass and changes in viscosity when proteins are added on the crystal are the measured variables. This is an accurate method and suitable for all proteins. The QCM-D would actually be a useful technique for many of the studies conducted in our laboratory. [48; 49]

A group of techniques used to study proteins adsorbed on surfaces in surface science are surface spectroscopies such as x-ray photoelectron spectroscopy, or XPS, Auger electron spectroscopy, or AES, time-of-flight ion mass spectrometry, or ToF-SIMS, and of course the scanning electron microscopy or SEM [82]. These methods are usually used for studying interactions of single molecules on the sample surface and not for entire coated surfaces. All these are very surface sensitive methods with penetration depths from a few atoms to nanometers and micrometers for SEM. The ECM proteins

can be too complex molecules for these methods, as a common example is studying dissociation of CO_2 molecules on metallic surface. Organic molecule on organic surface can be difficult for these due to similar electronic and atomic structures. [47; 49; 82]

The rotary shadowing technique in SEM is a method primarily for studying sizes and shapes of larger proteins. The basis of this technique is spraying dilute protein-glycerol mixture on mica substrate, evaporating the liquid and then coating the substrate by platinum evaporated on it. As the sample is rotated during platinum coating, the molecules are covered evenly with platinum and are visible in SEM. The advantage of this technique is that it can reveal small details in very large molecules while still also showing the full structure. This however is not very usable for characterizing ECM protein coatings as the scale is larger than individual molecules and the mica substrate is not used in cell cultures, so the protein adsorption behavior can be different. [22]

2.5.2 Fluorescent labeling

Fluorescent labeling of ECM protein coatings is a good way of visualizing the otherwise invisibly thin and transparent protein layers and also studying them qualitatively. It is basically using immunocytochemistry on coatings without cells. As a basic characterization method, fluorescent labeling first of all gives the information if the protein coating has attached to surface at all or not. As the labeling is based on antibodies, it means that if coating is labeled, it is also bioactive. If antibodies cannot attach to the coating neither can the cells. With colorimetric assays and fluorimetric measurement devices this method could even be used quantitatively, similar to Ca-imaging measurements. [54] Another labeling possibility is radiolabeling, where some of the hydrogens of the protein are changed for radioactive ^{3}H-isotopes and then their activity is measured by radioactivity counting. This could be used to verify protein concentrations is solution or on surface after coating. [83; 84]

Fluorescent resonance energy transfer, or FRET, is one technique actually usable for studying whole coated surfaces. It is based on modifying the ECM proteins by addition of fluorophores that emit fluorescent light. This emission changes as cells attach to the coating, or as molecules are stretched. Combining with laser scanning microscopy the forces cells exert to surroundings and adhesion stiffness can be studied with this technique. It can also be used to study the intermolecular deformation of proteins under stretching and this has been used for example to study how the RGD peptide is exposed in adsorbed fibronectin molecule. [45; 73]

2.5.3 Atomic force microscopy

Scanning probe techniques are ways of studying micro- or nanoscale surfaces with a probe moving close to the surface. In scanning tunneling microscopy, or STM, an electron flow from a tip to the surface and back is maintained to receive information on the sample. Combining STM and XPS equipment creates possibilities to study metallic surfaces in nanoscale and even atom-by-atom interactions and crystal lattice defects. The

information that can be gained by STM includes Ångström-scale topography, electrical state of surface atoms or molecules via adsorption or dissociation. However, this technique usually requires a vacuum where to operate, if not studying gas adsorption on the surface. Usually a thin metal film is needed to coat the biomolecules studied, which means the limitation are same as with SEM. And the protein coatings are in a notch larger scale than what this surface science technique is meant for. [85]

The better technique for samples not suitable for high vacuum, such as biological ones, like proteins, is atomic force microscopy (AFM). In atomic force microscopy the sample surface is scanned by actually touching or tapping by a fine tip. The tip is attached to a cantilever that responds to height changes and is monitored by laser diode and photodetector. This then creates the topographical map of the surface. The AFM working principle with most important parts is shown in Figure 2.13. Piezoelectric ceramics are used to move either the sample or the tip with high precision in 3D. The scanning is done in feedback loop when moving during the scan the bending of cantilever remains constant in order to maintain constant force. Then the up-and-down motion is recorded as the sample topography. As there is no transfer of electrons required for AFM imaging, it can be performed in liquid, which is a major benefit comparing to electron microscopies and many other vacuum requiring techniques. [45; 49; 86]

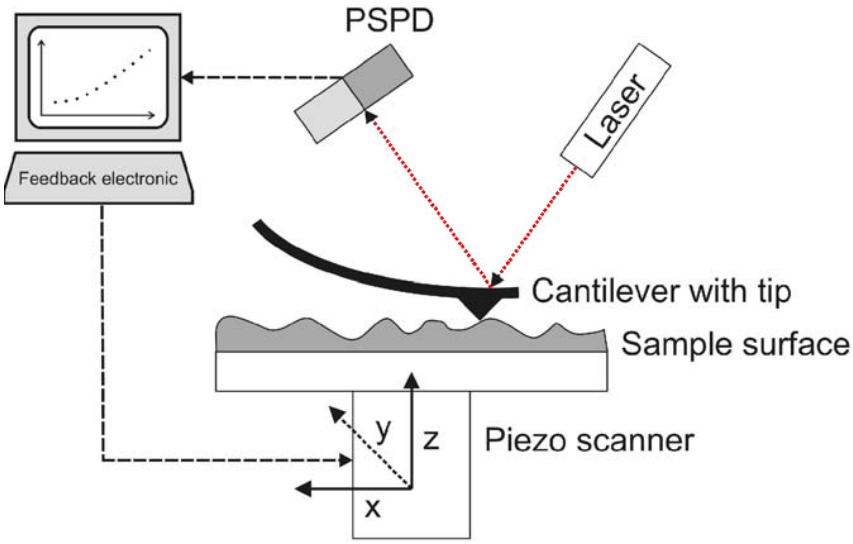

Figure 2.13: *Schematic operation principle of atomic force microscope. Modified from reference* [45].

There are three main modes used in AFM called contact mode, non-contact mode and tapping mode and the names are pretty self-explanatory. The contact mode is usually only used for hard samples while the other two are better suited for soft and biological ones. The modes where tip is not in direct contact with the surface are achieved by oscillating the cantilever at near-resonant frequency with piezoelectric actuator. The oscillation is reduced when the tip is very close to the sample and this reduction is oscillation amplitude then becomes the feedback signal usable for measuring surface topography. The use of tapping mode in liquid is challenging because of viscous damping

effects. The tapping and non-contact modes also lose some lateral resolution compared to contact mode, but the vertical height measurements are identical.[86]

The properties of cantilever tip such as spring constant and chemical stability have a affect the scanning results a lot and different materials are used for tips to scan different surfaces, aluminum or silicon nitride tip being kind of general and cheap alternatives. Another possibility is immuno-AFM, where the tip is coated with antibodies and the interactions between the tip and the surface are studied more specifically. Example of this molecular recognition mapping is coating the tip with biotin and having streptavidin patterns microprinted on the sample surface and as these two biomolecules bind well to each others, the streptavidin pattern on the surface is discerned from the spots where the tip binds to the surface. This technique could be used even further in studying protein mechanics. [87; 88]

Atomic force microscopy can also be used for applications where no actual scanning and imaging is required, when the AFM tip is used as a sensitive force sensor. The benefit here is gaining quantitative information of the sample instead of just pictures for qualitative assessment. [88] This is one of the best and most used methods to study mechanical properties of ECM coatings and is also used for hydrogels. The loading force is calculated from deflection and spring constant of the cantilever. This can then be translated into Young's modulus of the material by fitting the force-indentation-curve into the Hertz model which describes the elastic deformation of two spherical surfaces under load. Other properties possible to study with AFM related to force mapping are friction and adhesion and the strength needed to puncture through a cell membrane. [45; 86]

Combining AFM with fluorescent microscope is not uncommon and this combination can reveal new information on many biological samples. This is especially usable for cell samples that can be processed and labeled immunocytochemically and then studied with both techniques at once. The microscope light source just needs to be under of the sample, so that it does not interfere with the laser in AFM. For example this technique has been used to study the cytoskeleton of cardiomyocytes. [86; 89]

A study of different cell fixatives by Moloney et al. 2004 [90] showed that 4 % paraformaldehyde is the best fixation method for AFM studies of fibroblast cells, leaving the least imaging artefacts. One other possible fixative is glutaraldehyde. It is also used as coupling agent when covalently bonding proteins on surfaces to make them bioactive, usually in addition to other reagents and can be used as fixative for cells as well. It has been used as fixative for studying Matrigel™ with AFM, but glutaraldehyde fixed surfaces tend to have more debris than paraformaldehyde fixed ones. [49; 79; 90; 91]

The ECM proteins have been studied in AFM to some degree before, but the focus has been on single proteins and usually only one protein has been studied in one study. In Figure 2.14 is a compilation of AFM reference images of the coatings used in this thesis as well. The scanned area and magnification of the image greatly affect on how the ECM proteins look like and as the areas shown in Figure 2.14 are not very large, it is difficult to know how representative these are of the whole. In the gelatin image the spherical aggregates are easy to see and the study by Yang and Wang 2009 [58] was the

only one of references to have many enough AFM images to make a more complete view of the gelatin coating. The others would have been good to see in a view with larger scanned area. The reference images here also have coating concentrations as close to ones used in this thesis as possible. [58; 79; 92--94]

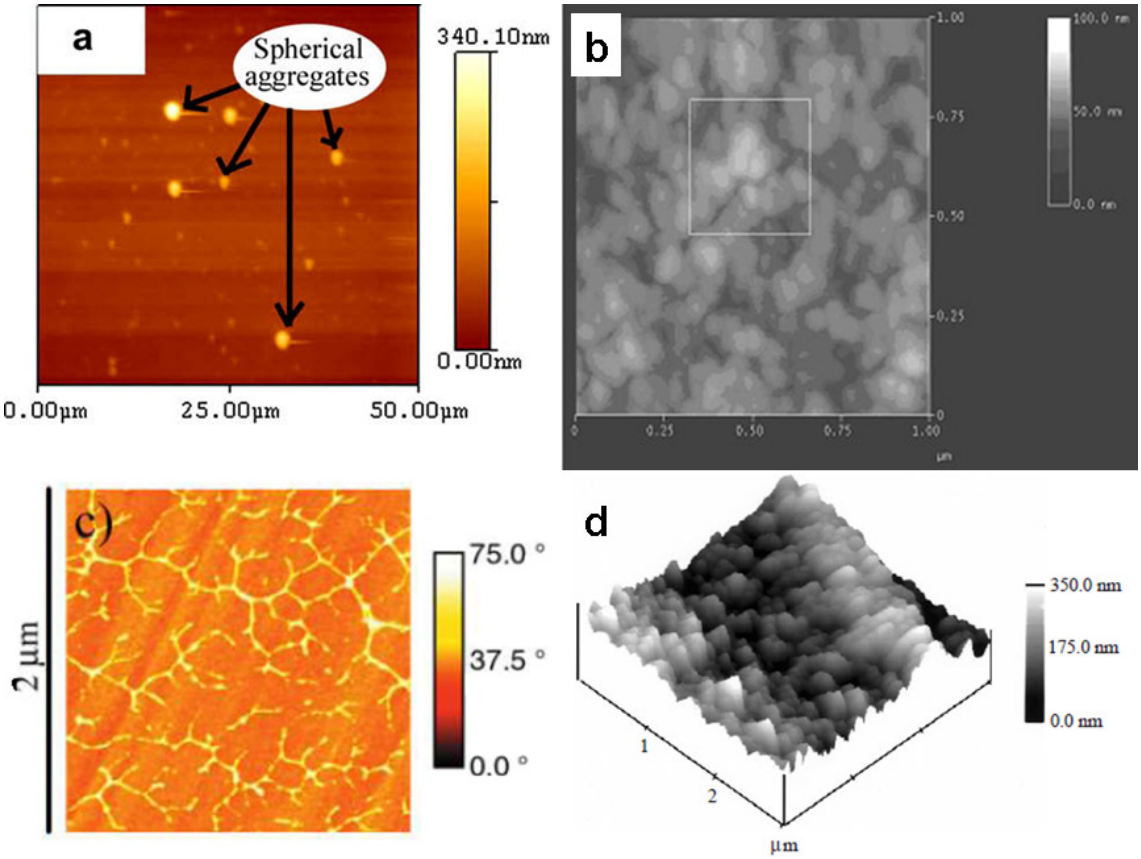

Figure 2.14: *Reference AFM images of the four ECM protein coatings studied in this thesis. A) 50x50 µm scanned are image of 1 % gelatin coating showing spherical aggregates and smoother surface* [58]. *B) 1x1 µm scanned area on laminin coating from 100 µg/ml concentration showing many round features and the molecules have attached on top of each others* [93]. *C) 2x2 µm scanned area of fibronectin coating from 3,3 µg/ml concentration* [94]. *D) 3x3 µm scanned area of Matrigel™, 1:1 dilution from stock and fixation with glutaraldehyde* [79].

As a conclusion, the unique capabilities of AFM for biomedical research are imaging of biological samples with even submolecular resolution, imaging under physiological conditions, measurement of mechanical properties and intermolecular forces with nanometer-scale spatial resolution and studying even dynamics of biomolecules and living cells. It is a very diverse technique usable in multidisciplinary research. AFM is also just robust enough to have been used in measuring protein coating thicknesses and could be used to study cells on the surfaces as well. [20; 49; 86]

2.5.4 Contact angle measurement

The contact angle measurement is a method to study the interface between a liquid and a solid, hence the name. It is used to quantitatively study the wetting, free energy and thermodynamics of the surface. The angles can be measured either for static liquid drops or for moving drops, if dynamic characteristics of the surface are studied. In the basic measurement system, a drop of liquid is administered on the solid sample surface. An interface is formed between the solid and liquid phases and the atmospheric gas phase and the angle between these phases is then recorded with high performance camera and measured via software. The different possibilities of the drop shape and the contact angles are shown in Figure 2.15 with indications of hydrophobicity or hydrophilicity. [95; 96]

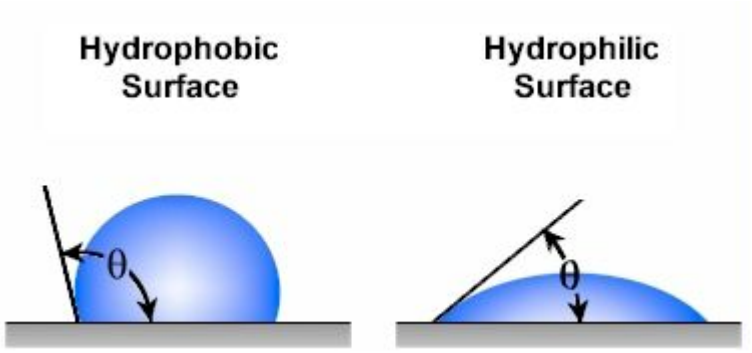

Figure 2.15: *Contact angle possibilities, θ angle of over 90° means that the sample surface is hydrophobic and less than 90° means hydrophilic. Modified from reference* [95].

The measurements are done with a camera on the level of the surface and then analyzing the pictures with computer. It should be noted that the measurement liquid can be something else than water, in which case hydrophobicity or –philicity is not the correct term, however, they are used here in the absence of better terms like 'medium-philicity'. Nevertheless, if the contact angle is less than 90**°,** the liquid can wet the surface and angle of zero indicates complete wetting. [95; 96; 96]

In the beginning of Chapter 2.4.1 are reviewed the effects the surface hydrophilicity has on protein attachment. The concepts of hydrophilicity and hydrophobicity are directly linked to the binding strength of water molecules to the studied surface, which is reflected into the contact angle of the water droplets. There has been controversialities on how hydrophilic or –phobic a surface should be for optimal cell and protein attachment, but so far the conclusion seems to be that very hydrophilic and very hydrophobic surfaces are the worst and close to 90° angels are good, depending on the exact cells, surfaces and proteins. It should also be kept in mind that temperature, humidity and the quality of water affect the measurements. [49; 54]

Use of contact angle measurement in characterizing ECM coatings has been done for example by Choi et al. 2012 [97] who measured first the angle on non-coated surface and then the coated surface and saw that it had changed from hydrophobic to hydrophilic, so the coating had been successful. Modification of surface by organic func-

tional groups is also seen in contact angle, as for example OH-groups make the surface hydrophilic and CH_3-groups clearly hydrophobic [98]. Measuring contact angles with varying pH buffered solutions can also be used to determine the surface pKa value, or acid dissociation constant, and then used to optimize the reagents for covalently bonding proteins on the surface. When comparing to most surface science methods, contact angle measurements are fast and easy to do, even though the results only tell about changes in hydrophilicity and not about exact protein orientations or dynamics, sometimes this kind of simpler characterization is needed. [54]

3 MATERIALS AND METHODS

All cell culture work was done in IBT Heart group laboratory, under laminar flow hood and cell culture plates were kept in incubator at +37 °C with atmospheric CO_2 concentration 5 %. All cell culture work was done as sterile as possible to avoid contaminations that could cause harm to these cells or others stored in the same incubator. A total of 13 batches of stem cells were differentiated during this thesis.

3.1 Cell culturing and differentiation protocol

The cell lines used in this thesis were human induced pluripotent cell lines UTA.00112, H7 (human embryonic stem cell line, WiCell Research Institute, USA), UTA.05208 and UTA.05105, of which the last two are fully produced by the Heart group and the first two are commercially available lines. The feeder cell line used was PA6 mouse bone marrow-derived stromal cell line (RIKEN Cell Bank, Tsukuba, Japan) [99] and same as used in the data by Pomp et al. 2008 [2; 3]. Most of the differentiation experiments were done with UTA.00112 cell line.

The used differentiation protocol was obtained from Pomp et al. 2008 and Goldstein et al. 2010 [2; 3]. The culture of stem cells before differentiation is not of concern here. To start a new batch of differentiation the stem cell colonies were mechanically separated from their mouse fibroblast feeder cells by scraping with the tip of pipette, treated with 1 ml collagenase IV per well with 5 minutes incubation in +37 °C. The colonies were then rinsed with cell culture medium. About 20 µl of generated suspension, approximately 60 000 cells, was used per cell culture well and transferred to new plate. The first phase of differentiation towards peripheral neurons was done in Induction medium. Induction phase culturing was as co-culture with 95 % confluent PA6 feeder cell layer in 6-well cell culture plates with 0.1 % gelatin coating. Medium was changed three times a week but the first change was done four days after plating to ensure cell attachment. The compositions of all the used mediums are shown in Table 3.1 and the producers of reagents are listed in Appendix 1. [3]

The PA6 feeder cell layer was plated in the cell culture wells, in PA6 medium, at least a day before adding undifferentiated iPS or hES cells. PA6 cells used as feeders were growth inactivated by irradiation and stored in liquid nitrogen -freezer. PA6 cells were produced for experiments by growing them on their own in gelatin coated 75 cm^2 cell culture flasks in PA6-medium and irradiated and frozen as a larger batch. PA6 cell cultures in flasks were also used for generating conditioned medium. [3]

Table 3.1: *Compositions of used differentiation mediums listed by differentiation phase.*

PA6 medium		**Induction medium (1st)**	
base	KO-DMEM	base	GMEM (BHK-21)
10 %	Fetal bovine serum	10 %	Knock-out serum replacement
0.1 mM	Non-essential amino acids	0.1 mM	Non-essential amino acids
2 mM	Glutamax	2 mM	Glutamax
0.25ml	Penicillin/Streptomycin	1 mM	Na-pyruvate
		1 mM	Penicillin/Streptomycin
		0.1 mM	β-mercaptoethanol
Neurosphere medium (2nd)		**DRG medium (3rd)**	
base	DMEM/F12	base	DMEM/F12
1 %	B27-supplement	1 %	B27-supplement
2 mM	Glutamax	2 mM	Glutamax
1 mM	Penicillin/Streptomycin	1 mM	Penicillin/Streptomycin
20 ng/ml	Basic fibroblast growth factor	10 ng/ml	Neural growth factor (NGF)

After 12 days in Induction medium, cell colonies with distinct round and solid shape were visible. These colonies were cut off with microsurgical scalpel under microscope and moved to low-cell bind 12-well culture plate. This second phase of differentiation protocol was called Neurosphere phase and it used Neurosphere medium. Cell suspension was around 20 spheres per 1 ml medium and medium was changed twice a week. Neurospheres were cut into smaller pieces every week, to keep their diameter roughly less than one millimeter so the cells inside the sphere will not die because of too slow nutrient diffusion. Cutting neurospheres was done with microsurgical scalpel and micro lancet needle, under microscope in laminar flow hood. The cells were cultured in this phase for four to eight weeks. [3]

The third phase of differentiation was called DRG-phase, from dorsal root ganglion. The neurospheres were moved to this phase by first dissociating them with trypsin for 5-10 minutes in +37 °C. Then they were rinsed first in trypsin and then trypsin was neutralized with DRG medium and rinsing was continued. When the spheres had clearly started to dissociate and clusters of a few cell were visible besides the spheres and individual cells were visible in the suspension, they were moved to the final plates. In DRG phase the cells were cultured either over PA6 feeder layer with gelatin coating same way as in Induction phase or without PA6 cells on the three studied ECM protein coatings: laminin, fibronectin or Matrigel ™. The protocol for these coatings is explained in detail in Chapter 3.3.1. Medium was changed twice a week. NGF was added to new medium right before the medium change as it does not stay active in the refrigerated medium. When culturing cells without PA6 feeder layer, we also tested if conditioning the DRG medium first with PA6 cells has effect on cells growing without the feeder layer. [3]

3.2 Cell characterization

3.2.1 Phase contrast microscopy

The cells were observed during and throughout the whole differentiation process using light microscope (Olympus IX51, Olympus Corporation, Tokyo, Japan). Cell morphologies during different phases were observed and micrographs were taken. Another light microscope inside laminar flow hood was used when performing the parts of cell culturing that needed microscopic precision. In the DRG phase cells were monitored almost daily to see the changes in morphology. Cell morphologies were used in induction and neurosphere phases to sort out which cells are moved to later phases and which are removed.

3.2.2 Immunocytochemistry

Mature DRG cells were fixed and stained by double fluorescence protocol. Cell culture wells were first drained empty of medium, then washed two times with phosphate buffere saline (PBS) solution for five minutes. The fixation was done with 4 % paraformaldehyde (PFA) solution, incubated in room temperature for 20 minutes, under laminar flow hood. The PFA was then drained and wells were washed by PBS, first for five minutes and after last wash PBS was left in the wells and the plates were stored in +4 °C.

Immunostaining was done either right after fixation or after cold storage. In staining wells were first treated with blocking solution containing 10 % normal donkey serum, 0.1 % Triton-X 100, 1 % bovine serum albumin in PBS, incubated for 45 minutes in room temperature with a shaker, as were all other incubations if not stated otherwise. Then wells were washed briefly with solution similar to blocking except for concentration of normal donkey serum is only 1 %. The same solution was used as base in mixture of primary antibodies. Concentrations of primary antibodies were optimized between consequent cell batches. Used concentrations are shown in Table 3.2. All primary antibodies used in this study are from abcam® (Cambridge, UK) and secondary antibodies from Molecular Probes® (Invitrogen, USA) After applying the primary antibodies the plates were stored overnight in +4 °C over a shaker and handled light protected.

Table 3.2: *Used primary and secondary antibodies, their concentrations and sources.*

Primary antibodies:	**Tested concentration range**	**Concentration with best results**	**Source**
Anti-Peripherin	1:800-1:200	1:400	Rabbit
Anti-Brn3a	1:160-1:50	1:80	Mouse
Anti-TRPA1	1:500-1:250	1:250	Mouse
Secondary antibodies :	**Concentration**	**Source**	
Antirabbit Alexa flour 488 IgG	1:800	Donkey	
Antimouse Alexa flour 568 IgG	1:800	Goat	

The primary antibody solution was washed away by washing three times with 1 % bovine serum albumine in PBS solution for 5 minutes. Secondary antibodies were applied in solution with same composition as previous wash. The used secondary antibodies were Alexa 488 IgG donkey, anti-rabbit and Alexa 568 IgG goat, anti-mouse, listed in Table 3.2. Both were used at 1:800 dilutions and one hour incubation. Then wells were washed first three times with PBS for 5 minutes and then two times with phosphate buffer without saline for 5 minutes. Lastly wells were aspired dry and VECTASHIELD® (Vector Laboboratories, USA) with DAPI dye for nuclei staining and cell mounting was applied with a cover slip on top. After staining the plates were stored at +4 °C for up to a few months.

The immunostaining results were studied using fluorescence microscope (Olympus IX51 fluor, Olympus Corporation, Tokyo, Japan) and pictures were taken and combined with DP Manager and DP Controller software (Olympus Corporation, Tokyo, Japan).

3.2.3 RT-PCR

The gene expression of the differentiating cells was studied by reverse transcriptase-polymerase chain reaction (RT-PCR) and gel electrophoresis. The cell samples were collected in the following time points: at the start of induction phase, at the end of induction phase, once every week of neurosphere phase at the same time as cutting the spheres and at the end of DRG-phase. Cell samples were collected by lysing cells in microcentrifuge tube with RA1-buffer supplemented with β-mercaptoethanol according to NucleoSpin® -protocol. The mRNA was isolated and purified from samples using NucleoSpin® RNA II –kit (Macherey-Nagel, Germany) and NucleoSpin®-protocol. The RNA concentration of samples after isolation was measured with Nanodrop spectrophotometer (ND-1000, Technologies Inc., USA). Both the lysed cell samples and the isolated RNA samples were stored in -80 °C.

The RNA was converted to complementary DNA, or cDNA, using high capacity cDNA kit (High Capacity cDNA RT-kit, Applied Biosystems Inc, USA). The cDNA reaction reagents were compiled into a master mix and the sample volumes were 10 µl master mix plus 10 µl lysed cell sample. The RNA-cDNA thermal conversion was done with the PCR device (Mastercycler Personal 5332, Eppendorf, Germany) with the following program: 25 °C 10 min, 37 °C 120 min, 85 °C 5 min and then to the final temperature of 4 °C. The cDNA can be stored at -20 °C.

In the actual polymerase chain reaction step the master mix was made from DyNAzyme™ II reaction mixture (DNA Polymerase Kit, Finnzymes, Finland). The gene primers used were peripherin, Brn3a, TRPA1, p75, SNAI1, SOX9, NTRK1 and AP2a. GAPDH was used as a housekeeping gene to confirm that the reaction is successful and RNA is present. The sample volume was 1-5 µl, depending on RNA concentration. The PCR device program for this step was: first 94 °C 2 min, then 40 cycles of 94 °C 30 s, annealing temperature of 52-62 °C depending on primers, 72 °C 1 min and in the end 72 °C 10 min and finally cooled to 4 °C.

The results were studied with gel electrophoresis. The gel used was 1,5 % agarose gel, made from TBE buffer (Amresco Inc., USA) and agarose powder (MP Biomedicals, USA). The gel solution was boiled in microwave oven to let agarose dissolve, cooled down for a short while before an addition of 10 mg/ml ethidium bromide as fluorescent tag and then cast in mold with 15-40 wells for the samples. An addition of 4 µl of loading buffer (Fermentas, USA) was added per PCR sample. After an hour of gelation the gel was put in electrophoresis machine (Electrophoresis, Midigel 2, Apelex, Massy, France), and loaded with samples and 5 µl of 50 base pair gene ladder (Fermentas, USA) was used. The gel electrophoresis was done with 90 V, 400 mA, 100 W and 42 minutes. The results were studied and recorded with gel imaging equipment including UV light, microscope and camera (Uvidoc, DOC-008.XD, Uvitec, Cambridge, England).

3.2.4 Calcium imaging

The calcium imaging experiments were done with similar protocol as in video article by Barreto-Chang and Dolmetch 2009 [36] about calcium imaging of cortical neurons using fura-2. The differentiated cells were tested for correct calcium ion channel functioning using calcium imaging system consisting of inverted Olympus IX51-microscope (Olympus Corporation, Hamburg, Germany) with UApo/340 x20 air objective (Olympus) for visual inspection of cells. Images were acquired with an ANDOR iXon 885 CCD camera (Andor Technology, Belfast, Northern Ireland) synchronized with a Polychrome V light source by a real time DSP control unit and TILLvisION software (TILL Photonics, Munich, Germany). During imaging cells were on cover slip in RC-25 imaging chamber (Warner Instruments Inc., USA). [37]

Perfusion liquids for cells were based on articles by Barreto-Chang et al. 2009 [36] and Koivisto et al. 2012 [24]. The used Tyrodes solution is made to mimic cerebrospinal fluid and two versions of Tyrodes solution were used here, low-K Tyrodes and high-K Tyrodes, with solution concentrations listed in Table 3.3 and reagents from Sigma Aldrich, except Hepes from Thermo Fischer Scientific. When raising KCl concentration, the osmolarity of the solution was maintained by changing NaCl concentration accordingly. The solutions were adjusted to pH 7.4 with NaOH addition. [2]

Table 3.3: *Compositions of Tyrodes solution used as perfusion during Ca-imaging.* [36]

Ingredient	**Low-K Ca^{2+} Tyrodes (mM)**	**High-K Ca^{2+} Tyrodes (mM)**
NaCl	129	74
KCl	5	60
$CaCl_2$	2	2
$MgCl_2$	1	1
Glucose	30	30
Hepes	25	25

Cells were cultured over cover slips, so they can be taken with the slip from culture plate to the imaging chamber. Fluorescent calcium indicator acetoxy-methyl-ester Fura-2 (Fura-2 AM, Life Technologies, UK) was used. Cells were loaded with Fura-2 AM by taking cover slip with cells to small petri dish, adding 1 ml low-K Tyrodes solution and 4 µl of 1 mM Fura-2 AM and incubated 30 min in +37 °C in dark before imaging. After loading cells were put in imaging chamber by attaching the cover slip in place from the edges with silicone grease. Cells were continuously perfused with low-K Tyrodes solution during imaging.

Regions of interest were selected according to cell morphology. Fura-2 was excited with 340 nm and 380 nm light and the emission was recorded at 505 nm. The Ca^{2+} levels are presented as ratiometric values of F340/F380. Cells were recorded with baseline in low-K Tyrodes solution, and activated with high-K Tyrodes solution or capsaicin (Sigma Aldrich, USA). Capsaicin was dissolved to ethanol and used at concentrations varying from 1µM to 10µM concentration in low-K Tyrodes solution. Perfusion times with different perfusate lasted for 50 to 150 seconds with a total recording time of 400 seconds. Baseline was recorded after each change to wash out the high-K or capsaicin containing perfusate.

3.3 Characterization of ECM protein coatings

3.3.1 Coating protocol for ECM protein coatings

The ECM coating were done either on glass cover slips (VWR, USA) or straight on cell culture well (Nunc, Roskilde, Denmark), made of polystyrene and pretreated by manufacturer with Nunclon™ Δ surface treatment to make polystyrene more hydrophilic [100]. The used coating materials were laminin-1 in 20 μg/ml solution extracted from Engelberth-Holm-Swarm mouse tumor (Sigma Aldrich, USA) diluted in PBS, fibronectin in 1 μg/ml and 10 μg/ml solutions (Fibronectin from human plasma, Sigma Aldrich, USA) diluted in PBS and Matrigel™ in approximately 168 μg/ml and 2.2 μg/cm^2 solutions diluted in cell culture medium base DMEM/F-12. Exact concentration of Matrigel™ is not known, as it is an ECM protein cocktail of slightly varying quality. Gelatin coating (Sigma Aldrich, USA) was used as control and in all cell cultures where differentiation was the main subject. Gelatin dilution was 0.1 % in PBS.

All the coatings were done as conventional passive coating with one hour incubation in room temperature and coating liquid was used enough to clearly cover the whole surface to be coated, usually 500 μl for one 24-well bottom of 1.9 cm^2 area. This coating protocol should yield an even and thin ECM protein layer as coating for all the materials used. Different protocols for ECM coating were tested to find, if they really produce different results in coating characteristics. First half hour of incubation was done in +37 °C or the whole incubation was done overnight in +4 °C. These were done because there are many different coating protocols in literature with varying incubation times and temperatures for the same ECM protein coating materials.

For coating characterizations, coatings were also done for only half or part of a cover slip, for analyzing the edge of coating. This was done by putting a piece of tape on the reverse side of the slip to hold the slip in upright position inside a cell culture well, as shown in Figure 3.1. The slip was then at least partially dipped in coating liquid and taped in place for duration of incubation. Touching the coating liquid with tape was avoided, as impurities might have dissolved from the tape and the attached with coating on the sample slip. It is important to handle the cover slips at all times only with tweezers to prevent transfer of dust and dirt from gloves onto the surfaces.

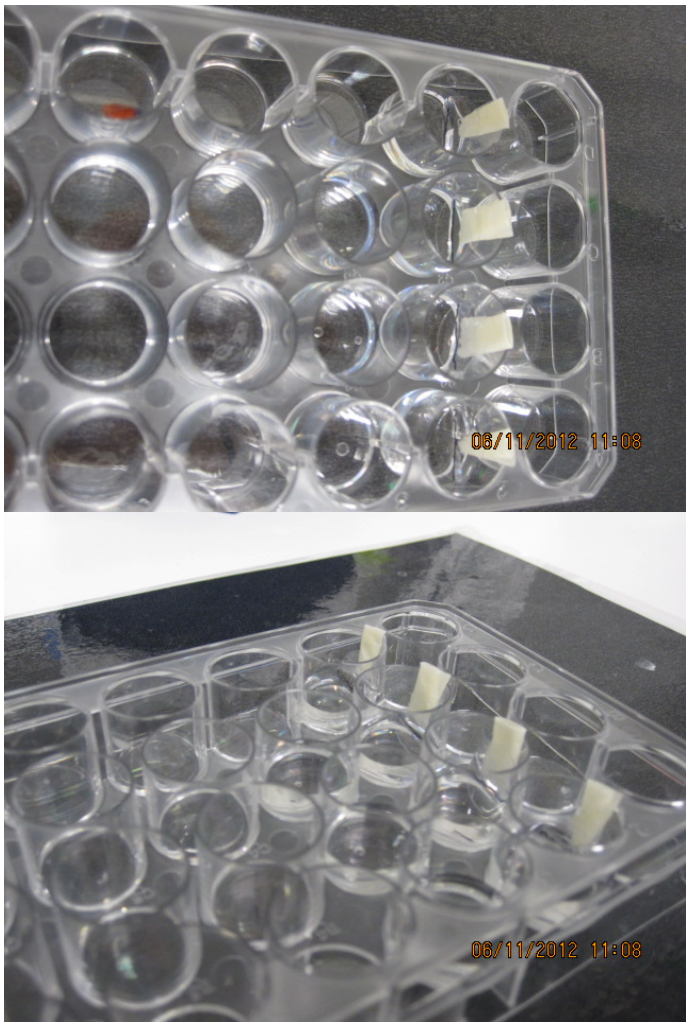

Figure 3.1: *Coating glass cover slips partially by dipping the in coating liquid and taping them in upright position.*

The ECM coating was done similarly for characterizations as for cell culture use. Clean and dry glass cover slips were also studied with the same characterization methods as controls. All characterizations were done to all the coating materials. The AFM and contact angle studies of ECM coatings without cells were done in laboratories of Biomedical Engineering Department and Automation Science and Engineering Department of Tampere University of Technology. Protocols for ECM protein characterization were one objective of this work, so different combinations of steps were tested with each characterization method, to find the ones that give the most representative results.

3.3.2 Fluorescent labeling of coatings

The ECM coatings can be fluorescent labeled in similar way as making immunocytochemistry to cells. Immunocytochemistry protocol used for cells was modified for coating characterization by removing the cell permeabilizing Triton-X from blocking and primary antibody mixtures, as there is no cell membrane to permeabilize, and the overnight incubation with primary antibodies was shortened to one hour in room tempera-

ture. A form for making the modified fluorescence labeling protocol is added as Appendix 2 of this thesis. Used antibodies are listed in Table 3.4. It was also tested how the reduction of washes between steps and the mounting with VECTASHIELD® and cover slip will affect the fluorescence outcome. Fixation with 2 % glutaraldehyde and 4 % PFA for 15 minutes in room temperature was also tested, if it has effect on coatings and their fluorescence. With fixation, there were no washing steps before it, but washing twice with PBS after it. The non-fixed samples were also washed two times with PBS before blocking step.

Table 3.4: *Antibodies used for fluorescent labeling of ECM coatings.*

Primary antibodies:	**Concentration**	**Source**
Anti-fibronectin	1:250	Rabbit
Anti-laminin	1:1000	Rabbit
Secondary antibodies :		
Antirabbit Alexa flour 488 IgG	1:800	Donkey

3.3.3 Atomic force microscopy

Characterization was done with atomic force microscope XE-100 (Park Systems, South Korea) using non-contact and high voltage mode. Used scanning tip was multipurpose tip, model ACTA (Applied Nanostructures, Inc., USA), tip material N-type silicon coated on reflecting side with aluminum, frequency 200-400 kHz, spring constant 25-75 N/m. Exact AFM imaging parameters were found by trial and error during imaging. Cover slips were moved directly from coating liquid to AFM, but they dried too fast in the AFM sample chamber to be able to study them while wet or the tip did not recognize difference between liquid droplet and coated surface and did not get proper readings and images, so the coatings were studied dry. Images were taken from studied surfaces at areas of 1x1 µm, 5x5 µm, 10x10 µm and 45x45 µm to view the topographical features of all sizes possible with the current equipment. AFM images were studied and processed with scanning probe microscopy imaging software named XEI (Park Systems, South Korea). Images were used for both qualitative and quantitative studies, but there were not enough images for statistical analysis.

All studied coatings were made as mentioned in Chapter 3.3.1 for glass cover slips and inside cell culture plates. Fixation of coatings with glutaraldehyde (Sigma Aldrich, USA) or PFA was done to see, if the proteins could be preserved in similar condition as in cell cultures without denaturation and crystallization that seems to happen during drying. Glutaraldehyde was used as 2 % solution and PFA as 4 % solution, with incubation during fixation was 15 minutes for both in room temperature, after which fixative was washed with sterile water and cover slips were left in sterile water in room temperature. Samples were kept in sterile water while waiting for imaging, to prevent too much drying an also keep them clean from dust or other airborne contaminants.

3.3.4 Contact angle measurement

The contact angle measurement was done with Attension Theta Lite optical goniometer (Biolin Scientific AB, Sweden) with attached GASTIGHT® precision syringe (Hamilton Inc., USA) and Attension Theta (Attension/Biolin Scientific, Espoo, Finland) software. Sample preparation was similar to AFM, but slips were not fixed. Measurements were done in room temperature of 25±1 °C, for slips that had dried enough so that they are not visibly wet. The air humidity in measurement room varies between 20 %-50 %. For a visibly wet surface, the liquid drop will always spread in 0° angle and be impossible to measure. Cell culture medium and sterile water were both used as contact angle liquid to view differences that the cocktail of molecules in culture media have on liquid-coating interface and surface tension compared to water.

Measurements were done by taking three pictures of static ascending angles when liquid is applied to surface drop-by-drop and three pictures of static receding angles when liquid is drawn back to syringe and one final picture of surface after liquid is mostly drawn back. All samples were measured this way two times to yield a total of 14 measurement results per one liquid-coating pair. The pictures were first analyzed with Attension Theta software and if the automatic measurement did not find the contact angle, ImageJ (open source) software was used to manually fit the contact angle in the picture and measure it. This means that the accuracy of these measurements is not very good at small angles. The measurement data was analyzed in Excel (Microsoft, USA).

4 RESULTS

Every batch of cells cultured with the SDIA-protocol did produce cells with morphological and immunocytochemical resemblance to neural cells. The cell culture times varied with each batch of cells, as shown in Table 4.1, this was done to find if longer or shorter time to differentiate has effect on the maturity of cells. The most used time was 4 weeks in NSP phase and little over 2 weeks in DRG phase. The time in DRG phase was also limited by detachment of cell from the culture plate bottom, in literature it is acknowledged that PA6 cells stay attached for one month at longest [2], and similar behavior was noticed here. If cells seemed to start to detach, they were fixed and stored at +4 °C for immunocytochemistry, which causes the large variance on how long cells were cultured in the DRG phase. The cell culturing was an iterative process, as differentiation to peripheral neural cells had never been done before in this laboratory. The cell line UTA.00112 was used the most in the beginning, to see if results are at first reproducible with one cell line. The Table 4.1 also shows which characterization methods were used for the cells after the end of culturing period.

Table 4.1: *Differentiated cell lines, cell batch numbers, culturing times of different phases and was DRG-phase culturing done over feeder layer or ECM protein coating.*

Batch	Cell line	NSP-phase in weeks	Surface	DRG-phase in days	Characterization
1	00112, p. 34	4wk	PA6	16d	Immunocytochemistry, PCR, (Cell-IQ ²)
2	h7, p. 34	3wk	PA6	26d	Immunocytochemistry, PCR
3	00112, p.38	4wk	PA6	18d	Immunocytochemistry, PCR
		4wk	Laminin	33d	Immunocytochemistry, Conditioned medium
4	00112, p.40	3wk	PA6	12d	PCR, (Cell-IQ ²)
		3wk	Laminin, Fibronectin	25d	Immunocytochemistry, Conditioned medium
5	00112, p. 42	4 wk	PA6	13 d	PCR, (Cell-IQ ²)
		5wk	Laminin, Fibronectin, Matrigel™	44d	Immunocytochemistry, Conditioned medium
6	00112, p. 43	7wk	PA6	18d	Immunocytochemistry, PCR
7	00112, p. 44	6wk	PA6	18d	Immunocytochemistry, PCR
		6wk	Laminin, Fibronectin,	30d	Immunocytochemistry, Ca-imaging
		6wk	Matrigel™	25d	Immunocytochemistry
		7wk	Fibronectin	(¹)	-
8	00112, p. 52	4wk	PA6	11d	Immunocytochemistry
		6wk	Laminin, Fibronectin, Matrigel™	(¹)	-
9	00112, p.52	5wk	PA6	17d	Ca-imaging
		6wk	PA6	13d	Immunocytochemistry
		6wk	Laminin, Fibronectin, Matrigel™	13d	Immunocytochemistry
10	00112, p. 55	7wk	PA6	18d	Immunocytochemistry
		7wk	Laminin, Fibronectin, Matrigel™	18d	Immunocytochemistry
11	05208, p.60	6wk	PA6	24d	Immunocytochemistry, Ca-imaging
		6vk	Laminin, Fibronectin, Matrigel™	43d	Immunocytochemistry
		8wk	PA6	29d	Immunocytochemistry, Ca-imaging, PCR
12	05208, p.68	6wk	PA6	21d	Immunocytochemistry
		6wk	Laminin, Fibronectin	21d	Immunocytochemistry
13	05105, p.18	6wk	PA6	29d	Immunocytochemistry
		6wk	Laminin, Fibronectin	38d	Immunocytochemistry
		8wk	PA6	21d	Immunocytochemistry, PCR

(¹)Indicates that cells did not attach to culture well and experiment failed.
(²) The continuous time-lapse imaging system Cell-IQ™ was tested, but it did not produce any additional information, so it was left out of the thesis.

4.1 Cell morphology and identification

The cells were monitored throughout their differentiation process by microscopy and phase contrast micrographs were taken in every phase of differentiation. From these pictures it is clear that the cells change morphology especially in the third phase of differentiation quite dramatically. The observed cell morphologies are also similar with the ones found in literature for cells of the same phase of differentiation. Throughout the differentiation process, there was a slight difference between cell lines, so it might be that one line has more tendencies towards PSN than another.

In the first phase the iPS cells form clear colonies on the PA6 co-culture. Between different batches of cells there can be drastic changes in amounts of colonies and colony morphologies with the exact same procedures, culture mediums and conditions, but overall there does always emerge some clear-lined, homogenous and solid colonies, that can be passaged to the second phase. The definition of homogenous or heterogenous colony is not exact, so some batches might have had more heterogenous colonies passaged onwards than others, as there is always the human error involved. Sizes of the passageable colonies vary from around 500 µm to a few millimeters. Examples of typical induction phase colonies are shown in Figure 4.1 and Figure 4.2 shows a PA6 cell layer without iPS cell. Even with variance on exact morphologies, the cells in induction phase grew every time in the same way and the more important morphological changes and variations occurred in the later phases.

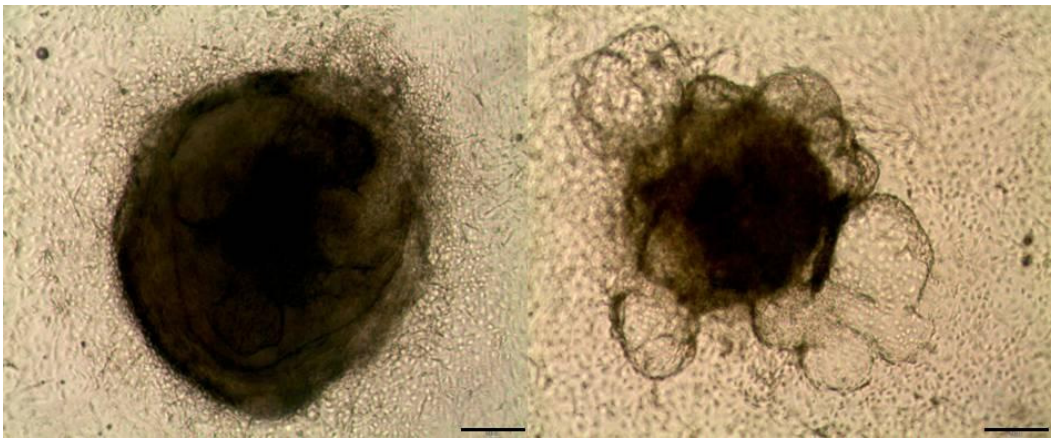

Figure 4.1: *On the left: example of homogenous colony at the end of induction phase. On the right: a more heterogenous colony from the same batch of cells. The cells are of batch 3, cell line h1/12 p. 38. The scale bar length is 200 µm.*

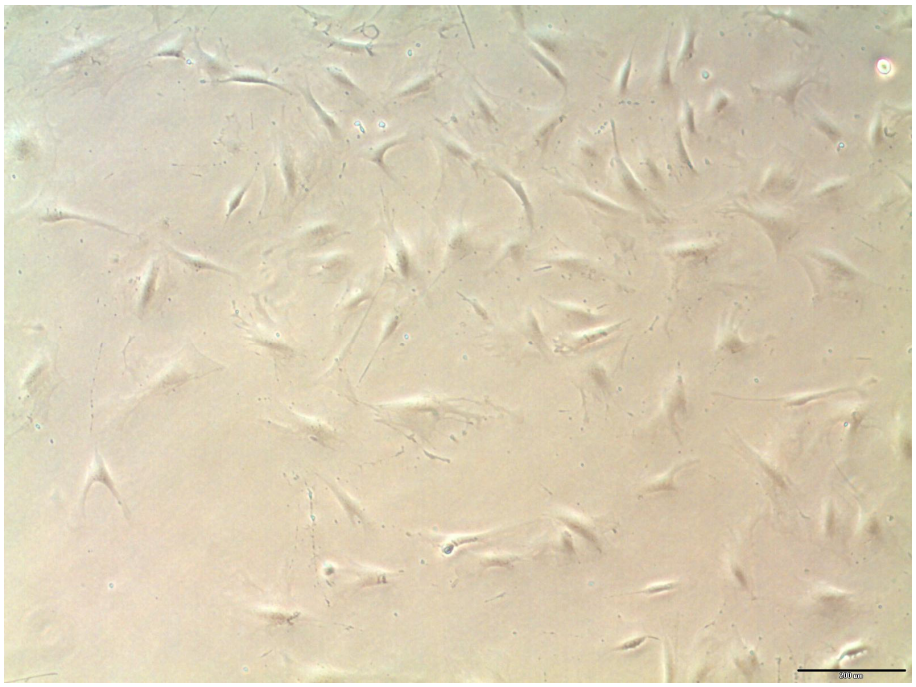

Figure 4.2: *Mouse PA6 stromal cells growing and multiplying for use in coculture. Two days after division, not as confluent as at the start of induction phase. The scale bar length is 200 μm.*

In the second phase, the different cell batches seemed to go through the morphological changes in a bit different order or timing, but this can be related to cell lines intrinsic qualities as well as differing homogeneity of the passaged cells. The basic unit of cells in this phase is a small, rather hard and solid sphere with round and spherical shape. These spheres can then grow in different ways in different batches with exactly same conditions. In Figure 4.3 are shown all the most often seen variations of neurosphere morphology. One variation is that the sphere just grows uniformly in diameter retaining its shape and staying hard, as in Figure 4.3b. Another variation is that the small spheres will infuse together on their edges and for a string or cluster of spheres, as in Figure 4.3c. These clusters can then grow on filling the space between cores of spheres with less dense and softer cell material, as in Figure 4.3d, but it is still possible to find the smaller spheres inside the larger ones. Especially during the weekly cutting of the spheres it is easier to cut along the softer parts of the sphere clusters. The large spheres and parts of sphere clusters can also turn into hollow spheres, as in Figure 4.3e, which might be because too slow nutrient diffusion inside the sphere or because a more heterogenic starting material. When cutting the hollow or the larger spheres there is sometimes a burst of loose cell material released from inside of the sphere, which might be dead cells.

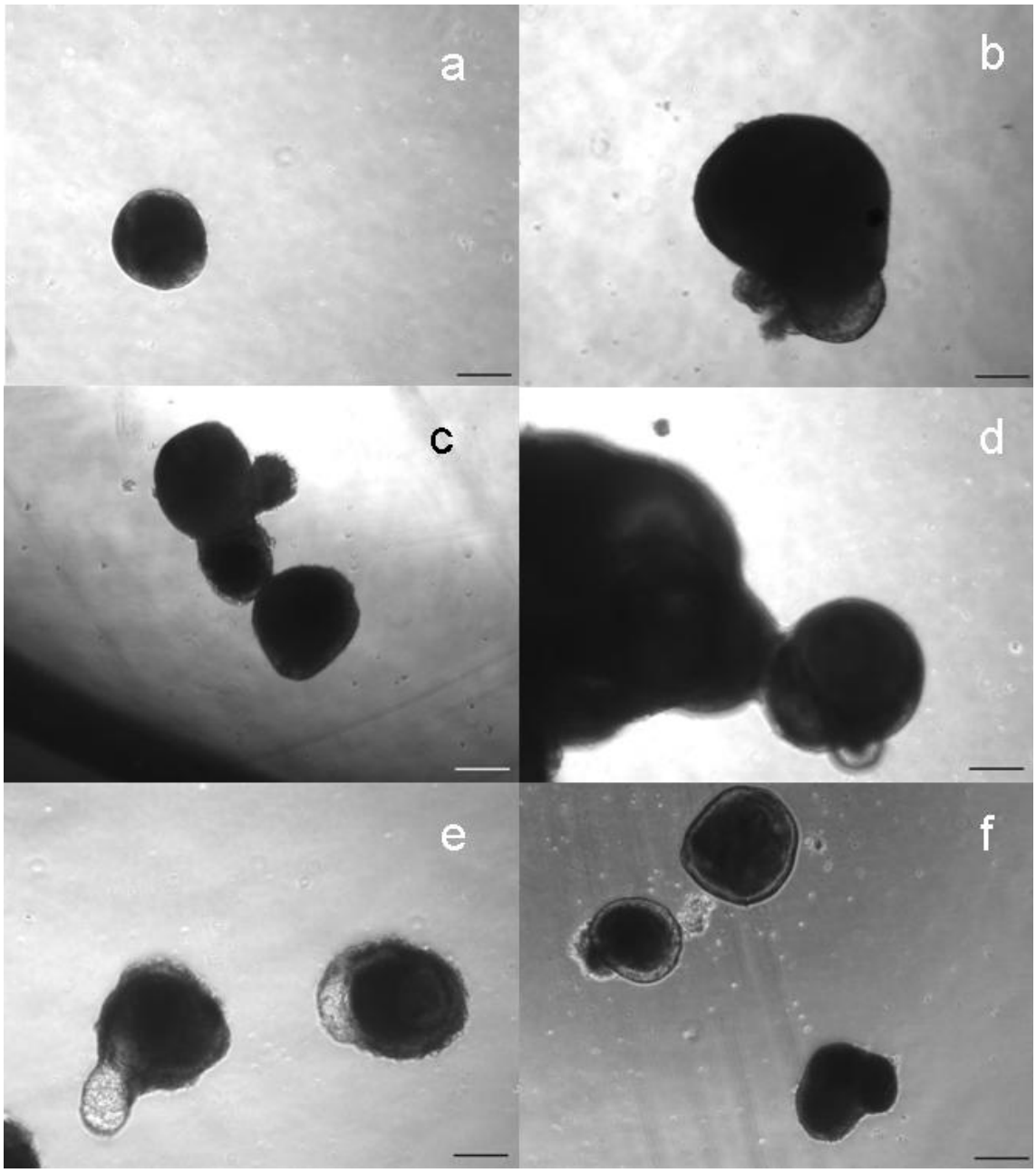

Figure 4.3: *Representative examples of different morphologies of neurospheres, all micrographs taken with same magnification. A) A neurosphere that is the basic building block of all the other sphere clusters. B) A neurosphere that has grown over 1 mm and should already be cut in half. C) A smaller cluster of neurospheres. D) Many neurospheres infused together and softer cell material filling the gaps between spheres. E) Two neurospheres with hollow parts on their sides. F) A couple of neurospheres of different sizes and a little bit of dead cell material floating around them. The scale bar length is 200 µm.*

In the third phase the neuronal cells are more difficult to distinguish from the PA6 cells at first, but after a few days they will have the bipolar morphology shown in Figure 2.3 and later they can grow into a variety of long neuronal processes and even neural network-like structures. The pseudounipolar morphology is hard to find in phase con-

trast images, but easier in fluorescence images, as the fluorescent colors define borders of single cell better. Mostly the larger networks have a non-dissociated sphere in their middle or attached to some point of the network, looking like the large neural process is growing from the sphere. The processes can also grow in width to be a lot wider than one cell, even approximately 100 µm wide. The length of one continuous process can be almost as big as the diameter of the cell culture well, over 10 mm, which means that they cannot be imaged with our equipment to show their full length. The processes have long straight parts and usually some bents as well, but it is not clear what causes the bending. In Figure 4.4 are shown some of the more typical morphologies of the mature peripheral-like neurons.

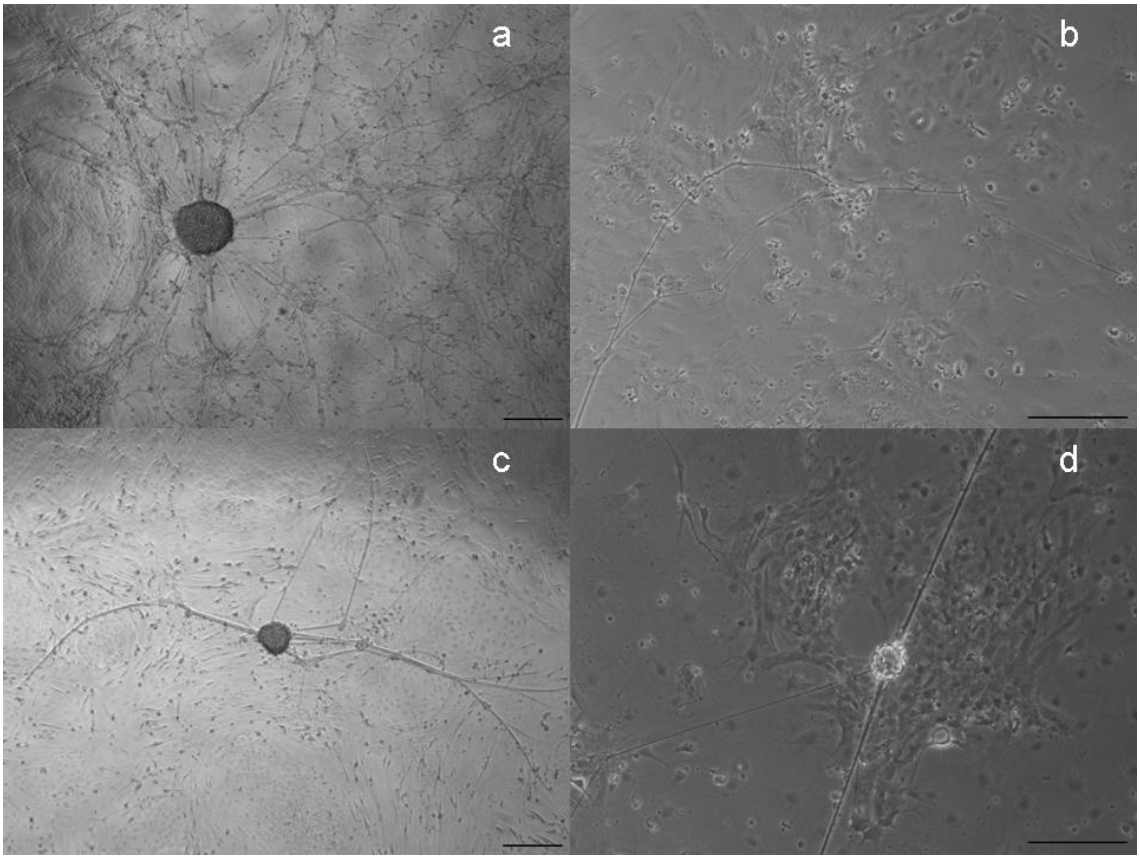

Figure 4.4: *Examples of neural cell processes after successful differentiation. A) An attached sphere has grown processes to all directions from it, scale bar 300 µm. B) A long process and non-neural like cells, scale bar 200 µm. C) An attached sphere with smaller neural network than in A, scale bar 300 µm. D) A small attached sphere with long neural processes growing to opposite directions and underneath typical non-neural like cell colony, scale bar 200 µm.*

The neurospheres passaged into DRG phase to the ECM coatings look different than the ones on PA6 co-culture. First of all, the big non-dissociated spheres or cell aggregates do not attach well on the ECM coatings, so the lack of these might cause lack on longer neural processes as well. The cells do, however, gain the bipolar morphology, slightly later than on PA6 co-culture, but they do not grow into fully mature network of neuronal morphology. In the first couple of days DRG phase cells on PA6 co-culture

look very similar to cells on ECM coatings. But the cells in co-culture change morphology quickly, while on the coatings they usually stick to this morphology or have only slight changes throughout the whole later part of culture. They also express more often a flat and spread out morphology, or at least this morphology is more visible, as there are no other types of cells to confuse with. The best acquired morphologies for third phase cells growing on all the tested ECM coatings are shown in Figure 4.5, Figure 4.6 and Figure 4.7, with the exceptional laminin culture explained later. The morphologies look so similar, that it is impossible to tell from the morphologies, which material is used in which picture and the coating itself is totally invisible. The cells do not attach to these coatings as well as they do on PA6 co-culture with gelatin coating in the bottom and especially the partly dissociated spheres did not attach as colonies to coatings as well as they did on feeder layer. Higher cell plating density was used compared to PA6 co-cultures, but it did not have significant effect. One conclusion could be that the coatings lacking the inducing effect of PA6 cells just cannot make the differentiation go further, which seems to be the case with fibronectin and Matrigel™, but not with laminin.

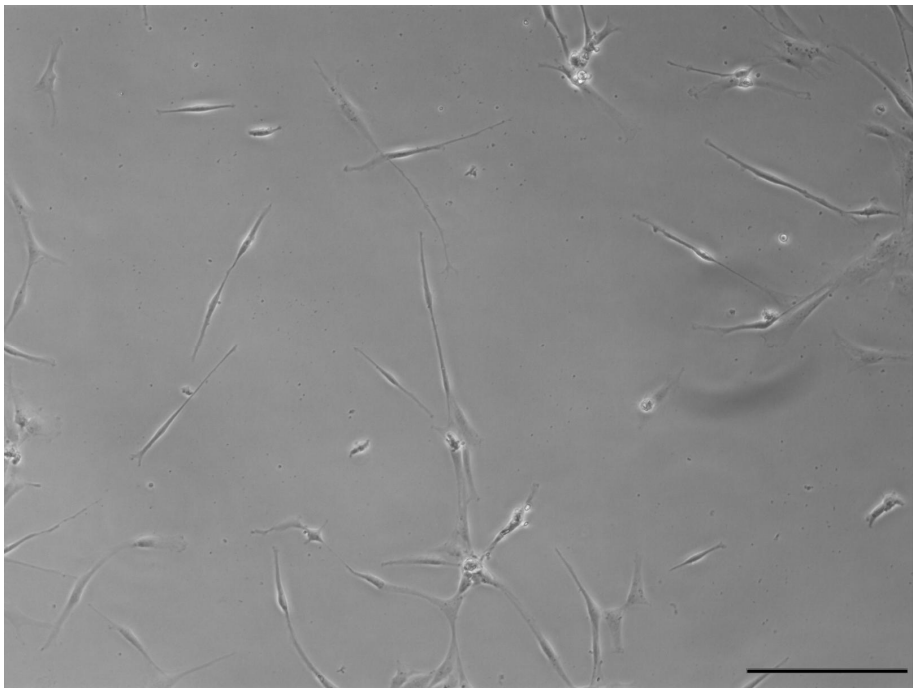

Figure 4.5: *Typical example of DRG phase cells plated on ECM coating, here on laminin. Cells have bipolar morphology, but are too far away from each other. The scale bar length is 200 μm.*

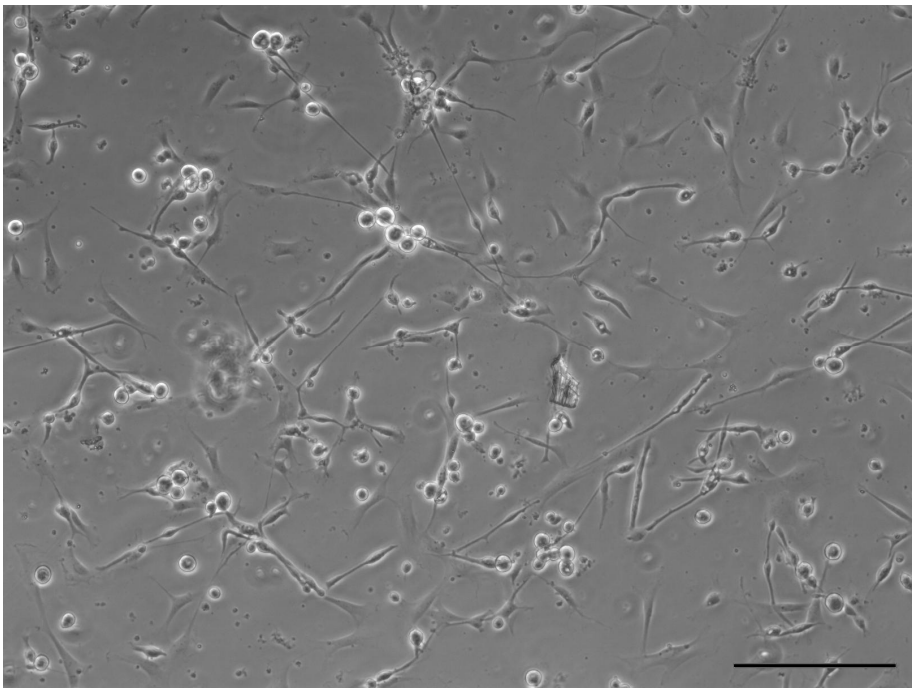

Figure 4.6: *Cells growing on fibronectin here have higher density and looks promising, but did not produce any actual networks. The scale bar length is 200 µm.*

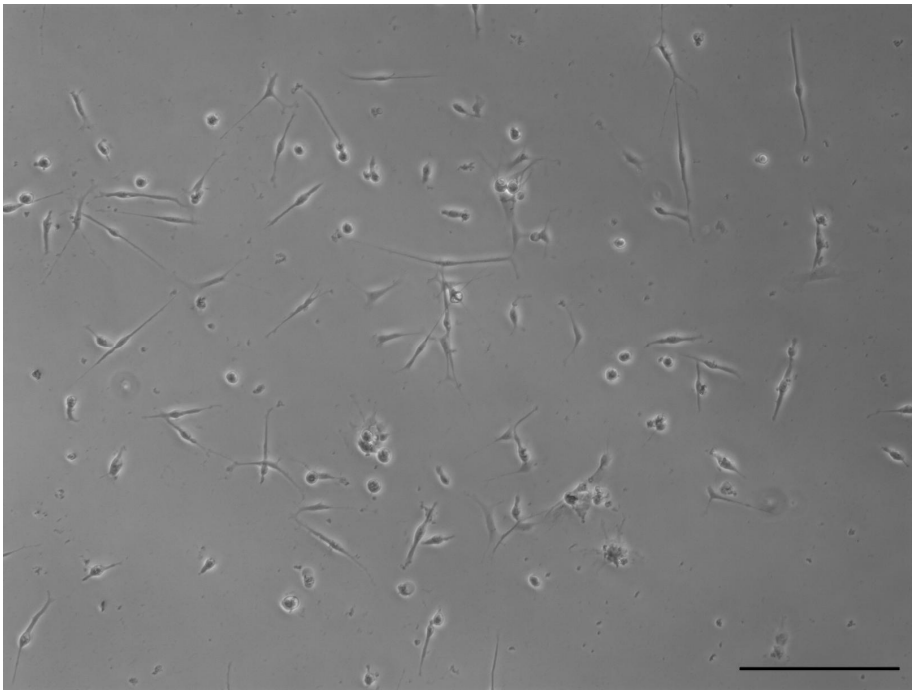

Figure 4.7: *Cells growing on Matrigel™ with morphology indistinguishable from the other ECM coating cultures. The scale bar length is 200 µm.*

There were two occasions that a larger colony did attach to the coatings, and when they did, they grew into having very large process networks. The largest network was with batch cell line UTA.05105 on laminin after eight weeks in neurosphere phase. This one large colony produced network extending for almost the full diameter of the cell culture well, about 13 mm long at longest, partly shown in Figure 4.8. In smaller scale

there was also one other successful process extending colony on laminin. So as total of ten cell batches were plated on ECM coatings, only three times some kind of neural network emerged and only once the network was as large as or even larger than network on PA6 co-culture.

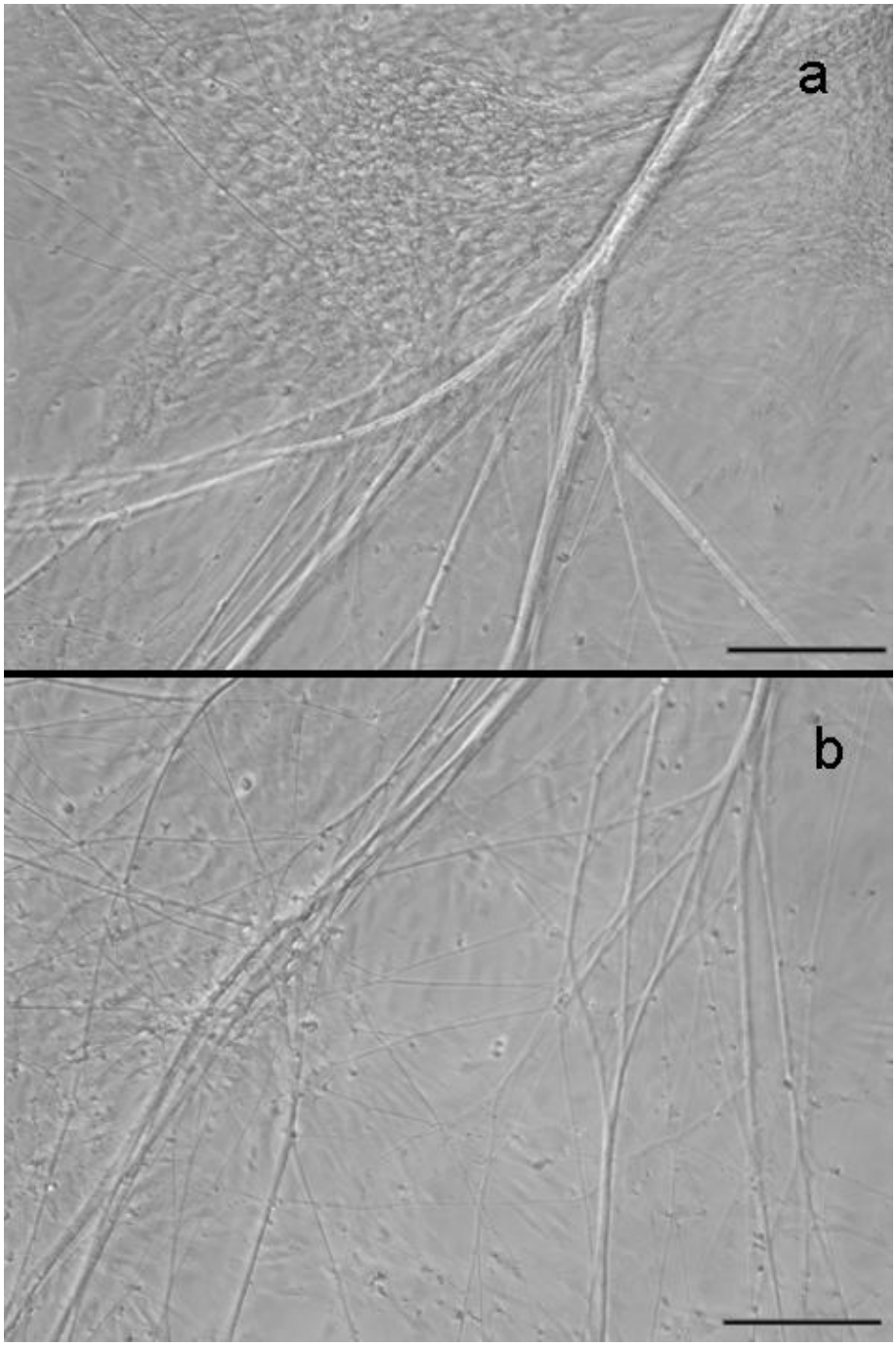

Figure 4.8: *The biggest neural network that was achieved on any ECM coating, with total length of processes around 10 mm, all coming from two closely attached colonies. Cell line was UTA.05105, which has later also proven to be very good in all neural differentiation, whatever the protocol. The scale bar length is 200 µm.*

The first cell batches were less successful than the later ones mainly because the culture time in neurosphere phase was four weeks at first, but it was later extended to six

and even eight weeks. It was noticed during the cell culture experiments that both six and eight weeks neurosphere cultures give more cells with correct morphology than three or four weeks. Even though the protocol said the neurosphere phase takes 2-8 weeks, 6-8 weeks is a better estimate. The cell line UTA.05105 had the highest tendency to differentiate towards neural cell type. Also the small detail of extending the incubation time from five to ten minutes during dissociation of spheres in the transition from neurosphere to DRG phase has clear effect on how the cells maturate in the DRG phase. This means that the spheres need to be disrupted and broken enough for cells to be able to proliferate outside the tight spheres. But there still needs to be spheres, as the longest processes always have a sphere or colony at one end or along the process somewhere. The spheres should not be completely dissociated to single cell level, only so that there are both individual cells and smaller and larger spheres to make colonies.

4.2 Immunocytochemistry

The cells with the right kind of neuronal morphology observed also stained positive for peripherin. Clear positive staining for Brn3a or TRPA1 was rarely seen. During the immunocytochemistry protocol some of the neural processes apparently detached partly from the surface and as a result are seen in coiled shapes that were not seen in phase contrast microscope before the fixation and staining procedure. Also colonies and individual cells were probably lost because of detachment during washing steps. Immunocytochemistry was performed to all differentiated cell batches, but here are shown only some representative examples of results as the cells look very similar between different batches and showing pictures of all of them would not be meaningful.

Typical examples of peripherin positive stainings are shown in Figure 4.9, from which it is clear that large peripheral-like neural networks did form during differentiation. The pictures are from varying cell batches, showing that the networks were formed reproducibly. The length of peripherin positive processes can vary from a few micrometers to ten millimeters, with the size of cell culture plate starting to be a limiting factor for process growth.

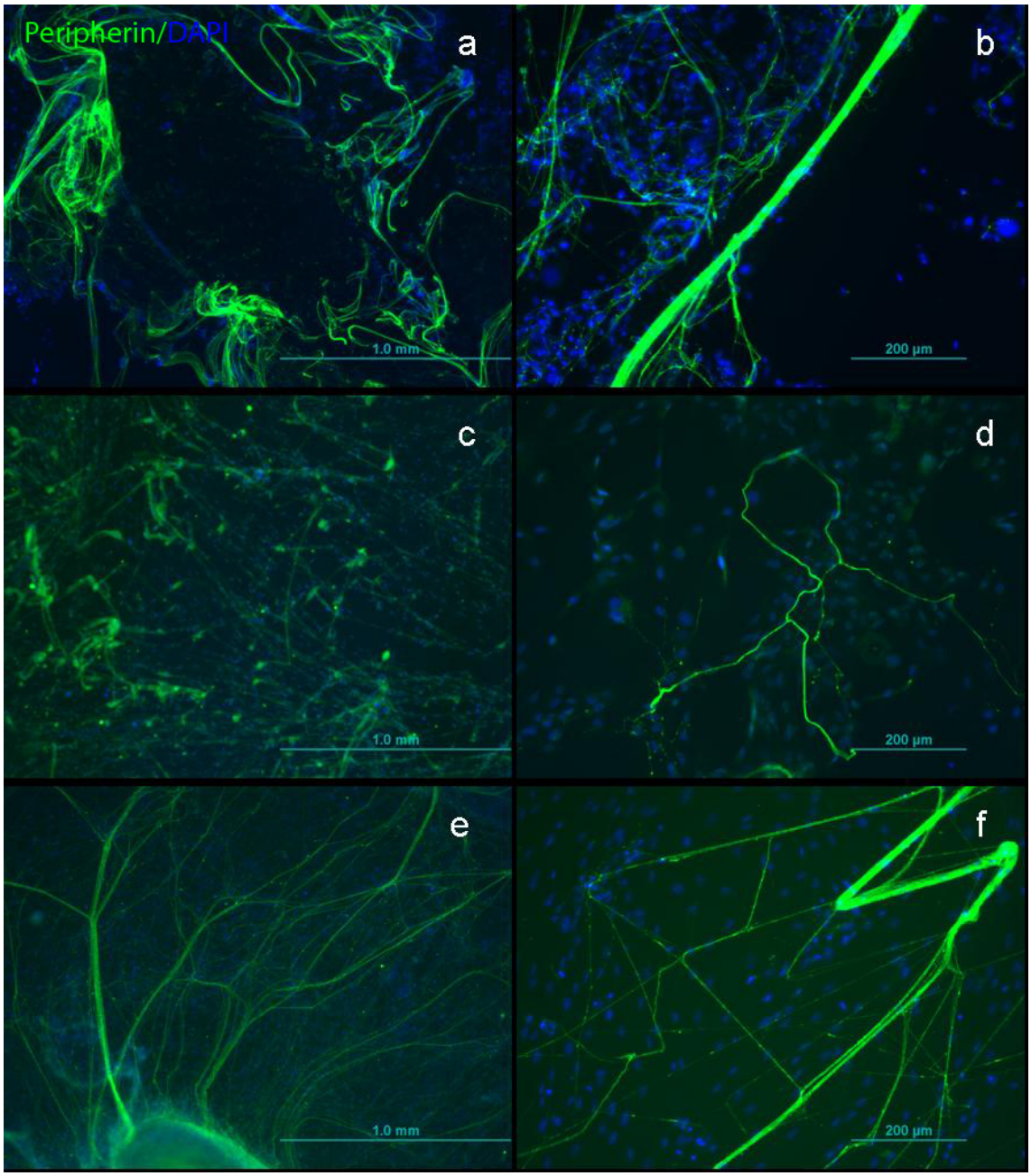

Figure 4.9*: Examples of peripherin positive cell processes shown green, taken from different cell batches. Nuclei of cells are stained blue with DAPI. A) Unstained colony in the middle with peripherin positive processes emanating to all directions. Processes have partly detached during immunocytochemistry so they look wavelike. B) A very strong and long process with smaller ones on the left side. C) A network of individual processes. D) A smaller detail of curvy process and non-specific background staining along nuclei not related to the process. E) Positively stained colony sending processes to all directions. F) A network still strongly attached and keeping its original shape. Scale bars on the left 1,0 mm and on the right 200 µm.*

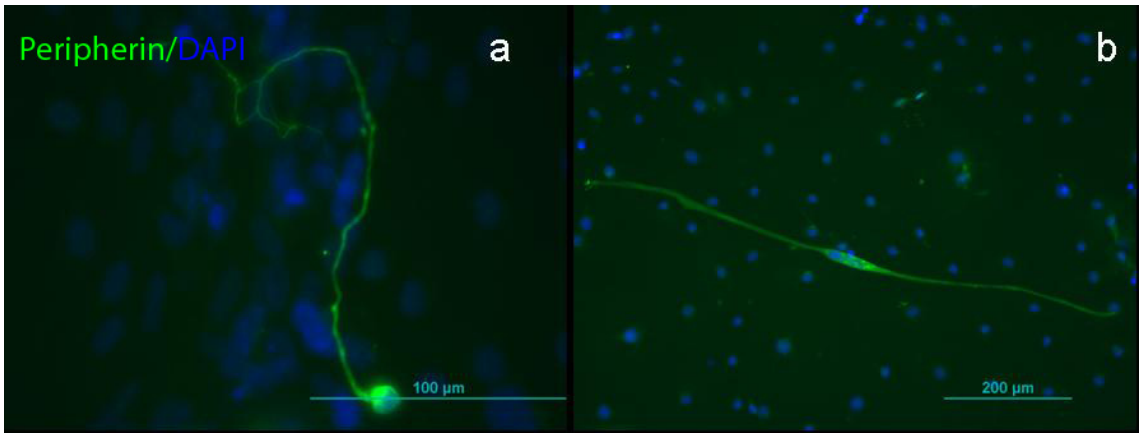

Figure 4.10: *Higher magnification of two individual cells with peripherin positive processes and peripheral neural morphology. A) A unipolar cell and B) a bipolar cell. Scale bars 100 µm on the left and 200 µm on the right.*

When studying individual cells it is often hard to distinguish, which nucleus is the one where a long process comes from and the longest processes also have many nuclei on their length, as is the case in the Figure 4.9. On a smaller scale, the processes of individual cells can be seen and the characteristic bipolar or pseudounipolar morphology of peripheral neurons is also seen, as in Figure 4.10. The true peripherin positive cells are clearly distinguished from false positives when seen next to each others in microscope, as the true positive ones are much brighter. In Figure 4.9d is one successful example of one bright peripherin process and dull false positives around it.

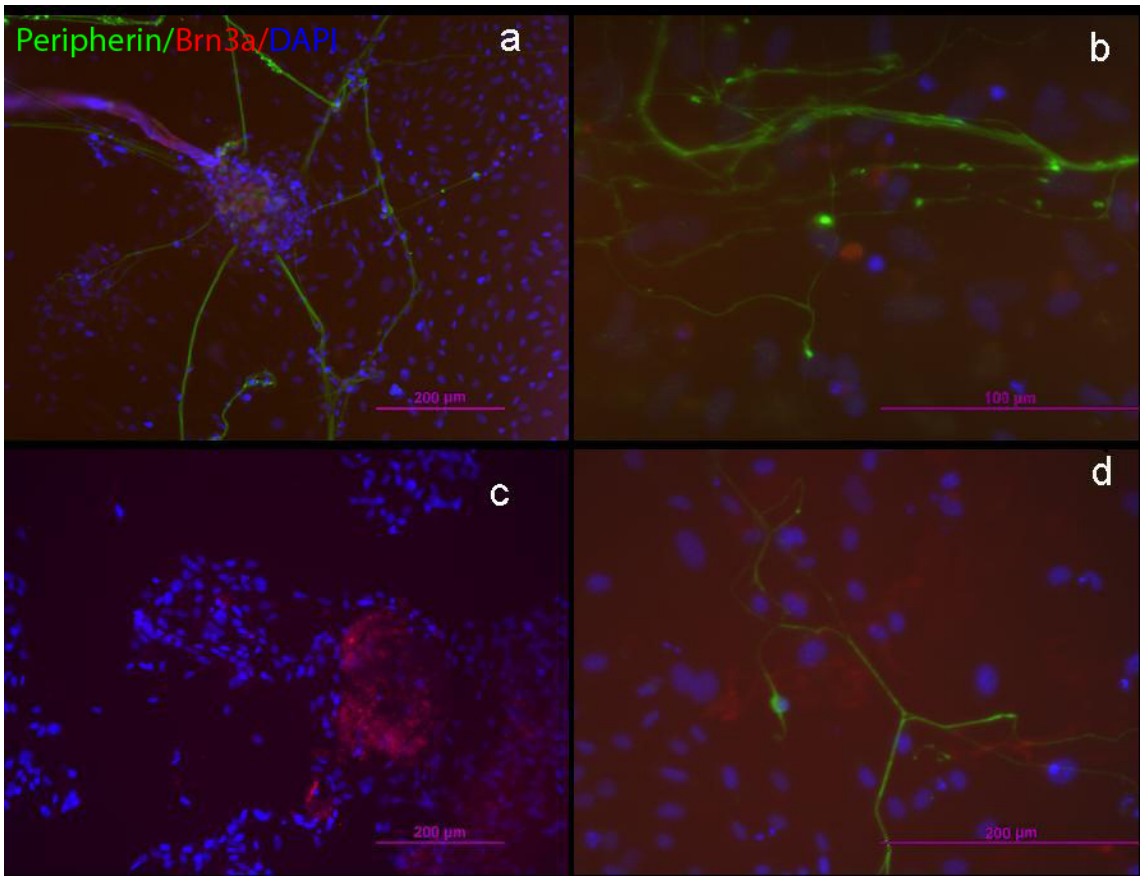

Figure 4.11: *Examples of cells seemingly positive for Brn3a, shown in red, peripherin in green and DAPI in blue. However the red fluorescence in these micrographs is not as strong as would be hoped, so the results are questionable. A) A colony with Brn3a positive centre and peripherin positive processes protruding outwards and the thicker red protrusion is likely some debris. B) Brn3a stains areas close to the nucleus, as it should, but the fluorescence should be stronger. C) Colony seemingly positive for Brn3a. D) Areas slightly positive for Brn3a around nuclei and peripherin positive process. Scale bars 200 µm except 100 µm in B.*

Dense cell colonies do not usually stain positive for peripherin, but they sometimes do for the Brn3a and TRPA1 markers, although the specifity of these positive staining results is debatable. These other markers should stain the soma around the nucleus of individual peripheral neurons with peripherin staining the processes extending from the soma, but no such results were consistently gained. So the cells in Figure 4.10 should be stained red around the nucleus, but they were not. Examples of slightly positive staining with Brn3a and TRPA1 are shown in Figure 4.11 and Figure 4.12 respectively. However, the strong background fluorescence might have interfered with these markers, which is why reversed secondary antibodies were also tested, but it was in vain. The marker expression should concentrate on the soma and not on the long processes, so the peripherin background should not interfere as much as it did.

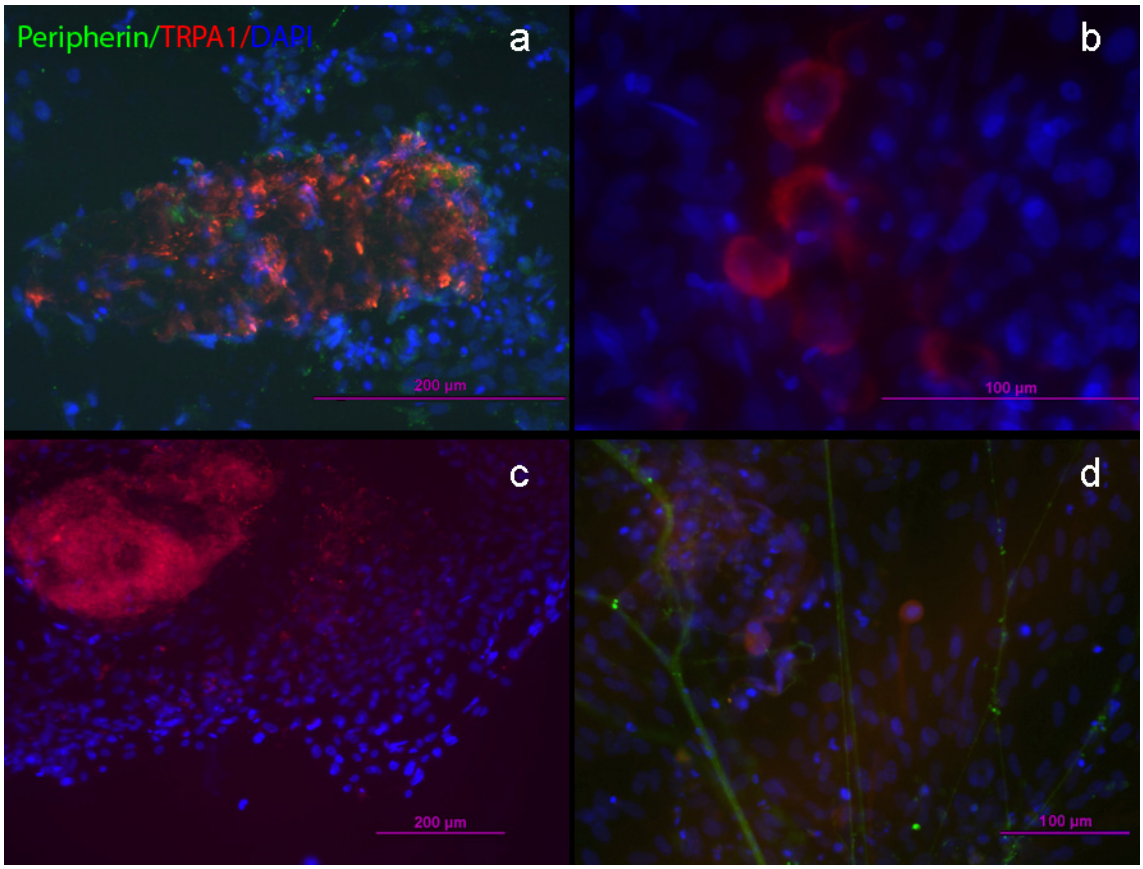

Figure 4.12: *Examples of cells seemingly positive for TRPA1, shown in red with peripherin shown in green and DAPI in blue. A) A colony positive for both TRPA1 and peripherin, but no protruding peripherin processes. B) High magnification of TRPA1 localized around the nucleus. C) Colony positive for TRPA1, looking very similar to colony in Figure 4.11c. D) TRPA1 positive staining around nuclei and peripherin positive processes around and connected to them. Scale bars on the right 200 µm and on the left 100 µm.*

When comparing Figure 4.11 and Figure 4.12 which have different markers in same color, they look very similar. For example the colonies were rather consistently stained positive in with both markers, which can either be a true positive or it can be that these antibodies just attach to the colonies more than on individual cells. As both of these markers use the same secondary antibody, there are no Brn3a/TRPA1 double positive fluorescence pictures. With these inconsistent results, the peripheral sensory nature of the differentiated cells is not yet confirmed fully. All the antibodies also produce false positive staining, that can be distinguished from the dull fluorescence compared to true positive ones. It seems that strong peripherin staining comes through to the red wavelengths in fluorescence, which can be confusing.

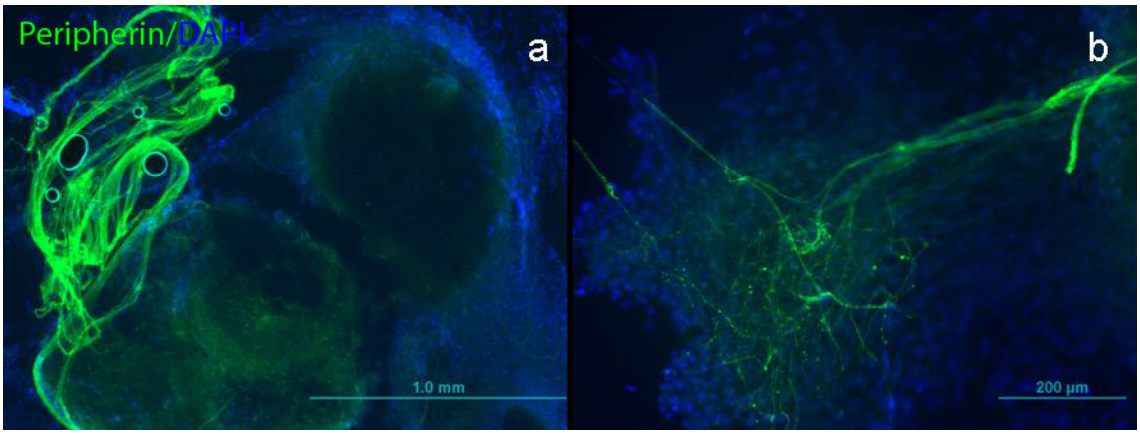

Figure 4.13: *Examples of neuronal colonies grown on laminin, these are the same colonies shown in Figure 4.8. A) The long and strong process coming out of the colony has detached during fixation, but the colony itself has stayed attached, so the process is curled along the colony. B) Higher magnification showing peripherin positive processes penetrating a thicker cell area. Scale bar on the left 1.0 mm and on the right 200 µm.*

The cultures on ECM protein coatings often did not produce large networks, but when they did, the cells looked similar to the ones cultured in PA6 co-culture, as can be seen if one compares Figure 4.13 and Figure 4.9. laminin was the only material to yield larger networks, twice, so this would indicate it as the best choice for PSN differentiation, but more successful cultures on laminin would still be needed to back up any conclusions. The same problems of Brn3a and TRPA1 expression were present on all ECM coating cultures and no good and clear examples of their expression were recorded.

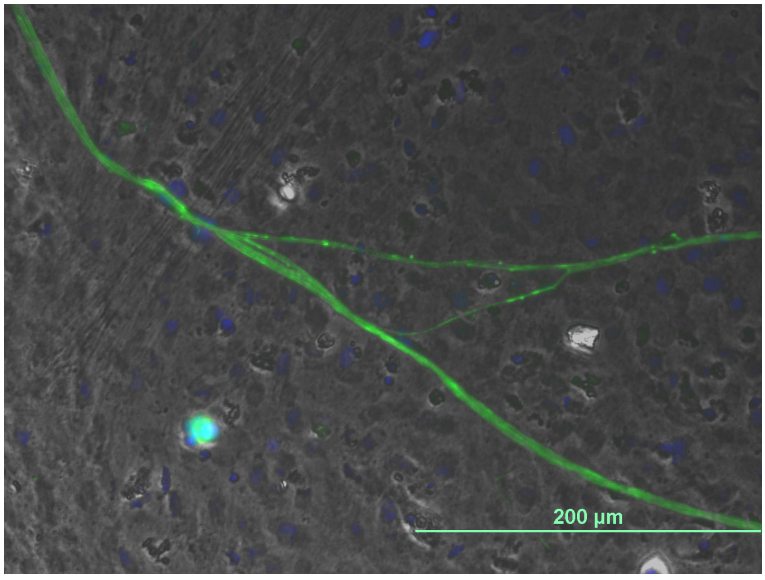

Figure 4.14: *Combined picture from phase contrast and fluorescent micrographs. Scale bar length 200 µm.*

When comparing the fluorescent micrographs and phase contrast micrographs of cells, it is clear that when long processes are seen on phase contrast microscope, they

are the peripherin positive ones. So there were not seen any long processes that were not peripherin positive. But the fact that processes detach partly during fixation of cells makes it difficult to appoint, which fluorescent colony or process was which from the phase contrast micrographs. But in Figure 4.14 is an example of fluorescent and phase contrast micrographs combined to show how well processed stain with peripherin.

4.3 RT-PCR

There were a lot of difficulties in gaining results from RT-PCR and due to that, only few genes tested successfully. The PCR enzymes and gene primers would need more optimization before use or the method could be changed from RT-PCR to quantitative- or qPCR. The GAPDH band was visible in gel electrophoresis pictures, as seen in Figure 4.15, so there was functioning RNA in the cell samples. There was also some kind of peripherin band, but it was constantly seen at a wrong part of the reference gene ladder, so the results are questionable. Other markers did not produce reproducible results, but as even the housekeeping gene GAPDH was sometimes difficult to visualize, it means that the problem here is more on the samples and the method than on cells actually expressing wrong markers.

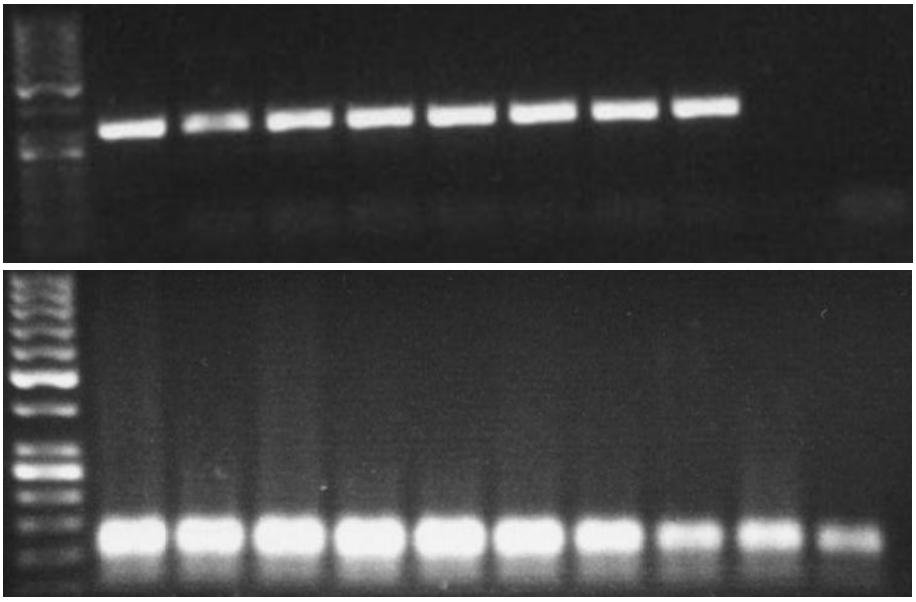

Figure 4.15: *Pictures of the two successful examples of RT-PCR gel electrophoresis. The upper one is GAPDH band and the lower one is peripherin band, which should be higher on the ladder.*

The peripherin band is clearly less bright on the two right-most sites in Figure 4.15, which are controls without cells. So the cell samples did have RNA from active peripherin genes, but the peripherin markers also react together without any RNA, which makes the results more difficult to interpret. The GAPDH controls are totally empty, as they should be.

4.4 Calcium imaging

The functionality of cells with neuronal morphology was tested with calcium imaging. Most of the cells did respond strongly to changes in potassium concentration of perfusion, meaning that they are putative functioning neurons. The responses on one measurement are shown in Figure 4.16 as change in fluorescent ratios calculated by the analysis program from selected regions of interest, chosen by morphology and visible fluorescent flashing in the analyzed video recording. The potassium response here has the right kind of shape, starting soon after concentration change and decreasing right away when the perfusion is changed back to normal with the baseline returning close to original. The cell batch 11 named UTA.05208 gave the most successful Ca-imaging data. In these graphs about Ca-imaging results the x-axel shows time in seconds and y-axel shows the ratio of fluorescence measured at two different wavelengths. So the units of y-axel are arbitrary but the strength of cell response is assessed by height differences in the curve.

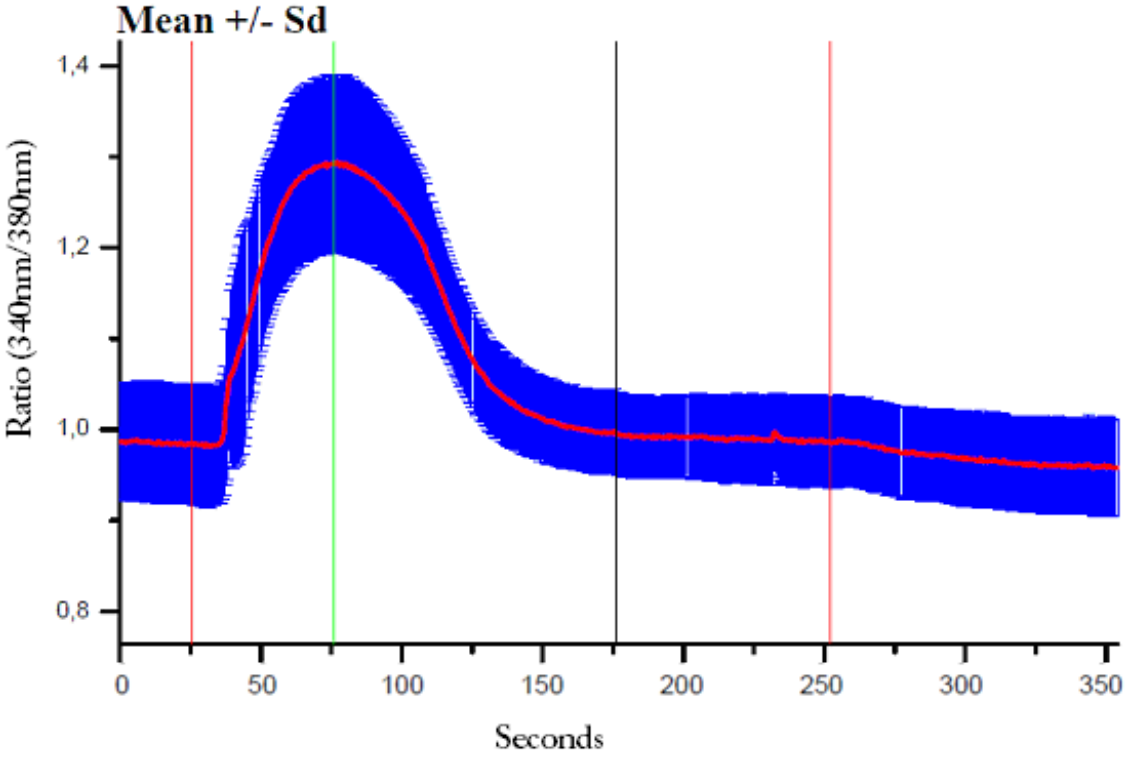

Figure 4.16: *The mean graph of fluorescent ratio of eight reacting cells with standard deviation included. The left red line represents iso-osmolaric change of Na^+-ions to K^+-ions in perfusion, green line is wash-out of extra K^+-ions, black line is addition of capsaicin in the perfusion and the right red line is wash-out of capsaicin. The response to K^+-ions is robust. There is also very small response to capsaicin in one analyzed cell.*

In general, no rapid response to capsaicin was observed, but in a few cells a rise in calcium was observed after approximately 100 seconds exposure to capsaicin. The response to capsaicin is a lot harder to see than response to potassium and even in best samples of cell batch 11 it is only seen in about 5 % of cells responding to potassium.

Cell should respond to capsaicin faster than was seen on these results. There is also possibility that changes in perfusion osmolarity or the potassium activation done first or something else irritating cells in the calcium imaging can interfere with the cells so that they start firing action potentials irregularly and without stimulation, which is seen as random peaks in fluorescent ratios. Proving that the response thought as capsaicin provoked is actually that would need more experiments than was possible to do during this thesis. But in Figure 4.17 is shown the one cell from the experiment of Figure 4.16 that did respond to both capsaicin and potassium concentration change.

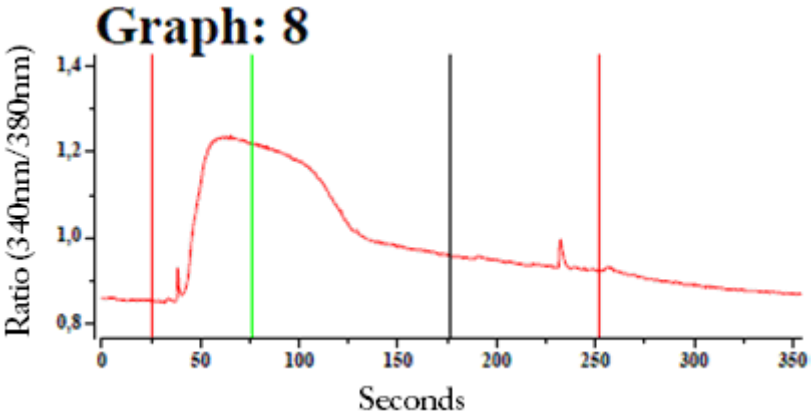

Figure 4.17: *The only cell from this recording that did respond to both K^+-ion change and capsaicin. The capsaicin peak is of typical shape, but could be more robust.*

However, repeating the experiment many times with cells from the same batch 11 showed some variation in the cell reactions. The capsaicin responses were sometimes seen on one from twenty cells but sometimes there was a more random looking response with many cells responding at different times in a time frame of 50 seconds. In Figure 4.18 is an example of many cellular responses that shows the large variance. In the same figure can also be seen that some cells have calcium signaling activity all the time or start having it after capsaicin exposure at random. So the capsaicin might disrupt the normal cell signaling more permanently. It seems that the response to capsaicin here is either delayed as administration of substance is too slow or perhaps something else activates the cells the second time.

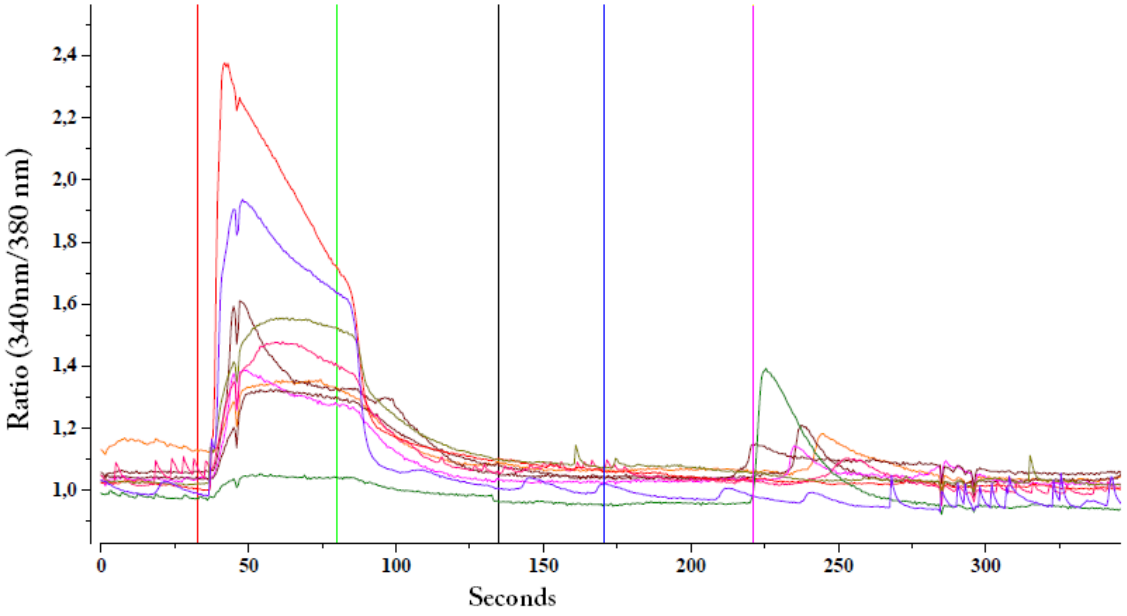

Figure 4.18: *The best ratios from one Ca-imaging measurement combined in one graph. The vertical red line represents iso-osmolaric change of Na^+-ions to K^+-ions in perfusion, green line is wash-out of extra K^+-ions, black line is, not important, adjustment of camera, blue line is addition of capsaicin and pink line wash-out of capsaicin.*

If studying more closely some of the curves in Figure 4.18, first of all, the red curve shows strongest response to K^+-concentration, but no response to capsaicin. The purple curve responds to K^+-concentration but also has small calcium activity all the time and after capsaicin addition the signal is disrupted more than others. The green curve has smallest response to K^+-concentration, but very robust to capsaicin. This reaction occurs at wrong time to be caused just by change in osmolarity from changing capsaicin back to normal perfusate as the new liquid has not reached the cells yet, which can be seen if comparing the curves after the red vertical line and the pink vertical line. A strong but delayed response to capsaicin is also seen in Figure 4.19. This time capsaicin was administered first and K^+-concentration changed later to see if this has effect on responses. It was hypothesized that strong K^+-reaction might deplete the cells of calcium and they would just be unable to respond to capsaicin as strongly as possible. The measurements proved that order of perfusate changes does not have much effect on cellular responses.

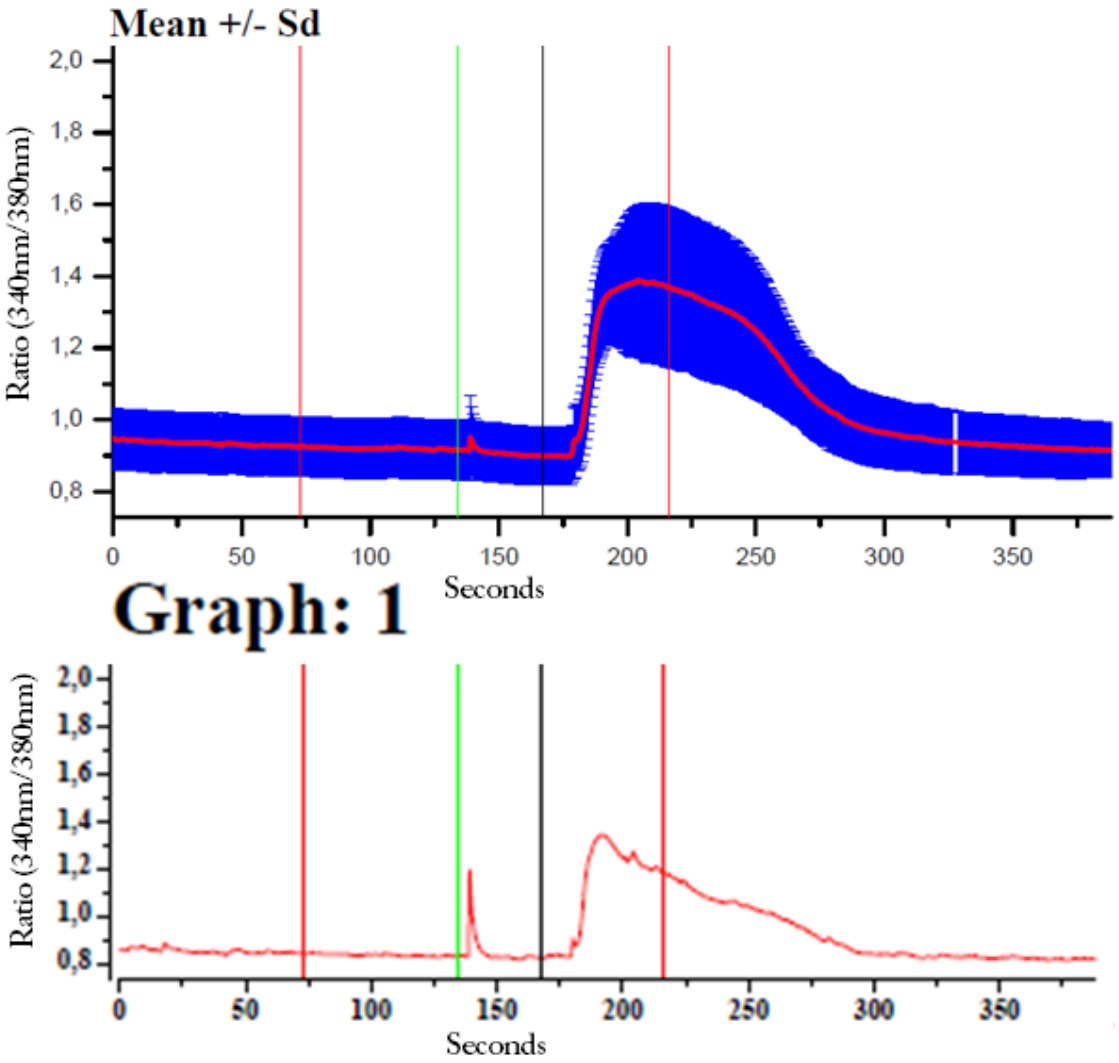

Figure 4.19: *The mean of ten different cells drawn with standard deviation and the curve of the one cell that did have robust response to both substances and very sharp rise in capsaicin response. First red line is capsaicin addtition, green is capsaicin wash-out, black is iso-osmolaric change of Na^+-ions to K^+-ions in perfusion, second red line is wash-out of extra K^+-ions.*

The capsaicin response seems often to be delayed but it cannot be anything else than capsaicin, as the intervals after each perfusate change are too short for the change to have effect yet. This can be seen when comparing Figure 4.19 with Figure 4.17 and Figure 4.18 where the capsaicin administration times are different but both have the capsaicin response peak at slightly over 100 seconds after capsaicin addition. So, faster pumping or longer capsaicin administration would have been needed if there had been more time for these measurements. However, even with this data it seems that the differentiated cells actually were C-fiber-like peripheral sensory neurons.

4.5 Characterization of ECM protein coatings

A large part of the functionality of the coatings used in cell culture is based on their biochemical characteristics, as reviewed in the Chapter 2.4, but there are also physical characteristics that differ between ECM protein coatings and that can have an effect on the success of cell culture. The thickness and topography of the coating as well as hydrophobicity caused by surface tension can affect cell attachment a lot. It would be important to distinguish the reasons why one coating works better than another and is it based on biochemical functionality or can similar results be achieved with chemically different coatings having same physical characteristics. However, these characteristics proved to be more difficult to measure accurately than was assumed.

4.5.1 Fluorescent labeling

Fluorescent labeling protocol was formed based on immunocytochemistry protocol and tested a few times in this work and already in other studies as well. The concentration used in cell culture for laminin was higher than for fibronectin, which caused labeled laminin samples to be brighter than fibronectin. The Figure 4.20 shows the different features seen in micrographs of fluorescent labeled laminin and fibronectin coatings. The fixation methods tested for preserving coatings in a more natural state did not actually help much. Samples treated with fixative before coating had features that looked like detached shreds of coating sheet floating around and more brightly fluorescent debris. The fixatives can bind antibodies as well, causing small false positive areas to be seen in non-coated areas.

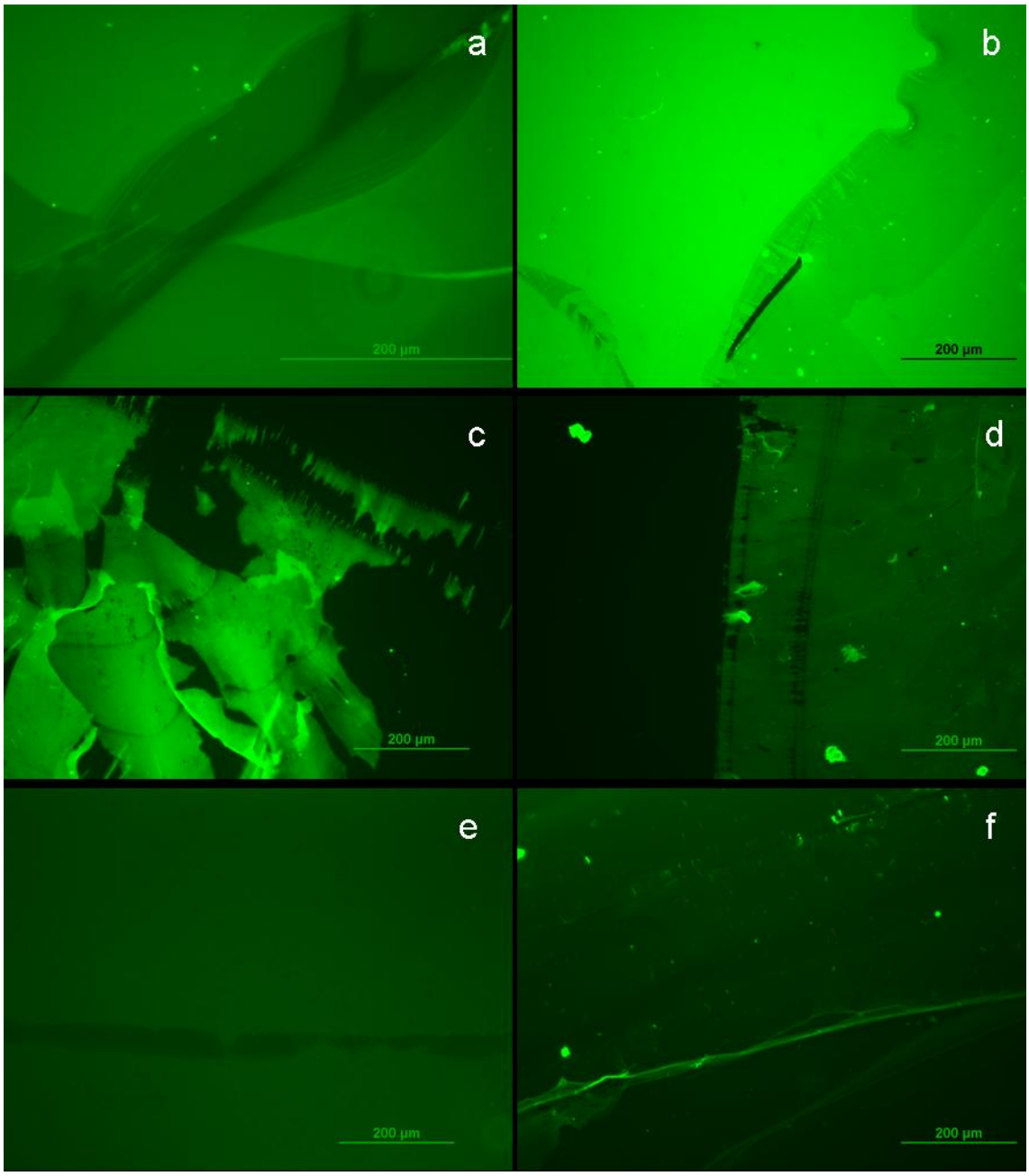

Figure 4.20: *ECM protein coatings labeled with green fluorescence. A) Micrograph for middle of laminin coating shows the layered structure. B) Layered structure and a small scratch on laminin coating. C) The edge of laminin coating made by coating only half of cover slip. The feature could be caused by liquid receding because of drying. D) A very sharp edge of laminin coating and false positive debris on the left. E) Even and flat fibronectin coating. F) Fibronectin coating that has started to detach from surface as a thread or sheet. Scale bar length 200 µm.*

From these micrographs it can be concluded that coatings do cover the whole surface where the coating liquid is applied, but the coating topography is by no means flat everywhere. Especially laminin seems to attach on top of other laminin layer, this creates more features and contours to focus on when studying the surface with microscope,

as in Figure 4.20a. A totally uniform monocolored layer is difficult to take pictures of as there is no place to focus on, even though it could be good result of uniformly coated surface. As used fibronectin concentration was only a fraction of the used laminin concentration, it is no wonder that there is seen more coating material on laminin coated wells compared to fibronectin coated ones. The proteins also attach to themselves more firmly than on the glass surface as they can detach from the surface as sheets or shreds.

4.5.2 AFM imaging of ECM protein coatings

The AFM pictures show that the ECM coatings on used surfaces are not flat or uniform, but have many topographical features. The interpretation of AFM pictures is not simple as one mostly has to rely on reference data during qualitative analysis. All the coating materials studied in this thesis have also been studied with AFM in some other published data, to some degree at least, so reference images are available.

The uncoated glass cover slip was imaged, to know what kind of topography there is without any added proteins. From Figure 4.21 can be seen that the surface is not flat, but has averagely 5 nm features all over it, with some larger different areas as well. This can be uneven glass surface, or it can be small dust and debris, as the cover slips are straight from the package but not cleaned.

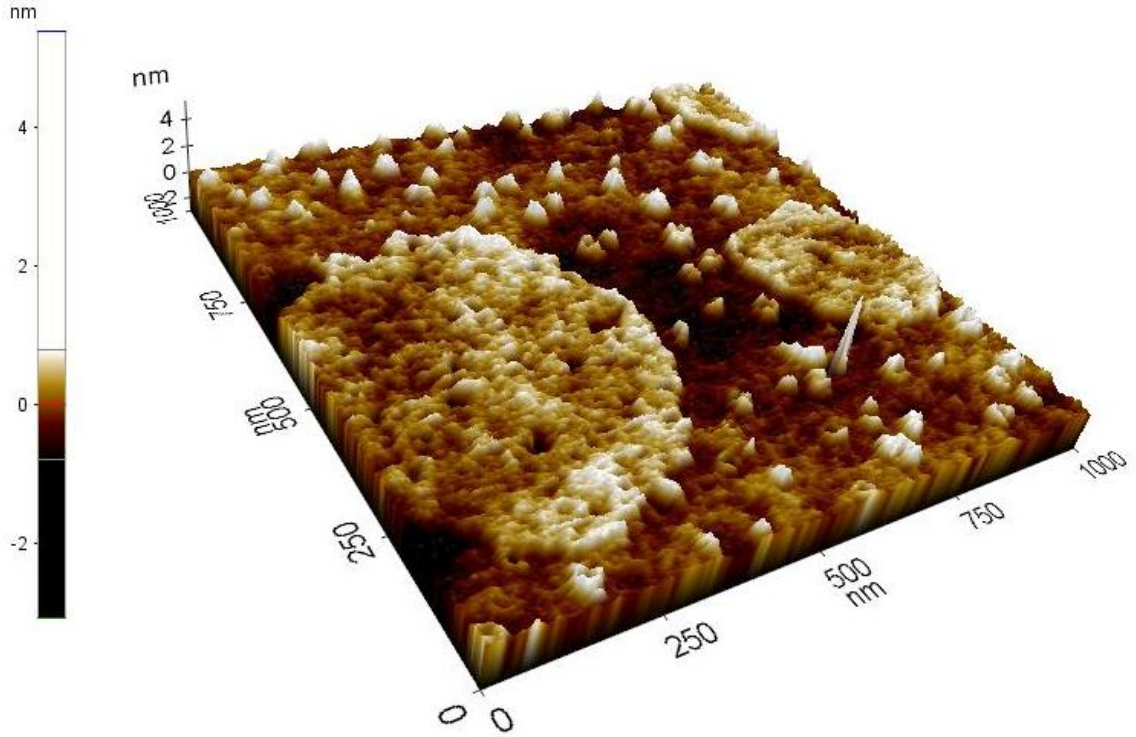

Figure 4.21: *3D view AFM image of cover slip straight from the package. The surface has topographical features at height of five nanometers and width of even 500 nm.*

The gelatin coating, which is a standard coating for our cell cultures, is seen on AFM images as a smooth surface with 500 nm high peaks at random intervals of some tens of micrometers. These peaks could be non-dissolved gelatin crystals or some gelatin aggregates. Gelatin coating was only imaged as air-dried. In Figure 4.22 is shown an AFM image of gelatin coating, in the image the high peaks produce large imaging artefact on the horizontal and vertical lines. The reference in Figure 2.14a has higher gelatin concentration, so the peaks are closer to each other, but the two images are so similar, that it can be confirmed this is what gelatin coating generally looks like if concentration is under 1 %.

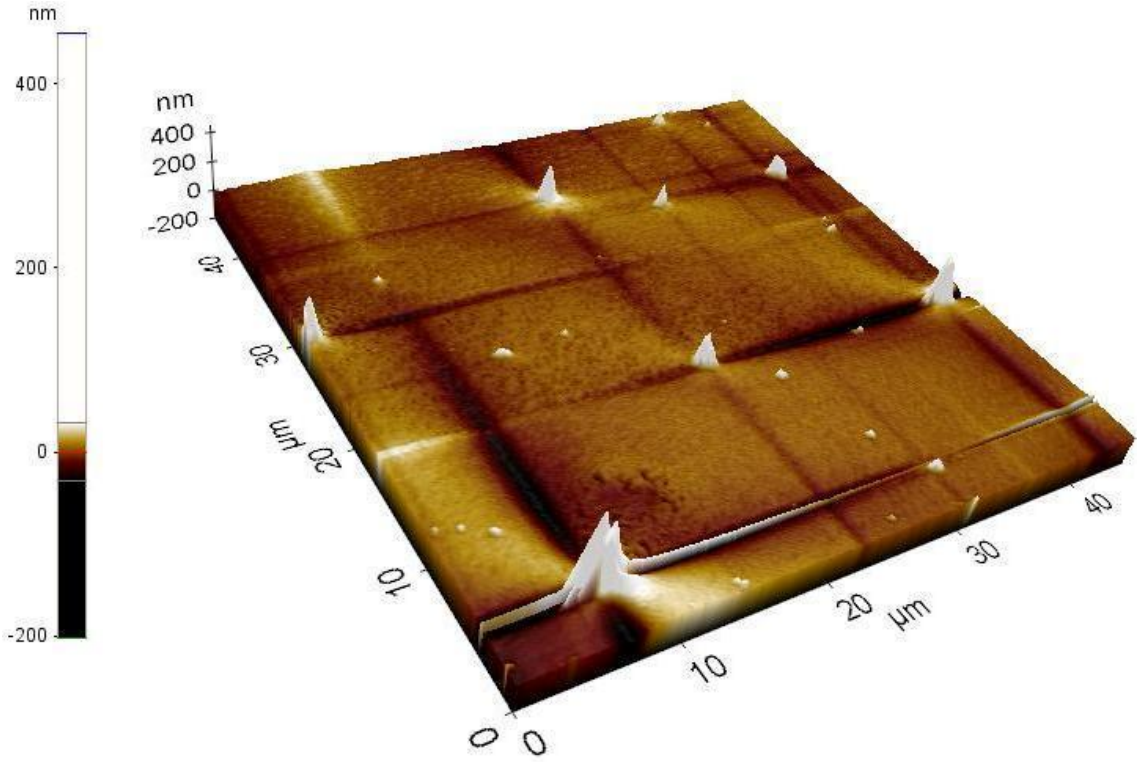

Figure 4.22: *AFM image of gelatin coated cover slip from 3D view. The inherent topography of the slip is no longer seen and gelatin is seen to form aggregates or crystals at random intervals. Dark areas emanating from peaks are imaging artefacts. The scanned area size is 45x45 µm.*

The laminin coating was imaged as air-dried and as a glutaraldehyde fixed version and they looked very different compared to each others. The air-dried laminin coating looks like it has crystallized, while fixed laminin coating has repetitive round shapes. The size of laminin molecules is in same range as the features seen in Figure 4.23, which increases the possibility of this actually being what laminin coating looks like. Most of the higher plateau parts in Figure 4.23 left image are around 40-50 nm high, which is known to be the length of laminin-1 short arms, so this could be what is in the image. In the right image, first of all the flat looking area is a lot more flat than in the left picture, the height variance is about 3 nm, while in the left image it is about 10 nm. One domain of a laminin molecule is known to be about the size of 3-4 nm. The large shapes in the lower image are about same height as most of the highest areas in the upper image as well.

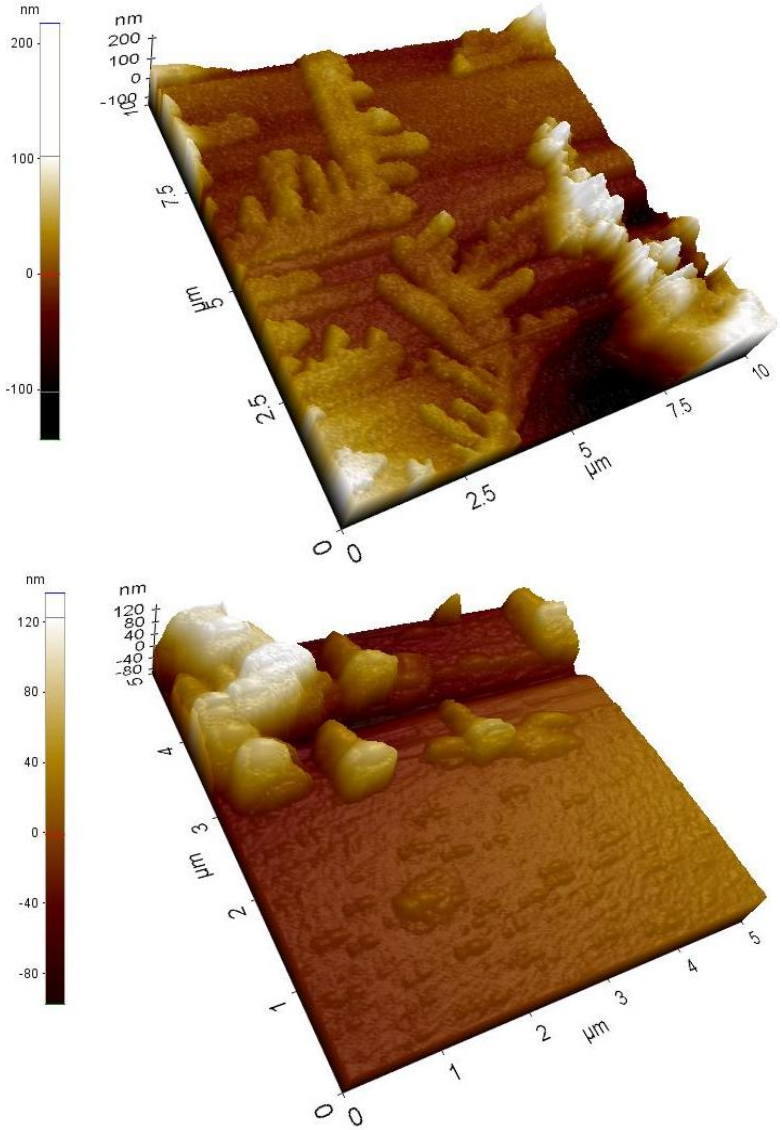

Figure 4.23: *AFM images of laminin coatings. The left image is air-dried laminin coating, scanned area 10x10 µm and the lower right image is glutaraldehyde fixed laminin coating with scanned area 5x5 µm.*

Fibronectin coating was only imaged in air-dried form. From the AFM images of fibronecting can be seen very large fiber structures that could be fibronectin fiber bundles or again crystallized fibronectin. The smallest features in Figure 4.24 are around the same size, few hundred nanometers, as known dimensions of fibronectin molecules, but most of the features shown here are of far greater size than any in the other AFM imaged samples. The fibronectin concentration used was 500 times less than used laminin concentration, so it seems odd that the fibronectin features are so much larger, or at least it cannot be because of concentration. The features in reference image are in totally different scale than in our image, so conclusions are hard to make.

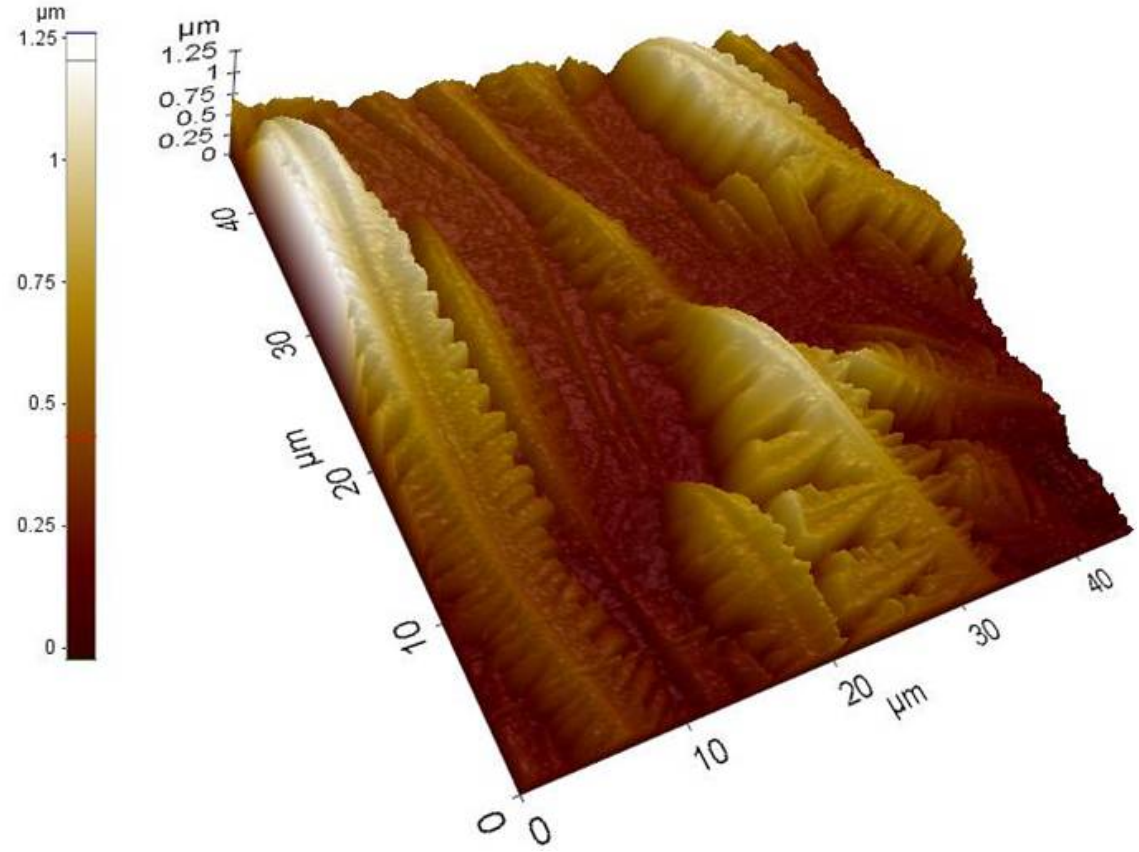

Figure 4.24: *AFM image of fibronectin sample, air-dried fibronectin coating with scanned area 45x45 µm and with features of micrometer scale.*

Matrigel™ was imaged in both air-dried and glutaraldehyde fixed forms, but we were unable to get good images from the glutaraldehyde fixed samples. In the air-dried samples in Figure 4.25 the shape looks crystallized as well. The reference image in Figure 2.14 could be taken from the middle of our Matrigel™ image, so it cannot be said which is more representative of a whole and the reference is also made from larger concentration of coating liquid [79]. The resemblance between Matrigel™ and laminin images is not surprising, as laminin is important part of Matrigel™. However, there is a larger height variance on the higher parts of the Matrigel™ image, ranging from 100nm to over 300 nm.

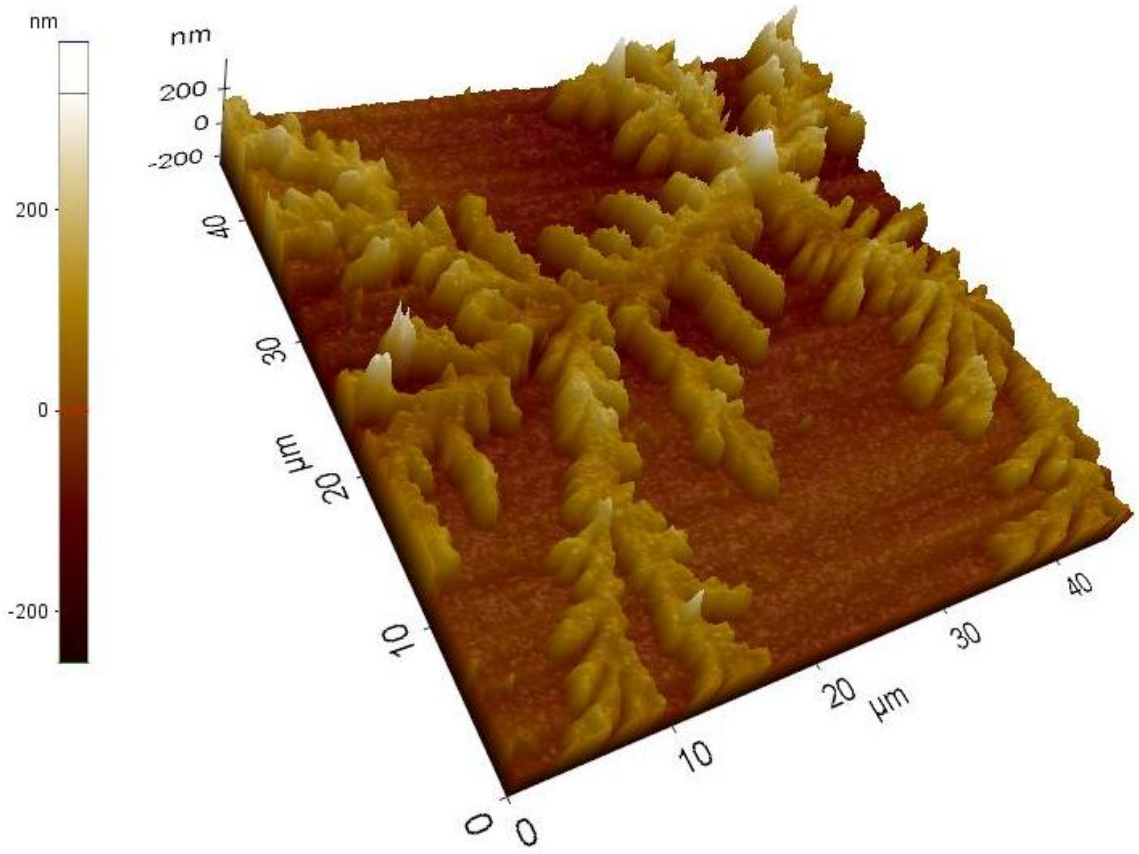

Figure 4.25: *AFM image of Matrigel™ coating, air-dried, scanned area 45x45 µm.*

As a conclusion from AFM images, it can be said that all the studied coatings did look different, but without further study of many more reference images, it is not possible to tell, what is actually seen in the AFM images. The gelatin and Matrigel™ images seem to be most like their references, so they are more reliable. From all the images it can be said that the surfaces are not at all flat, even if nothing can be seen in phase contrast microscopy of these coatings. The coating thickness varies a lot, but imaging the edge on half coated cover slips did not succeed, so the exact thickness could not be measured with this protocol.

4.5.3 Contact angle

The contact angle measurements show that the plain surfaces without coating are not as hydrophilic as coated surfaces, as was expected. There are differences in hydrophilicity between surfaces, which can affect the cell attachment, but more studies would be needed to draw conclusive results on contact angle and surface tension effect on cell attachment in these cases. It was also seen that using cell culture medium instead of water as contact fluid does not affect the measured surface tension much, but the medium does behave very differently during the measurement than water, as seen in Figure 4.26. The measurement is trickier to do with medium, even though the end results are very similar. The contact angle results are shown in Figure 4.27.

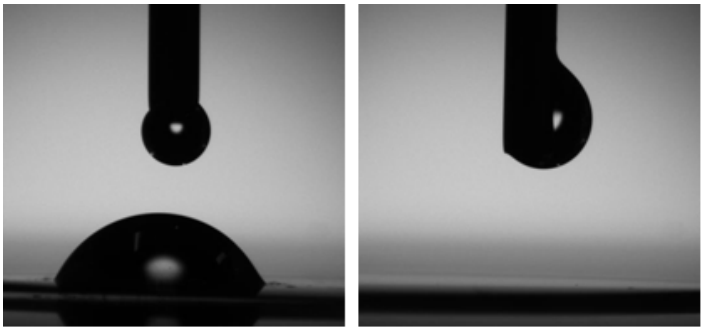

Figure 4.26: *Examples of liquid behavior in contact angle measurement when pushed out of the capillary on fibronectin coated cover slip. On the left water drop is dropping right from the capillary tip and on the right the cell culture medium drop starts to climb the capillary immediately after getting out of the tip and is difficult to administer on the surface.*

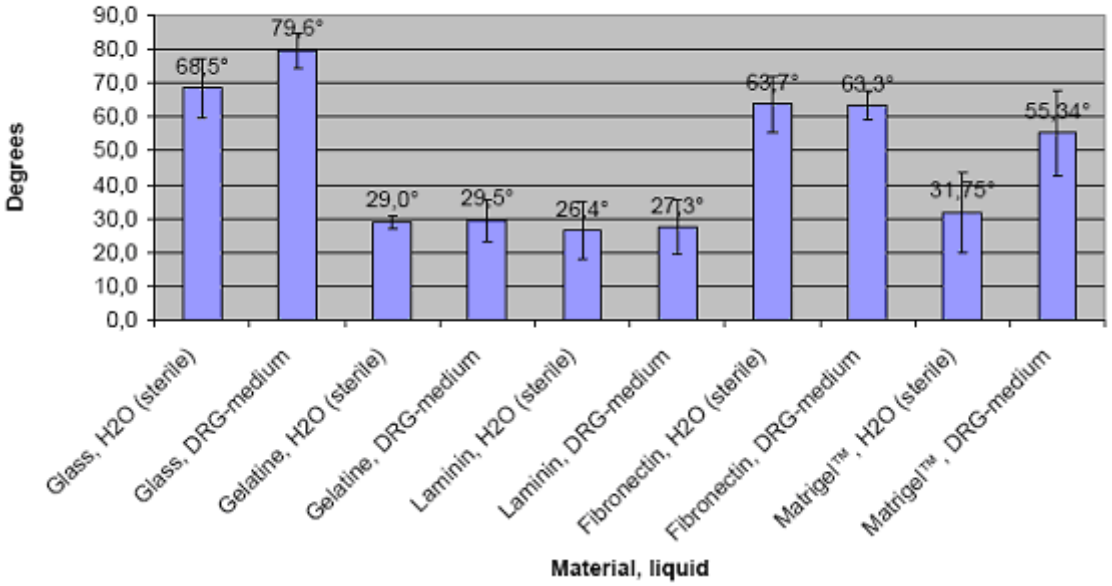

Figure 4.27: *Results of the contact angle measurements shown with contact angle in degrees and different coating material-liquid pairs and glass surface used as control and substrate for coating.*

The smallest contact angles and so smallest surface tension is with gelatin and laminin coatings, independent of contact liquid used. Fibronectin was used in this whole study at lower concentration than laminin, which might explain the large difference between them. This also shows that even if the proteins have denatured partly while drying, they still affect the hydrophilicity of the surface and through that would affect the cell attachment as well. Matrigel™ coated surfaces were difficult to measure, as the coating was visibly not flat and so the exact contact angles were not so accurately measured and the results for Matrigel™ here should be viewed with caution and the error bar could be taller than just standard deviation. The only material with large variance in contact angle between water and culture medium is Matrigel™, but due to slight difficulties in both use of medium as contact liquid and measurements on Matrigel™ surface, this would need more studies to confirm the large difference in surface tension. However, all the tested surfaces were clearly hydrophilic as the definition of hydrophobicity is 90° contact angle. This confirms that the theories for protein and cell attachment on hydrophilic surfaces are the ones to be used for these materials and that ECM coating does make glass surface more hydrophilic.

5 DISCUSSION

Two different areas were studied in this thesis, the differentiation of pluripotent stem cells into functioning peripheral neural cells and the use of extracellular matrix proteins as coatings in the neural cell culture. The differentiation protocol was successful and the results were reproducible, but the exact subtype or types of the differentiated cells were difficult to distinguish. Mostly based on calcium imaging data the differentiated cells can be called as putative C-fiber-like peripheral neuronal cells. The study of ECM protein coatings showed that they have differences in their physical characteristics as was assumed. More studies on coating would be needed to draw conclusions on how the characteristics affect the cells.

5.1 Differentiation into peripheral neural cells

The SDIA-protocol used has three distinct phases and is most importantly based on the inducting activity of mouse PA6 stromal cells, and the cell process outgrowth supporting effect of NGF. The morphology of cells produced with this protocol is definitely neuronal as seen in both light microscopy and fluorescent immunocytoshemistry micrographs. Their active genes were tested with RT-PCR and their functionality with calcium imaging and those results are promising but would still require more studies. Especially RT-PCR should be optimized on more in later studies.

When the differentiation was successful, the processes and networks often grew in such lengths that they could not possibly be representatively shown in micrographs. At largest, the networks could even be seen by plain eye. When studying the immunocytochemistry results, it was noted that the background fluorescence fades quickly, so the peripherin positive cells are much more distinctive when photographed a few days after the dyeing than right on the same day. The background staining also interferes with Brn3a and TRPA1 results and makes them harder to analyze, so in most cell batches only the peripherin staining was certain.

As the differentiation success in this study was good, in later peripheral neural differentiation studies would be advisable to use the Chambers et al. 2012 [15] small molecular inhibition protocol, which yields a lot faster differentiation and even though it was developed for general neural differentiation, it seems to lean towards peripheral and nociceptive neurons, so exactly what was the objective of this study as well. Both the accelerated differentiation and better yield percents are in favor of that protocol over the SDIA-protocol.

The PA6 cells can be changed to ECM protein coatings that induce neuronal differentiation as well. The cultures on ECM protein coatings did produce bipolar neuronal

cells, but the efficiency was not even nearly as good as with PA6 cells. ECM protein coatings also mostly failed to produce the larger neural networks, which were achieved with PA6 cells. The three different ECM protein coatings: laminin, fibronectin and Matrigel™ were also compared to each others and with gelatin, which is the standard coating used in our laboratory. All these ECM protein coatings have slight differences and it seems that laminin would be the best one for this application, but more studies are required to make further distinction between them.

At the final phase of differentiation, if the cells were on one of these coatings, they did become bipolar, but then they did not differentiate further into pseudounipolar structures, that would indicate their maturity. So perhaps the differentiation does start over ECM coating, but does not go further because of the lacking effect of PA6 cells. Another fact to consider is that attachment over the coatings is poorer than on co-culture and thus less cells are interacting with each other and they have difficulty producing a network as they are so few. However, the two successful cases with larger peripherin positive neural-like networks of laminin means that differentiation is possible on coatings without PA6 feeder layer or PA6 conditioned medium, if enough cells attach. So the cell attachment on these coatings should also be studied more, to get to know all the factors affecting it. It would be interesting to combine PA6 co-culture with laminin coatings to see if the differentiation success is increased further.

5.2 Characteristics of ECM coatings

It seems, rather surprisingly, that even though there is a great variety of coating protocols in literature to use for ECM proteins, a simple method of adding the protein containing PBS liquid on top of the substrate for one hour, or more, incubating in room temperature and then removing the liquid is enough to coat cell culture grade polystyrene or glass. Incubation in +37 °C or overnight in +4 °C or for a couple of hours in room temperature does not seem to produce different coating characteristics. The exception here is Matrigel™, which is stored in freezer and when used first needs to be thawed on ice or in +4 °C and needs to be handled with cold equipment when used in coating as its gelation can occur partially very fast. And when gelled, it does not redissolve when cooled, so in general Matrigel™ is a trickier coating material than the others used in this study. Neither are coatings liquids let to dry, because of our hypothesis that it causes crystallization and denaturation of proteins, even though it is also used in some protocols, for example by Moran et al. 2007 [93]. And for example it is even said that letting a laminin coating dry will clearly reduce the biological activity, at least for laminin-8 which is apparently more sensitive for drying than laminin-1, as studied by Kortesmaa et al. 2000 [69].

The concentrations of coating liquids used in this study were based on previous studies at our laboratory, but varing them could have been a good aspect to study here. For example, Cunnigham et al. 2002 [101] stated that theoretical saturation density of fibronectin over a surface is 1 $\mu g/cm^2$, but on other fibronectin adsorption studies, for

example Lhoest et al. 1998 [83] there are concentrations as high as 500 μg/cm^2, which is rather confusing. An explanation to this might be the protein folding and different conformations over the surface, as was stated in Chapter 2.4.1 Figure 2.9, but if approaching a research plan theoretically, there would be needed more information on the protein adsorption theory. It is also stated by Lhoest et al. 1998 [83] that over polystyrene substrates fibronectin undergoes more significant denaturation at smaller concentrations than at higher ones because larger parts of the protein are accessible to hydrophobic interactions, which are prevented by higher amount of protein-protein interactions. For studying protein attachment and effects of concentration of coating liquid, the QCM-D method would be interesting and suitable.

In general the use of advanced coating methods and finding the perfect coating-surface pair for the desired cell type is a work requiring lot of literature reviewing, which is why in this work the coatings were done in the most conventional and easy way. The laminin-1 used in this study is the most easily available and cheapest isoform of laminin, but it might not be the best for peripheral nerve studies. The different isoforms have been proven to have different functions around the body and concentrate on different tissues. So laminin-2, -3, or -4 might have produced different and even better results as they are present in the peripheral neural tissue. This should be considered when continuing work with laminin.

It was repeatedly noticed in this study, that the PSN neurites grow along edges of cover slips or parallel to edges so much that the edges seems to induce neurite outgrowth. This is related to other studies [66] on how adjacent tracks of adhesive laminin and non-adhesive surfaces orientate the neurite growth. However, the sizes of these topographical changes need to be in same range as the neurite growth cone, as too large or narrow adjacent tracks do not have the same effect as the cell filopodia needs to sense the edge of the coating and the plastic. This also means that an even and flat coated surface is not the most wanted result when producing coatings for cell culture.

One of the most useful outcomes of this study was establishing and testing a fluorescent labeling protocol for ECM coatings without cells. This protocol can be used to verify protein functionality in other studies as the antibody binding in the fluorescent labeling implies that the protein is in functional form and cells could attach to it as well. This protocol has already been used for preliminary studies of ECM proteins covalently bonded polymer surfaces and to hydrogels functionalized with ECM proteins.

The atomic force microscopy is a rather difficult to use characterization method for ECM coated surfaces. Good references would be needed to analyze what exactly is seen in the pictures as the AFM only shows surface topography but does not provide information about the chemical composition in question. It is very difficult to know what is a representative AFM picture and what is an anomaly, if the material studied is not well known beforehand. As performing atomic force microscopy on biological samples and more specifically on ECM protein coatings had not been done before in our laboratory, useful knowledge was learned about AFM on protein coatings. First of all, the coatings produced are not uniform, but clusters of proteins gather on seemingly random sites of

the surface even though fluorescent labeling shows that the whole surface is covered with proteins. And the proteins seem attach as layers, probably because attachment on top of another protein is more energetically favorable than attachment on glass. The best resemblance of our AFM image with a reference image was with gelatin coating, as shown in Figure 5.1.

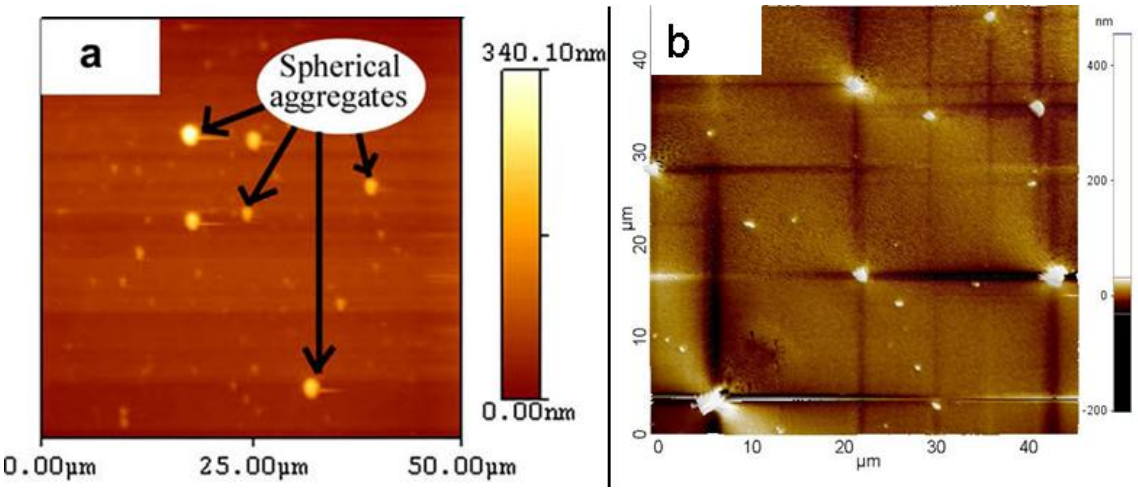

Figure 5.1: *Comparison of AFM images from gelatin coating. A) Reference image from Yang and Wang 2009* [58]. *B) Our image already shown in Figure 2.14 in similar top view as reference.*

The fixation of proteins on the surface by bonding them covalently with PFA or glutaraldehyde does not help to produce more easily interpreted pictures as the fixation molecules cannot be distinguished from ECM proteins by conventional topography mode. As the coatings seem to be rather firmly attached anyways, it is best to just use AFM on the coated surface as it is. The denaturation or crystallization or proteins was suspected, but cannot be confirmed with the simple AFM modes used. The use of AFM wet cell to image inside liquid would have been very interesting option, if that equipment had been accessible and usable. Also atomic force spectroscopy mode of AFM would have been interesting and is advisable, for someone continuing to study coatings on AFM. Immuno-AFM could be used to gain more information on protein functionality and to distinguish between proteins and fixation molecules. All of these would have been interesting possibilities to study the ECM protein coatings, but refining the protocols for these methods would have taken too long time for a master's thesis where AFM is not even the main research method. AFM is a promising and versatile study method of which more experience is needed to utilize it to the fullest and would be suitable subject for master's thesis on its own.

Contact angle measurement showed significant differences between coated surfaces and control samples in hydrophilicity. However, the use of water or cell culture medium as contact liquid does not have great difference, as the results are within the standard deviation of measurements. The gelatin and laminin coatings have the lowest surface tension and clean cover slip glass surface has the highest, which shows why the cover slips need to be coated before use in cell culture. This also confirms that protein attach-

ment on the surface occurs via more hydrophilic than hydrophobic interactions. To make contact angle measurement, the surface needs to be relatively dry, otherwise the used liquid will spread into 0° contact angle independent of liquid or material. This means that contact angle measurement does not represent the surface in exact same condition as in cell culture, where it is kept wet at all times to prevent possible protein denaturation, but it still shows that coating materials or at least coating concentrations have differences, even when dry. The requirements for surface hydrophilicity can also change by cell type, as here the best results for peripheral neurons were gained with materials with contact angles of 26- 29°, but for example the data by Ma et al. 2007 [49] the best contact angle for chondrocytes is seen as 76° and for epithelial cells as 70° on polycaprolactone-polymethacrylic acid surface.

Throughout the experiments, it would have been good to have polystyrene cover slips as one reference material, especially since cells seemed to differentiate more eagerly on polystyrene than on glass surface, regardless of the coating. However, commercial polystyrene cover slips have different surface treatment done at the manufacturer than the cell culture plate bottoms have. We could not get data from the manufacturer on how these surface treatments actually differ, but it can be assumed that they do differ as they have different trademarks, NunclonΔ for culture plates and Thermanox™ for slips [100]. Also the possibility of cutting off cell culture plate bottoms and studying them was not used, due to lack of time. If the coating studies are continued, this should be done to get another control. The polystyrene cover slips should also be tested in cell culture, if they have higher degree of differentiation than glass slips, then the cells used for calcium imaging could be grown on polystyrene slips as well.

6 CONCLUSIONS

The aim of this thesis was to produce peripheral neuronal cells from human induced pluripotent stem cells and validate that the used differentiation protocol is reproducible. These kinds of cells are needed for example for high-throughput screening of drugs with cell functional analysis methods such as calcium imaging. Peripheral neuronal cell produced from iPS cells also open a possibility of creating disease models as has already been done with other cell types, for example cardiomyocytes produced from iPS cells can be used to study genetic heart diseases [52]. The stem cells did differentiate into neural-like cells with high certainty, regardless whether they were hiPS cells or hESCs and with all the used cell lines. The subtype of neurons produced in this study is putative C-fiber-like peripheral sensory neuron, but some of the results are uncertain and the cell cultures are not purely PSN. But as a conclusion from all the cell characterization methods, it can be said that some of the cells were peripheral neurons. The cell culturing results were also slightly different between different batches of cells, even within one cell line in one batch the cells can have very different differentiation success in neighboring culture wells, but this is part of these biological processes.

Coating a cell culture well or cover slip with ECM proteins by applying the coating liquid and incubating in room temperature for one hour is enough to cover these surfaces with bioactive ECM proteins, on which cells can attach and differentiate. These coatings cannot be used to directly replace the PA6 co-culture in the used PSN differentiation protocol, as the differentiation success will drop dramatically. However, laminin was the best candidate for replacing PA6 co-culture, but results were not as reproducible as with PA6 cells. Combining PA6 co-culture with laminin coating would be interesting next step, if continuing with this differentiation protocol.

The used ECM protein coatings do differ from each others in both hydrophilicity and topography. AFM imaging is usable way for studying coatings, but more time is needed on tuning the method and for interpretation of the images. The fixation of coatings with glutaraldehyde or paraformaldehyde is not necessary and could even produce artefacts. Fluorescent labeling of ECM protein coatings with antibodies is a good method for visualizing the coating and studying coating methods. The labeling defined here has already been used in studying also hydrogels and microcontact printing results.

Important next step in PSN differentiation would be defining the produced cells better and comparison of the protocol used here with the small molecular inhibitor protocol published this autumn [2; 15]. The PSN cell phenotype, protein expression and functionality should be studied more. It also seems that some cell lines differentiate toward peripheral neurons more easily than others and this should be confirmed as well.

7 REFERENCES

[1] Takahashi K, Tanabe K, Ohnuki M, Narita M, Ichisaka T, Tomoda K, et al. Induction of Pluripotent Stem Cells from Adult Human Fibroblasts by Defined Factors. Cell 131(2007)5, pp. 861-872.

[2] Pomp O, Brokhman I, Ziegler L, Almog M, Korngreen A, Tavian M, et al. PA6-induced human embryonic stem cell-derived neurospheres: a new source of human peripheral sensory neurons and neural crest cells. Brain research 1230(2008)0, pp. 50-60.

[3] Goldstein RS, Pomp O, Brokhman I, Ziegler L. Generation of neural crest cells and peripheral sensory neurons from human embryonic stem cells. Methods in molecular biology (Clifton, N.J.) 584(2010) pp. 283-300.

[4] Haug E, Sand O, Sjaastad ØV, Toverud KC. Ihmisen fysiologia. 1.-2. ed. Porvoo; 1995: WSOY pp. 56-57, 64-67, 75, 102-106, 132-137, 150-152, 231, 305, 492-493, 497.

[5] Ylä-Outinen,Laura. Functionality of human stem cell derived neuronal networks : biomimetic environment and characterization. Tampere; 2012 Tampere University Press pp. 18-21, 26-32.

[6] Kumar KK, Aboud AA, Bowman AB. The potential of induced pluripotent stem cells as a translational model for neurotoxicological risk. Neurotoxicology 33(2012)3, pp. 518-529.

[7] Liu SV. iPS cells: a more critical review. Stem cells and development 17(2008)3, pp. 391-397.

[8] Sariola H, Frilander M, Heino T, Jernvall J, Partanen J, Sainio K, et al. Kehitysbiologia : solusta yksilöksi. 1.th ed. Helsinki; cop. 2003: Duodecim 311 s.

[9] Jiang X, Gwye Y, McKeown SJ, Bronner-Fraser M, Lutzko C, Lawlor ER. Isolation and characterization of neural crest stem cells derived from in vitro-differentiated human embryonic stem cells. Stem cells and development 18(2009)7, pp. 1059-1070.

[10] Lee G, Kim H, Elkabetz Y, Al Shamy G, Panagiotakos G, Barberi T, et al. Isolation and directed differentiation of neural crest stem cells derived from human embryonic stem cells. Nature biotechnology 25(2007)12, pp. 1468-1475.

[11] Joseph NM, Mukouyama YS, Mosher JT, Jaegle M, Crone SA, Dormand EL, et al. Neural crest stem cells undergo multilineage differentiation in developing peripheral nerves to generate endoneurial fibroblasts in addition to Schwann cells. Development (Cambridge, England) 131(2004)22, pp. 5599-5612.

[12] Pavan WJ, Raible DW. Specification of neural crest into sensory neuron and melanocyte lineages. Developmental biology 366(2012)1, pp. 55-63.

[13] Pomp O, Brokhman I, Ben-Dor I, Reubinoff B, Goldstein RS. Generation of Peripheral Sensory and Sympathetic Neurons and Neural Crest Cells from Human Embryonic Stem Cells. Stem cells 23(2005)7, pp. 923-930.

[14] Dhara SK, Hasneen K, Machacek DW, Boyd NL, Rao RR, Stice SL. Human neural progenitor cells derived from embryonic stem cells in feeder-free cultures. Differentiation 76(2008)5, pp. 454-464.

[15] Chambers SM, Qi Y, Mica Y, Lee G, Zhang XJ, Niu L, et al. Combined small-molecule inhibition accelerates developmental timing and converts human pluripotent stem cells into nociceptors. Nature biotechnology (2012).

[16] Brokhman I, Gamarnik-Ziegler L, Pomp O, Aharonowiz M, Reubinoff BE, Goldstein RS. Peripheral sensory neurons differentiate from neural precursors derived from human embryonic stem cells. Differentiation 76(2008)2, pp. 145-155.

[17] Baron-Van Evercooren A, Kleinman HK, Ohno S, Marangos P, Schwartz JP, Dubois-Dalcq ME. Nerve growth factor, laminin, and fibronectin promote neurite growth in human fetal sensory ganglia cultures. Journal of neuroscience research 8(1982)2-3, pp. 179-193.

[18] Woolf CJ, Ma Q. Nociceptors—Noxious Stimulus Detectors. Neuron 55(2007)3, pp. 353-364.

[19] Curchoe CL, Maurer J, McKeown SJ, Cattarossi G, Cimadamore F, Nilbratt M, et al. Early acquisition of neural crest competence during hESCs neuralization. PloS one 5(2010)11, pp. e13890.

[20] Li XJ, Du ZW, Zarnowska ED, Pankratz M, Hansen LO, Pearce RA, et al. Specification of motoneurons from human embryonic stem cells. Nature biotechnology 23(2005)2, pp. 215-221.

[21] Liem RK, Messing A. Dysfunctions of neuronal and glial intermediate filaments in disease. The Journal of clinical investigation 119(2009)7, pp. 1814-1824.

[22] Eriksson KS, Zhang S, Lin L, Lariviere RC, Julien JP, Mignot E. The type III neurofilament peripherin is expressed in the tuberomammillary neurons of the mouse. BMC neuroscience 9(2008) pp. 26.

[23] Gerrero MR, McEvilly RJ, Turner E, Lin CR, O'Connell S, Jenne KJ, et al. Brn-3.0: a POU-domain protein expressed in the sensory, immune, and endocrine systems that functions on elements distinct from known octamer motifs. Proceedings of the National Academy of Sciences of the United States of America 90(1993)22, pp. 10841-10845.

[24] Koivisto A, Hukkanen M, Saarnilehto M, Chapman H, Kuokkanen K, Wei H, et al. Inhibiting TRPA1 ion channel reduces loss of cutaneous nerve fiber function in diabetic

animals: Sustained activation of the TRPA1 channel contributes to the pathogenesis of peripheral diabetic neuropathy. Pharmacological Research 65(2012)1, pp. 149-158.

[25] Leonard DG, Gorham JD, Cole P, Greene LA, Ziff EB. A nerve growth factor-regulated messenger RNA encodes a new intermediate filament protein. The Journal of cell biology 106(1988)1, pp. 181-193.

[26] Xiang M, Zhou L, Macke JP, Yoshioka T, Hendry SH, Eddy RL, et al. The Brn-3 family of POU-domain factors: primary structure, binding specificity, and expression in subsets of retinal ganglion cells and somatosensory neurons. The Journal of neuroscience : the official journal of the Society for Neuroscience 15(1995)7 Pt 1, pp. 4762-4785.

[27] Dykes IM, Tempest L, Lee SI, Turner EE. Brn3a and Islet1 act epistatically to regulate the gene expression program of sensory differentiation. The Journal of neuroscience : the official journal of the Society for Neuroscience 31(2011)27, pp. 9789-9799.

[28] Anand U, Otto WR, Facer P, Zebda N, Selmer I, Gunthorpe MJ, et al. TRPA1 receptor localisation in the human peripheral nervous system and functional studies in cultured human and rat sensory neurons. Neuroscience letters 438(2008)2, pp. 221-227.

[29] Siemens J, Zhou S, Piskorowski R, Nikai T, Lumpkin EA, Basbaum AI, et al. Spider toxins activate the capsaicin receptor to produce inflammatory pain. Nature 444(2006)7116, pp. 208-212.

[30] Hille B. Ion channels of excitable membranes. Sunderland (Mass.); 2001: Sinauer pp. 2-7.

[31] Caterina MJ, Leffler A, Malmberg AB, Martin WJ, Trafton J, Petersen-Zeitz KR, et al. Impaired nociception and pain sensation in mice lacking the capsaicin receptor. Science (New York, N.Y.) 288(2000)5464, pp. 306-313.

[32] Szolcsányi J. Forty years in capsaicin research for sensory pharmacology and physiology. Neuropeptides 38(2004)6, pp. 377-384.

[33] Grienberger C, Konnerth A. Imaging calcium in neurons. Neuron 73(2012)5, pp. 862-885.

[34] Ghosh A, Greenberg ME. Calcium signaling in neurons: molecular mechanisms and cellular consequences. Science (New York, N.Y.) 268(1995)5208, pp. 239-247.

[35] Grynkiewicz G, Poenie M, Tsien RY. A new generation of Ca2+ indicators with greatly improved fluorescence properties. The Journal of Biological Chemistry 260(1985)6, pp. 3440-3450.

[36] Barreto-Chang OL, Dolmetsch RE. Calcium imaging of cortical neurons using Fura-2 AM. Journal of visualized experiments 23(2009)23.

[37] Kujala K, Paavola J, Lahti A, Larsson K, Pekkanen-Mattila M, Viitasalo M, et al. Cell Model of Catecholaminergic Polymorphic Ventricular Tachycardia Reveals Early and Delayed Afterdepolarizations. PLoS ONE 7(2012)9, pp. e44660.

[38] Bevan S, Hothi S, Hughes G, James IF, Rang HP, Shah K, et al. Capsazepine: a competitive antagonist of the sensory neurone excitant capsaicin. British journal of pharmacology 107(1992)2, pp. 544-552.

[39] Simonetti M, Fabbro A, D'Arco M, Zweyer M, Nistri A, Giniatullin R, et al. Comparison of P2X and TRPV1 receptors in ganglia or primary culture of trigeminal neurons and their modulation by NGF or serotonin. Molecular pain 2(2006) pp. 11.

[40] Ohshiro H, Ogawa S, Shinjo K. Visualizing sensory transmission between dorsal root ganglion and dorsal horn neurons in co-culture with calcium imaging. Journal of neuroscience methods 165(2007)1, pp. 49-54.

[41] Venstrom KA, Reichardt LF. Extracellular matrix. 2: Role of extracellular matrix molecules and their receptors in the nervous system. FASEB journal : official publication of the Federation of American Societies for Experimental Biology 7(1993)11, pp. 996-1003.

[42] Stevens MM, George JH. Exploring and engineering the cell surface interface. Science (New York, N.Y.) 310(2005)5751, pp. 1135-1138.

[43] Patterson J, Martino MM, Hubbell JA. Biomimetic materials in tissue engineering. Materials Today 13(2010)1–2, pp. 14-22.

[44] Shin H, Jo S, Mikos AG. Biomimetic materials for tissue engineering. Biomaterials 24(2003)24, pp. 4353-4364.

[45] Brandl F, Sommer F, Goepferich A. Rational design of hydrogels for tissue engineering: Impact of physical factors on cell behavior. Biomaterials 28(2007)2, pp. 134-146.

[46] Bott K, Upton Z, Schrobback K, Ehrbar M, Hubbell JA, Lutolf MP, et al. The effect of matrix characteristics on fibroblast proliferation in 3D gels. Biomaterials 31(2010)32, pp. 8454-8464.

[47] Kasemo B. Biological surface science. Surface Science 500(2002)1–3, pp. 656-677.

[48] Kasemo B, Gold J. Implant surfaces and interface processes. Advances in Dental Research 13(1999) pp. 8-20.

[49] Ma Z, Mao Z, Gao C. Surface modification and property analysis of biomedical polymers used for tissue engineering. Colloids and surfaces.B, Biointerfaces 60(2007)2, pp. 137-157.

[50] Ventre M, Causa F, Netti PA. Determinants of cell-material crosstalk at the interface: towards engineering of cell instructive materials. Journal of the Royal Society, Interface / the Royal Society (2012) pp. 2017-2032.

[51] He W, Bellamkonda RV. Nanoscale neuro-integrative coatings for neural implants. Biomaterials 26(2005)16, pp. 2983-2990.

[52] Kujala,Ville. Human pluripotent stem cell derived cardiomyocytes : differentiation, analysis and disease modeling. Tampere; 2012 Tampere University Press pp. 4, 44-45.

[53] Zhang S. Fabrication of novel biomaterials through molecular self-assembly. Nature biotechnology 21(2003)10, pp. 1171-1178.

[54] Goddard JM, Hotchkiss JH. Polymer surface modification for the attachment of bioactive compounds. Progress in Polymer Science 32(2007)7, pp. 698-725.

[55] Grinnell F. Fibronectin Adsorption on Material Surfaces. Annals of the New York Academy of Sciences 516(1987)1, pp. 280-290.

[56] Wang ,Yifen, Yang ,Hongshun, Regenstein ,Joe. Characterization of Fish Gelatin at Nanoscale Using Atomic Force Microscopy. Food Biophysics (2008)2, pp. 269-272.

[57] Relou IAM, Damen CA, van der Schaft DWJ, Groenewegen G, Griffioen AW. Effect of culture conditions on endothelial cell growth and responsiveness. Tissue and Cell 30(1998)5, pp. 525-530.

[58] Yang H, Wang Y. Effects of concentration on nanostructural images and physical properties of gelatin from channel catfish skins. Food Hydrocolloids 23(2009)3, pp. 577-584.

[59] Martini R. Expression and functional roles of neural cell surface molecules and extracellular matrix components during development and regeneration of peripheral nerves. Journal of neurocytology 23(1994)1, pp. 1-28.

[60] Hsia HC, Schwarzbauer JE. Meet the tenascins: multifunctional and mysterious. The Journal of biological chemistry 280(2005)29, pp. 26641-26644.

[61] Timpl R, Rohde H, Robey PG, Rennard SI, Foidart JM, Martin GR. Laminin--a glycoprotein from basement membranes. The Journal of biological chemistry 254(1979)19, pp. 9933-9937.

[62] Aumailley M, Bruckner-Tuderman L, Carter WG, Deutzmann R, Edgar D, Ekblom P, et al. A simplified laminin nomenclature. Matrix Biology 24(2005)5, pp. 326-332.

[63] Beck K, Hunter I, Engel J. Structure and function of laminin: anatomy of a multidomain glycoprotein. FASEB journal : official publication of the Federation of American Societies for Experimental Biology 4(1990)2, pp. 148-160.

[64] Hohenester E, Tisi D, Talts JF, Timpl R. The Crystal Structure of a Laminin G–like Module Reveals the Molecular Basis of α-Dystroglycan Binding to Laminins, Perlecan, and Agrin. Molecular cell 4(1999)5, pp. 783-792.

[65] von der Mark K, Park J, Bauer S, Schmuki P. Nanoscale engineering of biomimetic surfaces: cues from the extracellular matrix. Cell and tissue research (2010)1, pp. 131-153.

[66] Luckenbill-Edds L. Laminin and the mechanism of neuronal outgrowth. Brain Research Reviews 23(1997)1–2, pp. 1-27.

[67] Powell SK, Kleinman HK. Neuronal laminins and their cellular receptors. The international journal of biochemistry & cell biology 29(1997)3, pp. 401-414.

[68] Wondimu Z, Gorfu G, Kawataki T, Smirnov S, Yurchenco P, Tryggvason K, et al. Characterization of commercial laminin preparations from human placenta in comparison to recombinant laminins 2 (α2β1γ1), 8 (α4β1γ1), 10 (α5β1γ1). Matrix Biology 25(2006)2, pp. 89-93.

[69] Kortesmaa J, Yurchenco P, Tryggvason K. Recombinant laminin-8 (alpha(4)beta(1)gamma(1)). Production, purification,and interactions with integrins. The Journal of biological chemistry 275(2000)20, pp. 14853-14859.

[70] Hynes RO, Yamada KM. Fibronectins: multifunctional modular glycoproteins. The Journal of cell biology 95(1982)2 Pt 1, pp. 369-377.

[71] Potts JR, Campbell ID. Structure and function of fibronectin modules. Matrix Biology 15(1996)5, pp. 313-320.

[72] Wilson K, Stuart SJ, Garcia A, Latour RA. A molecular modeling study of the effect of surface chemistry on the adsorption of a fibronectin fragment spanning the 7-10th type III repeats. Journal of Biomedical Materials Research Part A 69A(2004)4, pp. 686-698.

[73] Klotzsch E, Smith ML, Kubow KE, Muntwyler S, Little WC, Beyeler F, et al. Fibronectin forms the most extensible biological fibers displaying switchable force-exposed cryptic binding sites. Proceedings of the National Academy of Sciences of the United States of America 106(2009)43, pp. 18267-18272.

[74] Koteliansky VE, Glukhova MA, Bejanian MV, Smirnov VN, Filimonov VV, Zalite OM, et al. A study of the structure of fibronectin. European journal of biochemistry / FEBS 119(1981)3, pp. 619-624.

[75] Price TM, Rudee ML, Pierschbacher M, Ruoslahti E. Structure of Fibronectin and Its Fragments in Electron Microscopy. European Journal of Biochemistry 129(1982)2, pp. 359-363.

[76] Kleinman HK, Martin GR. Matrigel: Basement membrane matrix with biological activity. Seminars in cancer biology 15(2005)5, pp. 378-386.

[77] Bilozur ME, Hay ED. Neural crest migration in 3D extracellular matrix utilizes laminin, fibronectin, or collagen. Developmental biology 125(1988)1, pp. 19-33.

[78] Burridge P, Keller G, Gold J, Wu J. Production of De Novo Cardiomyocytes: Human Pluripotent Stem Cell Differentiation and Direct Reprogramming. Cell Stem Cell 10(2012)1, pp. 16-28.

[79] Abrams G,A., Goodman S,L., Nealey P,F., Franco ,M., Murphy C,J. Nanoscale topography of the basement membrane underlying the corneal epithelium of the rhesus macaque. Cell and tissue research (2000)1, pp. 39-46.

[80] Soofi SS, Last JA, Liliensiek SJ, Nealey PF, Murphy CJ. The elastic modulus of Matrigel™ as determined by atomic force microscopy. Journal of structural biology 167(2009)3, pp. 216-219.

[81] Koch D, Rosoff W, Jiang J, Geller H, Urbach J. Strength in the Periphery: Growth Cone Biomechanics and Substrate Rigidity Response in Peripheral and Central Nervous System Neurons. Biophysical journal 102(2012)3, pp. 452-460.

[82] Galtayries A, Warocquier-Clérout R, Nagel M-, Marcus P. Fibronectin adsorption on Fe?Cr alloy studied by XPS. Surface and Interface Analysis 38(2006)4, pp. 186-190.

[83] Lhoest J-, Detrait E, van den Bosch de Aguilar,P., Bertrand P. Fibronectin adsorption, conformation, and orientation on polystyrene substrates studied by radiolabeling, XPS, and ToF SIMS. Journal of Biomedical Materials Research 41(1998)1, pp. 95-103.

[84] Elloumi Hannachi I, Itoga K, Kumashiro Y, Kobayashi J, Yamato M, Okano T. Fabrication of transferable micropatterned-co-cultured cell sheets with microcontact printing. Biomaterials 30(2009)29, pp. 5427-5432.

[85] Lahtonen K, Lampimäki M, Jussila P, Hirsimäki M, Valden M. Instrumentation and analytical methods of an x-ray photoelectron spectroscopy–scanning tunneling microscopy surface analysis system for studying nanostructured materials. Review of Scientific Instruments 77(2006)8, pp. 083901-083901-9.

[86] Colton RJ, Baselt DR, Dufrêne YF, Green JD, Lee GU. Scanning probe microscopy. Current opinion in chemical biology 1(1997)3, pp. 370-377.

[87] Heymann JB, Müller DJ, Mitsuoka K, Engel A. Electron and atomic force microscopy of membrane proteins. Current opinion in structural biology 7(1997)4, pp. 543-549.

[88] Hansma HG, Pietrasanta L. Atomic force microscopy and other scanning probe microscopies. Current opinion in chemical biology 2(1998)5, pp. 579-584.

[89] Geisse NA. AFM and combined optical techniques. Materials Today 12(2009)7–8, pp. 40-45.

[90] Moloney M, McDonnell L, O'Shea H. Atomic force microscopy of BHK-21 cells: an investigation of cell fixation techniques. Ultramicroscopy 100(2004)3–4, pp. 153-161.

[91] Charulatha V, Rajaram A. Influence of different crosslinking treatments on the physical properties of collagen membranes. Biomaterials 24(2003)5, pp. 759-767.

[92] Browne MM, Lubarsky GV, Davidson MR, Bradley RH. Protein adsorption onto polystyrene surfaces studied by XPS and AFM. Surface Science 553(2004)1–3, pp. 155-167.

[93] Moran MT, Carroll WM, Selezneva I, Gorelov A, Rochev Y. Cell growth and detachment from protein-coated PNIPAAm-based copolymers. Journal of Biomedical Materials Research Part A 81A(2007)4, pp. 870-876.

[94] Rico P, Rodriguez Hernandez JC, Moratal D, Altankov G, Monleon Pradas M, Salmeron-Sanchez M. Substrate-induced assembly of fibronectin into networks: influence of surface chemistry and effect on osteoblast adhesion. Tissue engineering.Part A 15(2009)11, pp. 3271-3281.

[95] ramé-hart instrument co. ramé-hart Contact Angle. 2012. Accessed 09/04, 2012 Available at: http://www.ramehart.com/contactangle.htm.

[96] Biolin Scientific. Applications | Attension Tensiometers. 2010. Accessed 07/18, 2012 Available at: http://www.attension.com/applications/application-notes-3.

[97] Choi BH, Choi YS, Hwang DS, Cha HJ. Facile surface functionalization with glycosaminoglycans by direct coating with mussel adhesive protein. Tissue engineering.Part C, Methods 18(2012)1, pp. 71-79.

[98] Keselowsky BG, Collard DM, García AJ. Surface chemistry modulates fibronectin conformation and directs integrin binding and specificity to control cell adhesion. Journal of Biomedical Materials Research Part A 66A(2003)2, pp. 247-259.

[99] Ibelgaufts H. PA6 (Cytokines & Cells Encyclopedia - COPE). 2006 . Accessed 05/29, 2012 Available at: http://www.copewithcytokines.de/cope.cgi?key=PA6.

[100] Thermo Scientifc. Specialized Surfaces. 2010. Accessed 10/19, 2012 Available at: http://www.nuncbrand.com/en/page.aspx?id=1275.

[101] Cunningham JJ, Nikolovski J, Linderman JJ, Mooney DJ. Quantification of fibronectin adsorption to silicone-rubber cell culture substrates. BioTechniques 32(2002)4, pp. 876, 878, 880 passim.

8 APPENDIX 1: REAGENTS AND PRODUCERS

Table 8.1: *List of reagents, producers and suppliers used in this work that are not listed in the Chapter 3.*

Reagent	**Producer**	**Supplier**
KO-DMEM	Gibco	Invitrogen
GMEM (BHK-21)	Gibco	Invitrogen
DMEM/F-12	Gibco	Invitrogen
Knock-out serum replacement	Gibco	Invitrogen
Glutamax	Gibco	Invitrogen
β-mercaptoethanol	Gibco	Invitrogen
B27-supplement	Gibco	Invitrogen
Fetal bovine serum	PAA Laboratories	Immunodiagnostic
Penicillin/Streptomycin	Lonza	Thermo Fisher Scientific
Non-essential amino acids	Lonza	Thermo Fisher Scientific
Trypsin	Lonza	Thermo Fisher Scientific
Phosphate buffered saline, PBS	Lonza	Thermo Fisher Scientific
Na-Puryvate	Sigma-Aldrich	
Paraformaldehyde, PFA	Sigma-Aldrich	
Bovine serum albumin	Sigma-Aldrich	
Triton-X 100	Sigma-Aldrich	
Phosphate buffer	Sigma-Aldrich	
Neural growth factor	R&D Tocris	
Basic fibroblast growth factor	R&D Tocris	
Normal Donkey Serum	Merck Millipore	

9 APPENDIX 2: FLUORESCENT LABELING PROTOCOL FOR ECM PROTEIN COATINGS

Samples: _____ **Date:**_____

- ☐ **COATING 1h RT**
- ☐ **FIXING 4 % PFA or 2% Glutaraldehyde 15 min RT**
- ☐ **WASH 2 * 5 min PBS** (1 ml, 0.01 M, pH 7.4)
- ☐ **BLOCKING: 10% NDS, 1% BSA in PBS 45 min RT** (for 24-well plate: 750 µl liquid/well)
- ☐ **WASH: 1% NDS, 1% BSA in PBS**
- ☐ **MIXTURE OF PRIMARIES: 1% NDS, 1% BSA in PBS RT 1 h**
  (24-well plate: 150 µl mixture of antibodies/well)

Well	ANTIBODY	DILUTION	ORIGIN
	I _____	_____	_____
	I _____	_____	_____
	I _____	_____	_____

- ☐ **WASH: 3 * 5 min 1% BSA in PBS**
- ☐ **MIXTURE OF SECONDARIES: 1% BSA in PBS 1 h RT in Dark**

Well	ANTIBODY	DILUTION	ORIGIN
	I _____	_____	_____
	I _____	_____	_____
	I _____	_____	_____

- ☐ **WASH 3 *5 min in PBS**
- ☐ **WASH 2 * 5 min in PB**
- ☐ **Dry and mount with Vectashield + coverslips**
- ☐ **Store at +4°C light protected**